



UNIVERSITÄT ZU KÖLN

Mathematisches Institut

MASTERARBEIT

Modern Methods for Signal Analysis: Empirical Mode Decomposition Theory and Hybrid Operator-Based Methods Using B-Splines

Laslo Hunhold

Erstgutachterin:

Prof. Dr. Angela KUNOTH

Zweitgutachter:

Dr. Boqiang HUANG

27. Mai 2019, überarbeitet am 11. März 2020

Preface

Signal analysis is as diverse as the data it tries to comprehend. The empirical mode decomposition is no exception to this rule and the great attention it has received over the years with numerous applications in many fields has always been overshadowed by the introduction of more and more increasingly powerful but also heuristical approaches.

Since I have been first roughly introduced to the topic by Prof. Dr. Angela KUNOTH, who has published in the field and managed to spark my interest, in 2015 I was always willing to further understand and advance it. With other endeavours in the meantime I was given the chance to work on this topic in the course of my master's thesis.

First of all I would like to thank Prof. Dr. Angela KUNOTH for introducing me to and supporting and entrusting me with this fascinating and complex topic. I would also like to thank Dr. Boqiang HUANG for his support with his deep insight as a researcher into the field, his patience and the in-depth discussions. Last but not least, I would like to thank my family for their unwavering support and encouragement.

*Wesseling, Germany
May 2019*

Laslo Hunhold

When I heard the learn'd astronomer,
When the proofs, the figures, were ranged in columns before me,
When I was shown the charts and diagrams, to add, divide, and measure
them,
When I sitting heard the astronomer where he lectured with much
applause in the lecture-room,
How soon unaccountable I became tired and sick,
Till rising and gliding out I wander'd off by myself,
In the mystical moist night-air, and from time to time,
Look'd up in perfect silence at the stars.

Walt WHITMAN (1819–1892)

Contents

Preface	iii
1. Introduction	1
2. B-Splines	11
3. Empirical Mode Decomposition Model and Analysis	19
3.1. Intrinsic Mode Functions	19
3.2. Cost Functions	24
3.2.1. Canonical	25
3.2.2. Leakage Factor	29
3.3. General Optimization Problem	30
3.4. Regularity	31
3.4.1. Convex-Like Optimization	32
3.4.2. SLATER Condition and Strong Duality	38
3.5. Conclusion	42
4. Operator-Based Analysis of Intrinsic Mode Functions	45
4.1. IMF Differential Operator	46
4.1.1. Properties	47
4.1.2. Simplification	52
4.1.3. Discretization	53
4.2. Examples	54
4.3. Discussion	60
5. Hybrid Operator-Based Methods	61
5.1. Classic EMD method	61
5.2. Envelope Estimation	63
5.2.1. Classic Envelope Estimation	64
5.2.2. Iterative Slope Envelope Estimation	64
5.2.3. Examples	66
5.3. Hybrid EMD Algorithm	70
5.4. ETHOS Toolbox	71
5.4.1. Initialization and Precomputation	71
5.4.2. Data Filtering	72
5.4.3. Boundary Effects and Extension	72
5.4.4. Decomposition	72
5.4.5. Plotting	73

Contents

5.4.6. Envelope Estimation	73
5.4.7. IMF Characteristic	73
5.5. Examples	74
6. Summary and Outlook	83
A. Function Space Order and Operators	85
B. Convexity Theory	89
C. Notation Directory	91
C.1. Chapter 1: Introduction	91
C.2. Chapter 2: B-Splines	91
C.3. Chapter 3: Empirical Mode Decomposition Model and Analysis	91
C.4. Chapter 4: Operator-Based Analysis of Intrinsic Mode Functions	92
C.5. Chapter A: Function Space Order and Operators	92
C.6. Chapter B: Convexity Theory	92
D. Code Listings	93
D.1. ETHOS Toolbox	93
D.1.1. ethos.h	93
D.1.2. ethos.c	94
D.1.3. config.mk	114
D.1.4. Makefile	115
D.2. Examples	115
D.2.1. emd.c	116
D.2.2. envelope.c	123
D.2.3. regop.c	129
D.2.4. util.h	133
D.2.5. util.c	134
D.2.6. config.mk	138
D.2.7. Makefile	139
D.3. License	140
Bibliography	141
Eigenständigkeitserklärung	145

1. Introduction

This thesis examines the empirical mode decomposition (EMD), a method for decomposing multicomponent signals, from a modern, both theoretical and practical, perspective. The motivation is to further formalize the concept and develop new methods to approach it numerically.

Multicomponent Signal Decomposition A signal is a time- or space-dependent univariate function $s(t)$ that carries information about the properties of a phenomenon in the form of variations of an observed quantity over space or time. For instance, time-varying signals can be financial or audio data, and space-varying signals can be images or maps.

Naturally, due to the complexity of reality, it is impossible to find a quantity that only contains information about the phenomenon you are interested in. Instead, it will contain information about multiple phenomena simultaneously. To give an example, if you observe bat calls using a powerful ultrasonic microphone outside at night, you will also pick up a lot of environment noise (birds, wind, cars, airplanes, et cetera) that is mixed with your bat calls. As humans we are good at filtering out audible noise intuitively due to the anatomy of our ears and function of our brains, which can for example be observed during a conversation at an event with loud music or background noise. The computer lacks such intuition. It is in our interest to quantify this separation process so that it can be applied to larger and more general problems automatically.

One way to approach this is to consider the concept of ‘frequency’, the rate of change of an oscillation over time or space. The signal is considered as a (weighted) sum of oscillations of different frequencies, a so-called ‘multicomponent signal’, where each summand is called a ‘component’ (see Figure 1.1 for an example). A single component does not

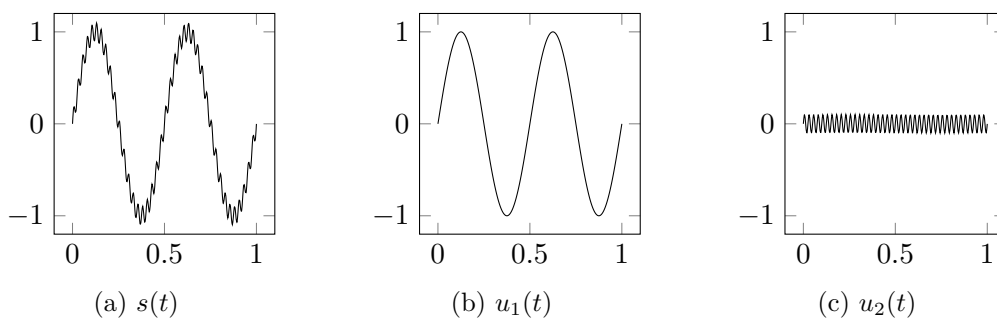


Figure 1.1.: An example for a signal $s(t)$ that is an additive composite of a low-frequency oscillation $u_1(t)$ and a high-frequency oscillation $u_2(t)$.

1. Introduction

necessarily correspond to the phenomenon we are interested in but this decomposition into components quantifies the signal and a subset of these components as a whole can convey the information we need. This process is called ‘signal decomposition’.

Reconsidering our bat call example, we can easily discard all components corresponding to frequency ranges that are above or below the frequency ranges of bat calls. More problematic are the frequency ranges of the bat calls themselves and how to decompose them usefully. To approach this issue, we will as follows introduce the three most popular signal decomposition methods. The last one, the Empirical Mode Decomposition (EMD), will be the main focus of this thesis.

Fourier Transform First proposed in 1822 by Jean-Baptiste-Joseph FOURIER (see [Fou22]), the *FOURIER transform* is the most well-known method in this context. It is based on the observation that for every 1-periodic function $\Phi(t)$ (which means that for all $t \in \mathbb{R}$ it holds $\Phi(t) = \Phi(t + 1)$) and $j \in \mathbb{Z}$ we can find $c_j \in \mathbb{C}$ such that

$$\Phi(t) = \sum_{j \in \mathbb{Z}} c_j \cdot \exp(2\pi i j t). \quad (1.1)$$

This is due to the fact that, roughly spoken, $\{t \mapsto \exp(2\pi i j t) \mid j \in \mathbb{Z}\}$ is an orthonormal basis of the HILBERT space (a real or complex vector space with an inner product that is a complete metric space in regard to the norm induced by the inner product) of square integrable 1-periodic functions. Equation (1.1) is called the ‘FOURIER series’ of $\Phi(t)$ and the coefficients c_j are calculated as

$$c_j := \int_{-\frac{1}{2}}^{\frac{1}{2}} \Phi(t) \cdot \exp(-2\pi i j t) dt. \quad (1.2)$$

The mapping $j \mapsto c_j$ is called the ‘FOURIER transform’ of $\Phi(t)$ and the parameter j corresponds to the frequency. The higher the j , the faster the $\exp(2\pi i j t)$ term oscillates over time t , resulting in a higher-frequency oscillation. If we cover $j \in \mathbb{Z}$ we obtain a complete coverage of low and high frequencies. In Figure 1.2 you can see an example of how a finite FOURIER series composes a 1-periodic function.

We can immediately see that this series is a c_j -weighted sum of oscillations $\exp(2\pi i j t)$, a property we desired based on the observations in the previous paragraph on multicomponent signals. We have to note here, though, that $\Phi(t)$ is 1-periodic, which a signal $s(t)$ is not in general. To extend the FOURIER transform to non-periodic signals, we first note that for any $T > 0$ a T -periodic function $\tilde{\Phi}(t)$ can be transformed into a 1-periodic function $\Phi(t)$ via $\Phi(t) := \tilde{\Phi}(t/T)$. If we apply this transformation to the above expression and let $T \rightarrow \infty$ we obtain the general FOURIER expression of a non-periodic signal $s(t)$ as

$$s(t) = \int_{-\infty}^{\infty} (\mathcal{F}s)(f) \cdot \exp(2\pi i f t) df \quad (1.3)$$

with the FOURIER transform

$$(\mathcal{F}s)(f) := \int_{-\infty}^{\infty} s(t) \cdot \exp(-2\pi i f t) dt. \quad (1.4)$$

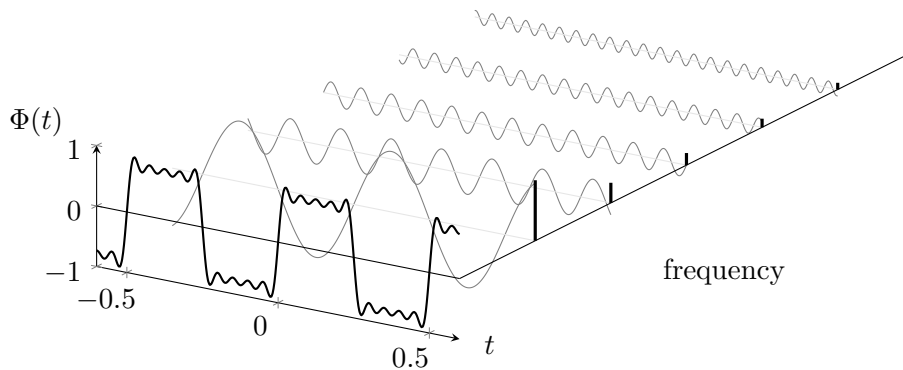


Figure 1.2.: Visualization of the FOURIER series composition of a 1-periodic function $\Phi(t)$ that is additively composed of 5 oscillatory terms.

The parameter f of the FOURIER transform $(\mathcal{F}s)(f)$ corresponds to a continuous form of the j we have seen earlier. During the FOURIER transform, each ‘frequency’ f ’s share is averaged over the entire interval the signal is defined on. In turn, if the signal’s frequency composition varies across this timeframe the FOURIER transform is unable to reflect these changes, and we can say that it is only suitable for *stationary signals*, which are signals whose frequency compositions do not change much over time.

One may approach this problem by reducing the area the FOURIER transform covers. This is done by applying a so-called ‘window function’ to the signal that zeros out all of the signal except on a compact interval. The window function is varied by employing a base window function (e.g. a GAUSS function) that is ‘moved’ to multiple parts of the time domain until it has been fully covered and all sub-intervals are analyzed. This method is called the Short-Time FOURIER Transform (STFT). The KÜPFMÜLLER uncertainty principle states that it is impossible to both clearly localize a signal in both the time and frequency domain (see [KK00, VII.47 (29a)]). This shows that the downside of the STFT is that with increasing tightness of the time-interval that is studied the frequency becomes more and more uncertain.

In summary, on the one hand, the classical FOURIER transform localizes the signal perfectly in the frequency domain, but has the worst possible time resolution. On the other hand, applying window functions presents the limits of signal analysis and leads to bad time-resolution for high frequencies, because the time-window is made arbitrarily small. For further reading on FOURIER analysis one may consult [Kö88].

Wavelet Transform The *wavelet transform* based on the groundwork by Alfréd HAAR in 1910 (see [Haa10]) is closely related to the STFT and makes use of by now so-called ‘wavelet’ functions that are ‘better-behaved’ as window functions than the ones used for STFT. ‘Better-behaved’ in this context means providing better frequency-resolution for shorter time-intervals and better time-resolution for high frequency bands.

1. Introduction

The fundamental idea is to consider the HILBERT space (a real or complex vector space with an inner product that is a complete metric space in regard to the norm induced by the inner product) $(\mathcal{L}^2(\mathbb{R}), \langle \cdot, \cdot \rangle)$ of square-integrable functions with the standard inner product $\langle \cdot, \cdot \rangle: \mathcal{L}^2(\mathbb{R}) \times \mathcal{L}^2(\mathbb{R}) \rightarrow \mathbb{R}$ defined as

$$\langle f, g \rangle := \int_{-\infty}^{\infty} f(t) \overline{g(t)} dt \quad (1.5)$$

and find an orthonormal basis (which means that the inner product of two distinct basis elements is zero and one for two same basis elements) for it. In the context of the FOURIER transform, we noted previously that the set $\{t \mapsto \exp(2\pi i j t) \mid j \in \mathbb{Z}\}$ was an orthonormal basis of the Hilbert space of the 1-periodic square-integrable functions. However, our interest here is to find basis functions with compact support (which means that they are zero everywhere except on a compact interval). An additional limitation with wavelets, in terms of an orthonormal basis, is that we, just like previously with the window functions for STFT, consider one basic function we in this context call ‘mother wavelet’ $\psi(t)$ that is moved and transformed across the time interval to generate all other basis functions. The transformations are so-called ‘dyadic translations’ and ‘dilations’ and are parametrized by $j, k \in \mathbb{Z}$, yielding a family of functions defined as

$$\psi_{j,k}(t) := 2^{\frac{j}{2}} \cdot \psi(2^j \cdot t - k). \quad (1.6)$$

If the mother wavelet $\psi(t)$ can be used to construct a HILBERT basis as described above, we call it an *orthonormal wavelet*. Then we can express any signal $s(t)$ with $(j, k) \in \mathbb{Z}^2$ and $c_{j,k} \in \mathbb{R}$ as

$$s(t) = \sum_{(j,k) \in \mathbb{Z}^2} c_{j,k} \cdot \psi_{j,k}(t) \quad (1.7)$$

with the wavelet coefficients

$$c_{j,k} = \langle s, \psi_{j,k} \rangle. \quad (1.8)$$

The advantage of this separation becomes apparent when we consider that the parameters j and k play special roles: The parameter j corresponds to the frequency (dyadic dilation), whereas k corresponds to the location (dyadic translation). When we group the sum by frequency, we obtain

$$s(t) = \sum_{j \in \mathbb{Z}} \sum_{k \in \mathbb{Z}} c_{j,k} \cdot \psi_{j,k}(t) =: \sum_{j \in \mathbb{Z}} g_j(t), \quad (1.9)$$

effectively yielding a separation of the signal into functions $g_j(t)$ reflecting the relative share of the frequency respective to j within the signal over time.

When discussing the wavelet transform one has to observe that the choice of the mother wavelet $\psi(t)$ is neither canonical nor domain-specific. Additionally, the range of the parameters j and k have to be determined in advance or adaptively, making it necessary to apply some kind of preprocessing to the signal. The dyadic translations (parametrized by k) impose the same grid-density across the entire interval, as $\psi_{j,k}$ is linear in $k \in \mathbb{Z}$. This is problematic when a small timeframe of the input signal has

high oscillations that might require a high local time resolution. Still, as opposed to the FOURIER transform, the wavelet transform can be used for non-stationary signals (those that exhibit changes of their frequency-composition over time) as well. For further reading on the wavelet transform, one may consult [Dau92] and [Mal09].

Empirical Mode Decomposition The method focused on in this thesis is the *empirical mode decomposition* (EMD) proposed in 1998 by HUANG et alii (see [HSL⁺98]) that has gained lots of attention since then. In contrast to the classic FOURIER and Wavelet transforms that depend on a predefined finite subset of a HILBERT basis to match a certain frequency range, the EMD is an iterative data-adaptive process. This means that there needs to be no preprocessing and it adapts to the incoming data as it analyzes it. In contrast to classical versions of the FOURIER and wavelet transforms, it also does not require the input data to be regularly aligned on a grid.

This method works as follows: The signal $s(t)$ is additively adaptively separated into S so-called ‘intrinsic mode functions’ (IMFs) $u_i(t)$, which each more or less correspond to the signal components laid out earlier, and a residual r_{S+1} that remains from the signal after the S extraction steps. The crucial difference compared to the previous methods is that the IMFs are allowed to slowly vary in frequency and intensity over time, whereas previously we had functions that were more or less fixed in the frequency- and time-domains. A formal definition of IMFs is given in 3.1.

Assuming we have determined the IMFs, we obtain the signal representation

$$s(t) = \sum_{i=1}^S u_i(t) + r_{S+1}(t) \quad (1.10)$$

and set requirements that are satisfied in the ideal case. Each IMF shall have the form

$$u_i(t) = a_i(t) \cdot \cos(\phi_i(t)),$$

with a so-called ‘instantaneous amplitude’ $a_i(t)$ and ‘instantaneous phase’ $\phi_i(t)$. The derivative $\phi_i'(t)$ of the instantaneous phase $\phi_i(t)$ is the frequency. Thus, this form allows the IMF to be both variable in amplitude and frequency. We require for all $t \in \mathbb{R}$ the natural conditions $a_i(t) \geq 0$ and $\phi_i'(t) > 0$. These are necessary given negative amplitudes or frequencies are not physically meaningful. We also want $a_i(t)$ and $\phi_i'(t)$ to be slowly varying, which will be formally laid out later. The residual shall at best be monotonic or have at most one local maximum or minimum, which of course is dependent on how many extraction steps S were taken.

Separating a signal $s(t)$ into IMFs is called ‘sifting’ (see Figure 1.3). This is a multi-step-process, but each step is more or less independent from the others. A single step extracts one IMF from the signal, subtracts the IMF from the signal and returns the result as the so-called ‘residual’, which is then again processed as a new input signal in the next step. For this reason, we will, as follows and in this thesis, almost exclusively focus on a single step of the sifting process. The classic procedure for a sifting step laid out in [HSL⁺98] is to determine lower and upper envelopes $\underline{a}(t)$ and $\bar{a}(t)$ of the signal $s(t)$,

1. Introduction

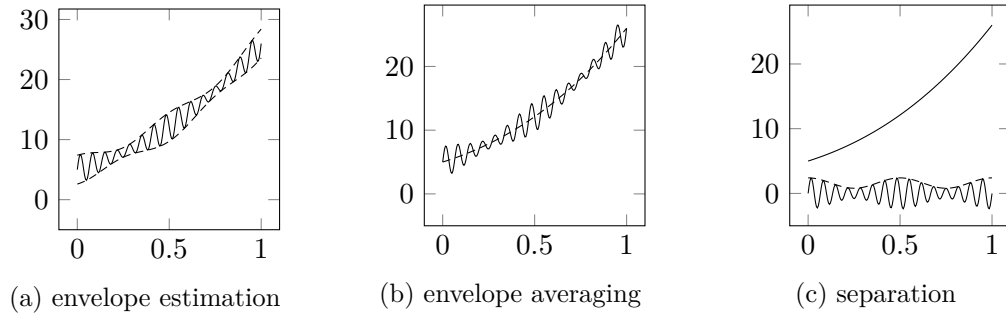


Figure 1.3.: Visualization of the EMD sifting process of a 1-component signal.

usually by interpolating local maxima and minima. The mean $\frac{1}{2} \cdot (\bar{a} + \underline{a}) =: r(t)$ is defined as the residual $r(t)$ for the next decomposition step and the difference $s(t) - r(t) =: u(t)$ between signal and residual is the desired intrinsic mode function. As a side-result, one obtains the amplitude $a(t)$ of the intrinsic mode function $u(t) := a(t) \cdot \cos(\phi(t))$ by the difference $\bar{a}(t) - r(t) := a(t)$ between the upper envelope and the residual.

The next (optional, depending on the application) step is to do a so-called ‘spectral analysis’ of the extracted IMFs, which means that for a given IMF $u(t)$ the instantaneous amplitude $a(t)$ and phase/frequency $\phi(t)/\phi'(t)$ are extracted. As the name implies, the EMD is an empirical method. Unfortunately, this procedure has up to now a relatively weak theoretical footing compared to the strong theory behind the FOURIER and wavelet transforms.

The big disadvantage of the EMD representation in Equation (1.10) is that it is not unique, making it difficult to formulate theoretical assessments. Without providing more conditions, the uniqueness guarantee is impossible to give. However, the big strength of the EMD is that both the instantaneous amplitude and phase can have arbitrary form within the bounds of physical meaningfulness and slow variation in Equation (1.10). This means that a single IMF can ‘track’ a subcomponent of a signal over the time- and frequency-domain even if this subcomponent happens to change in intensity or frequency and this rate of change falls within the previously set bounds.

When considering the decomposition provided by the FOURIER transform in Equation (1.4), we see that it has a constant ‘amplitude’ $(\mathcal{F}(f))(f)$ for each oscillation term $\exp(2\pi if t)$ belonging to the fixed ‘frequency’ f , given the FOURIER transform provides no time-resolution. The wavelet transform decomposition in Equation (1.9) improves upon this problem by having a decomposition into ‘frequency share’ functions $g_k(t)$. However, it is unable to reflect the condition when a signal component leaves the frequency-band relating to k without further post-processing of some kind. The empirical mode decomposition with its flexible instantaneous amplitude and phase for each intrinsic mode function is able to flexibly reflect both changes in amplitude and frequency over time.

Operator-Based Signal Separation and Null-Space-Pursuit The operator-based signal separation (OSS) was proposed in 2008 by PENG et alii (see [PH08] and [PH10]) as an

idea for a more formal foundation for the empirical mode decomposition. The basic concept is centered around the idea of an ‘adaptive operator’, which we will explain with an example as follows.

Consider you have a function $h(t)$ and you only know that it is of the form $h(t) := \cos(\phi(t))$. The function $\phi(t)$ is not known and it is your goal to determine it. Let us consider the first and second derivatives of $h(t)$. We obtain with the chain rule that $h'(t) = -\phi'(t) \cdot \sin(\phi(t))$ and $h''(t) = -\phi''(t) \cdot \sin(\phi(t)) - (\phi'(t))^2 \cdot \cos(\phi(t))$. If we then define a differential operator $\mathcal{D}_{\tilde{\phi}}$ with respect to the input function $h(t)$ as

$$\left(\mathcal{D}_{\tilde{\phi}}h\right)(t) := h''(t) - \frac{\tilde{\phi}''(t)}{\tilde{\phi}'(t)} \cdot h'(t) + (\tilde{\phi}'(t))^2 \cdot h(t), \quad (1.11)$$

it follows directly, because the terms cancel each other out, that

$$\mathcal{D}_{\tilde{\phi}}h \equiv 0.$$

The differential operator is defined in terms of the parameter $\tilde{\phi}(t)$. If we manage to choose it as $\phi(t)$, the ‘hidden’ function within the cosine-term of $h(t)$, the operator applied to $h(t)$ vanishes. In other words, we can say that then $h(t)$ is in the ‘null-space’ of the operator. The search for the correct parameter to annihilate the operator applied to $h(t)$ can consequently be called ‘null-space-pursuit’.

When we reconsider the EMD signal representation from Equation (1.10), it becomes clear that this operator-based approach can be used to process IMFs $u(t)$ in some fashion. The IMFs are of the form $u(t) := a(t) \cdot \cos(\phi(t))$ in regard to their instantaneous amplitude $a(t)$ and phase $\phi(t)$, but both are not known. For the purpose of spectral analysis, i.e. determining these factors, we use the adaptive differential operator that is parametrized by $\tilde{a}(t)$ and $\tilde{\phi}(t)$ and annihilate the IMF $u(t)$ when the parameters are tuned to $a(t)$ and $\phi(t)$, effectively yielding us the previously unknown instantaneous amplitude and frequency.

This however is not enough. To completely formally express the EMD, another important aspect is to grasp the IMF extraction itself. In each step, we split the input signal $s(t)$ into an IMF $u(t)$ and a residual $r(t)$. A canonical extraction condition is to demand that we extract as much as possible from the input signal, namely, that the residual $r(t) = s(t) - u(t)$ is ‘minimal’, in a sense that is to be made precise.

Combining both ideas, a single EMD extraction step for an input signal $s(t)$ can be expressed as a regularized optimization problem. We consider the residual $r(t)$ and use a fitting differential operator $\mathcal{D}_{(\tilde{a}, \tilde{\phi})}$ (see [PH10, Equation (3)]) with some real parameter $\lambda > 0$. The function-minimization-terms are put into norms so they yield a cost-function with values in \mathbb{R} as

$$(r, a, \phi) = \arg \min_{\tilde{r}, \tilde{a}, \tilde{\phi}} \left\{ \left\| \mathcal{D}_{(\tilde{a}, \tilde{\phi})}(s - \tilde{r}) \right\|_2^2 + \lambda \cdot \|\tilde{r}\|_2^2 \right\}.$$

This problem can be reformulated in terms of an IMF u with instantaneous amplitude a and phase ϕ as

$$(u, a, \phi) = \arg \min_{\tilde{u}, \tilde{a}, \tilde{\phi}} \left\{ \left\| \mathcal{D}_{(\tilde{a}, \tilde{\phi})}\tilde{u} \right\|_2^2 + \lambda \cdot \|s - \tilde{u}\|_2^2 \right\}. \quad (1.12)$$

1. Introduction

The first term in Equation (1.12) ensures that the resulting function u is an IMF and enables us to perform a spectral analysis in terms of a and ϕ , because it strives to annihilate the operator whose parameters we are tuning to. The second term ensures, as previously discussed, maximum extraction from the signal s , i.e. a minimal residual. This is referred to in [PH10] as the ‘greedy’ approach. Note that there are other ways to formulate an extraction condition other than the minimization of $r(t) = s(t) - u(t)$ within a norm. If we assume that our residual is reasonably smooth, the greedy approach is a valid approach compared to other approaches considering higher-order differentiation of the residual within the norm.

The approach of the operator-based signal separation with the null-space-pursuit provides an elegant formalization of the EMD, combining both the sifting and spectral analysis into one optimization problem. The previous difficulty that the separation of the signal into an IMF and residual directly relies on the spectral analysis of said IMF ‘in-situ’ is elegantly solved by weaving the spectral analysis in form of an adaptive operator into the extraction process itself.

An open question is the choice of such an adaptive operator and how well it enforces the IMF conditions, given the one in [PH10, Equation (3)] is not unique. To give an example, let us consider the differential operator $\frac{\partial^3}{\partial t^3}$ as an example for a differential operator to ‘match’ (i.e. annihilate) quadratic functions. Quadratic functions are in its null-space, which means that it is suitable for a null-space-pursuit to enforce quadratic functions. However, linear and constant functions are also in its null-space and will subsequently be also ‘matched’. The same problem, though much harder to grasp, might be present for IMF-annihilating adaptive operators.

EMD Optimization Problem Taking a step back from the formalized EMD by [PH10] in Equation (1.12), this thesis proposes to take a new look at the EMD as a constrained optimization problem for each step. The author calls this the EMD optimization problem (EMDOP) and investigates this in Chapter 3. It considers the operator-based method as a form of regularization over the set of IMFs (see 3.1) and generalizes it. The extraction condition is that $r(t) = s(t) - u(t)$ shall be minimal (maximum extraction, minimal residual), yielding the optimization problem

$$\begin{aligned} \min_u \quad & \|s - u\|_2^2 \\ \text{s.t.} \quad & u \text{ IMF.} \end{aligned}$$

This optimization problem corresponds to one single step of the EMD and is later generalized to arbitrary ‘cost functions’ other than $\|s - u\|_2^2$. The EMDOP will be the main focus of the theoretical groundwork of this thesis in Chapter 3. It provides new results for OSS/NSP and other similar regularization-based EMD-schemes. As previously stated, the only path toward an EMD-algorithm yielding unique results is to add more conditions to the extracted IMF. One path is to add more regularization terms which has consecutively been done in the analysis in [PH08] and [PH10]. Another way is to add more constraints to the EMDOP. This thesis considers the latter approach, as more regularization terms weaken the theoretical foundation of the EMD method even more.

Another reason for the latter approach is that regularization terms in the cost functions are in fact there to enforce some kind of condition on the extracted IMF, so it only makes sense to avoid this indirect route and directly state these conditions.

B-Splines Introduced by Isaac Jacob SCHOENBERG in 1946 (see [Sch46a] and [Sch46b]), B-splines (‘Basis-splines’) have become an integral part of numerical analysis due to their very useful theoretical and practical properties as basis functions for a space of piecewise polynomial functions. In the course of this thesis, we will make use of these properties.

The objects of interest in the presented signal analysis methods are functions, not scalars. Looking at the EMD, for instance, we have the functions describing the signal $s(t)$: IMF $u(t)$, residual $r(t)$, instantaneous amplitude $a(t)$ and instantaneous phase $\phi(t)$. Many publications, despite dealing with functions, express their algorithms in terms of discrete samples. The author considers this to be a problem as the process of fitting a function to samples opens up a new set of problems, for instance over- or underfitting the data in some way. This problem is discussed in [Die95] and, for reasons of scope due to the complexity of sampling theory, is left out in this thesis.

However, to explain this briefly, when analyzing a signal you are mostly interested in a certain frequency band. Frequencies above or below that are considered as ‘noise’. When taking a step back, though, there is really no such thing as ‘noise’, given this ‘noise’ is just a signal with frequencies we are not interested in. A strictly sample-based algorithm needs to be careful, given that samples can contain such oscillations depending on the sampling rate. When working with continuous signals, we allow such high oscillations but don’t make ourselves dependent on the sampling rate.

To avoid such problems with samples and discrete signals, B-splines are used to model smooth functions in a discretized (such that they are machine-representable) way in this thesis and all outside inputs considered to be functions rather than samples.

Goal of this Thesis The goal of this thesis is to take a both theoretical and practical look at the empirical mode decomposition. We want to answer the question how to classify the previously introduced OSS/NSP method (see Equation (1.12)) within the aforementioned strictly theoretical newly introduced EMD model EMDOP. After theoretical assessments, the canonical objective is to make use of the theoretical results to develop new EMD methods with regard to sifting and spectral analysis by employing the OSS/NSP method.

Structure of this Thesis Following Chapter 2, which introduces B-splines, Chapters 3 and 4 contain the main theoretical results of this thesis. Chapter 3 analyzes the empirical mode decomposition by first formalizing the aforementioned EMD optimization problem in Sections 3.1, 3.2 and 3.3 and proving it to be SLATER-regular in Section 3.4. Chapter 4 motivates the foundation of the operator-based signal-separation method and analyzes the operator-based analysis of intrinsic mode functions.

Using the results obtained in Chapters 3 and 4, Chapter 5 proposes an EMD approach that is a hybrid of classic and modern methods. In the course of this construction, a new

1. Introduction

'iterative slope' envelope estimation algorithm is motivated, presented and evaluated in Section 5.2. This yields the final hybrid operator-based EMD method in Section 5.3. As another coproduct, the 'ETHOS' toolbox is presented and documented in Section 5.4.

2. B-Splines

The central objects of interest in the empirical mode decomposition are functions. Our interpolated signals, intrinsic mode functions and instantaneous amplitudes and frequencies are all time-variant quantities and, thus, a good model for them is of high importance.

A priority we can note is that however we model functions, they should be easy to represent numerically. Another key aspect of interest, as we will make heavy use of it later, is the ability to evaluate the functions and their derivatives easily and quickly. The approach of many publications is to directly work with samples and use in-situ-approximated derivatives. However, this makes it difficult to formalize the process and distinguish between sampling errors and weaknesses in the process itself. Thus, even though the classic EMD algorithm presented in [HSL⁺98] works with discrete data-points, the main interest should be to strive to understand why such heuristics work and when and not mix the problem with one related to sampling theory. In other words: Oversampling should not affect the result and continuous rather than discrete signals help us mitigate this issue.

In general the basis function approach is that one considers a finite vector space of functions for which one can find a finite set of basis functions. Weighted sums of these basis functions can then be used to represent any function in this vector space. If we take \mathbb{R}^2 as an example, there exist numerous possible choices for bases, for instance the standard basis $\{(1, 0)^T, (0, 1)^T\}$ or $\{(1, 1)^T, (0, 1)^T\}$. Any element in \mathbb{R}^2 can be represented with a weighted sum of these basis vectors. For function spaces, which are also vector spaces, one can also consider different choices of basis functions accordingly.

The choice of basis functions used in this thesis are B-splines, a basis for the vector space of spline functions that has multiple useful theoretical and numerical properties. B-splines were first introduced by Isaac Jacob SCHOENBERG in 1946 (see [Sch46a] and [Sch46b]) and the term is short for ‘basis splines’. It had a big impact in many numerical fields since then. This thesis is the first to explore the solution theory of the empirical mode decomposition and the operator-based methods using B-splines and generally makes heavy use of them. This is why we introduce B-splines in this section in such detail, but leave out some of the more technical proofs. Before introducing B-splines, we naturally first have to define what a spline function is. To do that, we first introduce the

Definition 2.1 (Set of polynomials [dB01, I (1)]). *Let $k \in \mathbb{N}$. The set of polynomials of order k is defined as*

$$\Pi_k := \left\{ t \mapsto \sum_{i=0}^{k-1} a_i \cdot t^i \mid (a_0, \dots, a_{k-1}) \in \mathbb{R}^{k-1} \times \mathbb{R}_{\neq 0} \right\}.$$

2. B-Splines

We distinguish between ‘degree’ and ‘order’. A linear polynomial with degree 1 (largest t -exponent) has order 2 (degrees of freedom), a cubic polynomial with degree 3 has order 4. Now that we have defined polynomials, we can formulate what spline functions are.

Definition 2.2 (Spline function space [dB01, VII (1)]). *Let $k, \ell \in \mathbb{N}$ with $k \leq \ell - 1$ and $T := \{\tau_i\}_{i=0}^{\ell-1}$ with $\tau_0 < \dots < \tau_{\ell-1}$. The spline function space $\Sigma_{k,T}$ of order k on T is defined as*

$$\Sigma_{k,T} := \left\{ s \in \mathcal{C}^{k-2}([\tau_0, \tau_{\ell-1}]) \mid \forall_{i \in \{0, \dots, \ell-2\}} : s|_{[\tau_i, \tau_{i+1}]} \in \Pi_k \right\}$$

As we can see, a spline function is a smooth function that is piecewise-defined by polynomials. Analogous to the set of polynomials the set of linear splines is $\Sigma_{2,T}$ and the set of cubic splines is $\Sigma_{4,T}$. The first step towards finding a basis for $\Sigma_{k,T}$ is to determine the dimension, which we can say is finite as the grid T is finite.

Proposition 2.3 (Spline function space dimension [dB01, IX (44)]). *Let $k, \ell, m, p \in \mathbb{N}$ with $k \leq \ell - 1$, $p \in \{m, \dots, \ell - 1\}$ and $T := \{\tau_i\}_{i=0}^{\ell-1}$ with $\tau_0 = \dots = \tau_m \leq \dots \leq \tau_p = \dots = \tau_{\ell-1}$. $\Sigma_{k,T}$ is a real vector space with*

$$\dim(\Sigma_{k,T}) = k + \ell - 2.$$

Proof. That $\Sigma_{k,T}$ is a real vector space follows directly from the fact that $\mathcal{C}^{k-2}([\tau_0, \tau_{\ell-1}])$ and Π_k are real vector spaces.

We find the dimension by constructing an arbitrary $s \in \Sigma_{k,T}$. On the first piecewise interval $[\tau_0, \tau_1)$ we know that s is in Π_k , i.e. a polynomial of order k and thus with k degrees of freedom. We also have k degrees of freedom in the subsequent piecewise interval $[\tau_1, \tau_2)$, but require that $s \in \mathcal{C}^{k-2}([\tau_0, \tau_{\ell-1}])$. We thus need to demand the $k - 1$ continuity conditions

$$\forall_{i \in \{0, \dots, k-2\}} : s^{(i)} \Big|_{[\tau_0, \tau_1)} (\tau_1) = s^{(i)} \Big|_{[\tau_1, \tau_2)} (\tau_1),$$

leaving 1 degree of freedom for the interval $[\tau_1, \tau_2)$. This holds iteratively for all $\ell - 2$ intervals $[\tau_1, \tau_2), \dots, [\tau_{\ell-2}, \tau_{\ell-1})$, yielding in total $k + \ell - 2$ degrees of freedom corresponding to the dimension of $\Sigma_{k,T}$. \square

Now that we’ve explored the set of spline functions a bit, we know that a basis for this vector space needs to have $k + \ell - 2$ elements. If we for a moment take a step back and think of an iterative scheme to construct elements of $\Sigma_{k,T}$ starting with $\Sigma_{1,T}$ (piecewise constant splines), the underlying idea is to start with piecewise constant functions for $k = 1$, namely indicator functions, and define higher order splines recursively in such a way that we satisfy piecewise continuity.

Definition 2.4 (Indicator function). *Let $A \subseteq X$. The indicator function $\chi_A : X \rightarrow \{0, 1\}$ is defined as*

$$\chi_A(x) := \begin{cases} 1 & x \in A \\ 0 & x \notin A. \end{cases}$$

Definition 2.5 (B-spline [dB01, IX (13)]). Let $k, \ell, m, p \in \mathbb{N}$ with $k \leq \ell - 1$, $p \in \{m, \dots, \ell - 1\}$ and $T := \{\tau_i\}_{i=0}^{\ell-1}$ with $\tau_0 = \dots = \tau_m \leq \dots \leq \tau_p = \dots = \tau_{\ell-1}$. The B-spline of order k in τ_i with $i \in \{0, \dots, (\ell - 1) - k\}$ is defined for $k = 1$ as

$$B_{i,1,T}(t) := \begin{cases} \chi_{[\tau_i, \tau_{i+1})}(t) & i < (\ell - 1) - 1 \\ \chi_{[\tau_i, \tau_{i+1})}(t) & i = (\ell - 1) - 1 \end{cases}$$

and recursively for $k > 1$ as

$$B_{i,k,T}(t) := \frac{t - \tau_i}{\tau_{i+k-1} - \tau_i} B_{i,k-1,T}(t) + \frac{\tau_{i+k} - t}{\tau_{i+k} - \tau_{i+1}} B_{i+1,k-1,T}(t).$$

This recursive definition, also known as the DE BOOR-COX-MANSFIELD recursion formula, not only gives shape to the concept that has been discussed up until now, but also provides a convenient way to efficiently evaluate B-splines recursively, making it especially suitable for numerical implementations.

As a remark: When the knots τ_i and τ_{i+1} coincide, it holds for the indicator function $\chi_{[\tau_i, \tau_{i+1})} \equiv 0$, meaning the respective summand in the recursive formula of Definition 2.5 disappears. Without this knowledge, one might be tempted to assume that we are hitting a case of zero divided by zero in its coefficient.

Proposition 2.6 (B-spline properties). Let $k, \ell, m, p \in \mathbb{N}$ with $k \leq \ell - 1$, $p \in \{m, \dots, \ell - 1\}$ and $T := \{\tau_i\}_{i=0}^{\ell-1}$ with $\tau_0 = \dots = \tau_m \leq \dots \leq \tau_p = \dots = \tau_{\ell-1}$. It holds that

1. $\text{supp}(B_{i,k,T}) = [\tau_i, \tau_{i+k}]$,
2. $\forall t \in [\tau_0, \tau_{\ell-1}]: B_{i,k,T}(t) \geq 0$,
3. $\forall i \in \{0, \dots, \ell - 2\}: B_{i,k,T}|_{[\tau_i, \tau_{i+1})} \in \Pi_k$,
4. $\forall i \in \{0, \dots, (\ell - 1) - k\}: B_{i,k,T} \in \mathcal{C}^{k-2}([\tau_0, \tau_{\ell-1}])$.

Proof. See [dB01, IX (20)]. □

Another interesting property is that the evaluation of derivatives is also recursive in nature, similar to the DE BOOR-COX-MANSFIELD recursion formula.

Proposition 2.7 (B-spline derivatives). Let $k, \ell, m, p \in \mathbb{N}$ with $k \leq \ell - 1$, $p \in \{m, \dots, \ell - 1\}$ and $T := \{\tau_i\}_{i=0}^{\ell-1}$ with $\tau_0 = \dots = \tau_m \leq \dots \leq \tau_p = \dots = \tau_{\ell-1}$. It holds that

$$B'_{i,k,T}(t) = (k - 1) \cdot \left(\frac{B_{i,k-1,T}(t)}{\tau_{i+k-1} - \tau_i} - \frac{B_{i+1,k-1,T}(t)}{\tau_{i+k} - \tau_{i+1}} \right).$$

Proof. See [dB01, X (8)]. □

The obvious advantage is that we can not only efficiently evaluate B-splines themselves for a given grid, we can also do that for their derivatives, making it possible to work with derivatives in a way not possible with other means of modelling functions numerically

2. B-Splines

as easily and effectively. This is due to the recursive nature of B-splines, their compact support, smoothness and positivity, as we'll also see later in this thesis.

Before we can speak of B-splines as a basis though, we need to solve a remaining issue. Figure 2.1 shows all possible B-splines for varying k and indicates the problem: The number $\ell - k$ of B-splines on the grid decreases for increasing k , even though we want to have $k + \ell - 2$ basis functions, a number that is supposed to increase for increasing k . The solution is to just extend the knot vector in such a way that we conveniently match

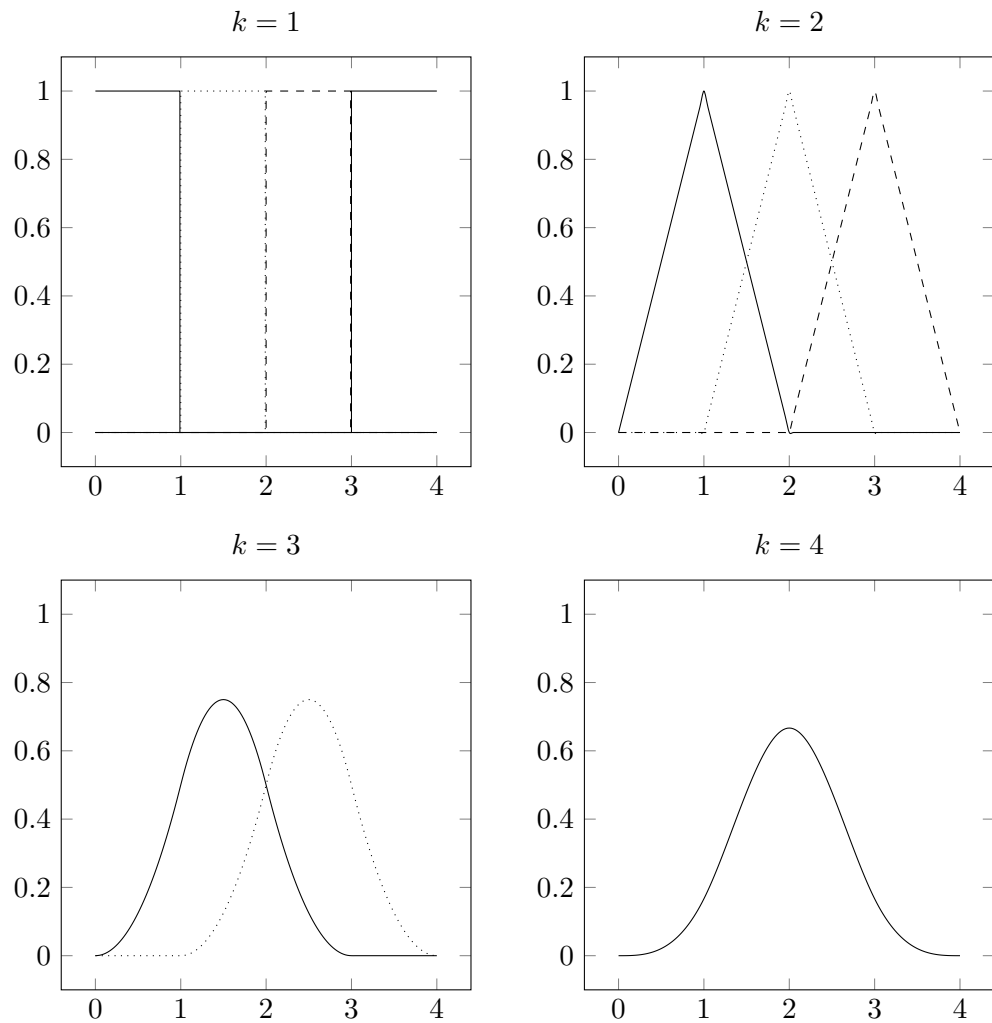


Figure 2.1.: Plots of all $\ell - k$ B-splines $B_{i,k,T}(t)$ for all possible $k \leq \ell - 1$ with the knot vector $T = \{0, 1, 2, 3, 4\}$ (hence $\ell = 5$) and $i \in \{0, \dots, (\ell - 1) - k\}$ (from left to right). With each increase of k the number of B-spline-functions is reduced by one.

the dimension of the spline function space, yielding the

Definition 2.8 (Extended knot vector). Let $k, \ell \in \mathbb{N}$ with $k \leq \ell - 1$ and $T := \{\tau_i\}_{i=0}^{\ell-1}$ with $\tau_0 < \dots < \tau_{\ell-1}$. The extended knot vector $\Delta_k(T)$ is defined with $n := k + \ell - 2$ as

$$\Delta_k(T) \ni: \delta_i := \begin{cases} \tau_0 & i \in \{0, \dots, k-1\} \\ \tau_{i-k+1} & i \in \{k, \dots, k+\ell-3\} = \{k, \dots, n-1\} \\ \tau_{\ell-1} & i \in \{k+\ell-2, \dots, 2 \cdot k + \ell - 3\} = \{n, \dots, n+k-1\}. \end{cases}$$

Intuitively, we repeat the first and last knot k times, and if we take a look at the resulting plots in Figure 2.2 we see that the number of B-splines on the extended grid matches the number of necessary basis functions for the spline function space. Granted, this argument does not yet prove that these B-splines based on the extended knot vector form a basis, but it should help to understand the motivation behind this step before we do that in the following

Theorem 2.9 (CURRY-SCHOENBERG). Let $k, \ell \in \mathbb{N}$ with $k \leq \ell - 1$ and $T := \{\tau_i\}_{i=0}^{\ell-1}$ with $\tau_0 < \dots < \tau_{\ell-1}$. It holds with $n := k + \ell - 2$ that

$$\Sigma_{k,T} = \text{span} \left(\left\{ B_{0,k,\Delta_k(T)}, \dots, B_{n-1,k,\Delta_k(T)} \right\} \right).$$

Proof. See [dB01, IX (44)]. □

With this knowledge we have reached our goal and found a basis for the spline function space. Given $\Sigma_{k,T}$ is a real vector space, it makes sense to define a mapping between it and coefficient vectors for the B-spline basis. In the following segment we make use of the results in Chapter A on the function space order \preceq and order-preserving isomorphisms.

Definition 2.10 (Coefficient spline mapping). Let $k, \ell \in \mathbb{N}$ with $k \leq \ell - 1$, $T := \{\tau_i\}_{i=0}^{\ell-1}$ with $\tau_0 < \dots < \tau_{\ell-1}$, $n := k + \ell - 2$ and $\mathbf{s} = (s_0, \dots, s_{n-1}) \in \mathbb{R}^n$. The coefficient spline mapping $\mathbb{B}_{k,T} : (\mathbb{R}^n, \preceq) \rightarrow (\Sigma_{k,T}, \preceq)$ is defined as

$$\mathbb{B}_{k,T}(\mathbf{s}) := \sum_{i=0}^{n-1} s_i \cdot B_{i,k,\Delta_k(T)}.$$

This mapping is both an isomorphism and preserves order, which we prove in the following

Proposition 2.11. Let $k, \ell \in \mathbb{N}$ with $k \leq \ell - 1$ and $T := \{\tau_i\}_{i=0}^{\ell-1}$ with $\tau_0 < \dots < \tau_{\ell-1}$. $\mathbb{B}_{k,T}$ is an order isomorphism of ordered vector-spaces (see Definition A.5).

Proof. This follows directly from Theorem 2.9 and $B_{i,k,\Delta_k(T)} \succeq 0$ for $i \in \{0, \dots, n := k + \ell - 2\}$ mentioned in Proposition 2.6. □

Setting the details aside, what one can take away from this result is that manipulations of B-spline functions can equivalently be expressed in terms of manipulations of their basis coefficients. In the context of optimization problems considered in Chapter 3, this enables us to formulate optimization problems in terms of B-spline basis coefficients.

2. B-Splines

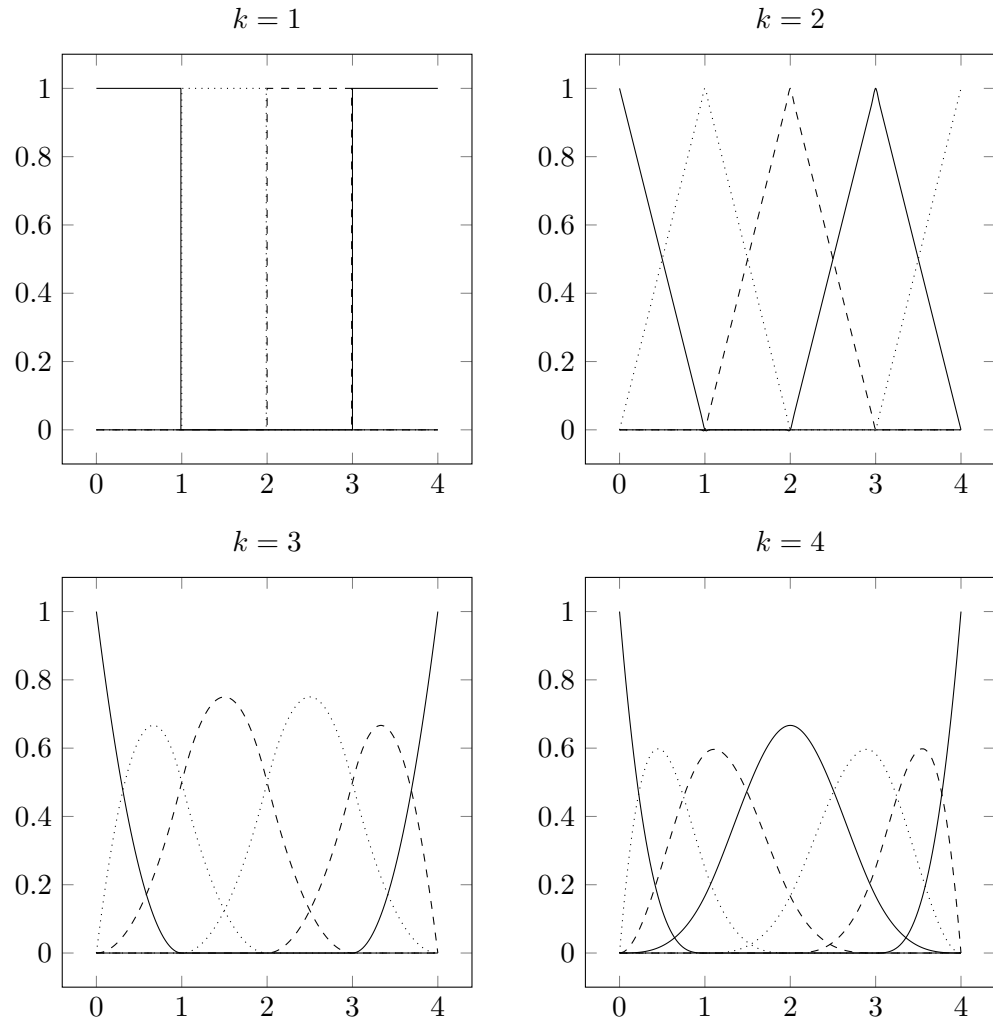


Figure 2.2.: Plots of all $k + \ell - 2$ B-splines $B_{i,k,\Delta_k(T)}(t)$ for all possible $k \leq \ell - 1$ with the extended knot vector $\Delta_k(T)$ with $T = \{0, 1, 2, 3, 4\}$ (hence $\ell = 5$) and $i \in \{0, \dots, (\ell - 1) - k\}$ (from left to right). With each increase of k the number of B-spline-functions increases by one, as desired.

From the numerical perspective, we want to find quality conditions with which we can compare two function space bases. One such aspect is orthogonality, which will be elaborated as follows. Consider \mathbb{R}^2 again with the standard basis $\{(1, 0)^T, (0, 1)^T\}$. This is an example for a so-called ‘orthogonal basis’, as these vectors are orthogonal to each other with regard to the EUCLIDEAN inner product. In turn, this means that in a basis decomposition, each basis vector only affects one entry of the resulting vector. In function spaces, which are also vector spaces, bases can also be orthogonal with regard to an inner product. A more general approach though is the concept of a basis to be ‘locally linearly independent’. This means that each basis function only affects a small area of the interval the function operates on (i.e. the function has local support). Thus, in turn, if one seeks to find fitting coefficients for each basis function to best approximate a given set of discrete datapoints, a locally linearly independent basis ensures that each coefficient is only affected by datapoints within that small area (which corresponds to the support of each basis function). A closely related concept is that of the well-conditioned basis, where we can relate the norm of the basis coefficients with the norm of the resulting function.

Proposition 2.12 (Well-conditioned basis). *Let $k, \ell \in \mathbb{N}$ with $k \leq \ell - 1$, $T := \{\tau_i\}_{i=0}^{\ell-1}$ with $\tau_0 < \dots < \tau_{\ell-1}$, $n := k + \ell - 2$ and $\mathbf{s} = (s_0, \dots, s_{n-1}) \in \mathbb{R}^n$. There exists $c_{k,2} \in (0, 1)$ (only depending on k) such that*

$$c_{k,2} \cdot \|\mathbf{s}\|_2 \leq \left\| \mathbb{B}_{k,\Delta_k(T)}(\mathbf{s}) \right\|_2 \leq \|\mathbf{s}\|_2.$$

Proof. It follows from [dB01, XI (8)] that there exists $c_{k,\infty} \in (0, 1)$ with

$$c_{k,\infty} \cdot \|\mathbf{s}\|_\infty \leq \left\| \mathbb{B}_{k,\Delta_k(T)}(\mathbf{s}) \right\|_\infty \leq \|\mathbf{s}\|_\infty.$$

Given that $\left\| \mathbb{B}_{k,\Delta_k(T)}(\mathbf{s}) \right\|_2 \leq \left\| \mathbb{B}_{k,\Delta_k(T)}(\mathbf{s}) \right\|_\infty$ and all norms are equivalent on \mathbb{R}^n the proposition follows. \square

This implies that if there are small disturbances in the B-spline-coefficients it only leads to small disturbances in the spline functions themselves, further underlining that B-splines are a good choice for numerical applications. Another result of this proposition is that we can find an upper and lower bound for the supremum norm of a given spline function by the supremum norm of its coefficient vector.

Another interesting observation is the

Proposition 2.13 (partition of unity). *Let $k, \ell \in \mathbb{N}$ with $k \leq \ell - 1$ and $T := \{\tau_i\}_{i=0}^{\ell-1}$ with $\tau_0 < \dots < \tau_{\ell-1}$. It holds with $n := k + \ell - 2$ that*

$$\mathbb{B}_{k,T}((1, \dots, 1)) := \sum_{i=0}^{n-1} B_{i,k,\Delta_k(T)} = 1$$

Proof. See [dB01, IX (36)]. \square

2. B-Splines

Remark 2.14. *The particular form of the extended knot vector according to Definition 2.8 is considered to be fixed in this thesis. To simplify notation and bring the focus on the topic at hand instead of technicalities we will write Σ_k , $B_{i,k}$ and \mathbb{B}_k instead of $\Sigma_{k,T}$, $B_{i,k,\Delta_k(T)}$ and $\mathbb{B}_{k,\Delta_k(T)}$. We just fix the chosen spline knot vector T and assume that in the contexts it is used in it has been well-chosen. This assumption is not hard to make, given when we prove statements with the general variables k, ℓ and $n := k + \ell - 2$ we do not lose generality even if we ignore T 's exact form.*

With the results of this section, we can take a look at other function space bases and argue why they were not used in this thesis. One possible choice are ‘orthogonal polynomials’. Orthogonality simplifies data fitting, but it comes at the cost of numerical behaviour with potentially high polynomial degrees. The many possible choices of orthogonal polynomials also require deeper analysis of the matter than what fits within the scope of this thesis.

Another possible alternative choice are ‘radial basis functions’ (RBF), which have been diversely explored in the context of EMD (see for example [YYJ12] and [LWW13]). They are the other extreme compared to orthogonal polynomials in terms of orthogonality, as each basis function spans across the entire interval. Additionally, they do not present a locally linearly independent basis, which can be at the cost of numerical stability. Given the many choices of radial functions it is also difficult to evaluate the quality of each choice. Numerically, due to their non-locality, they yield hard to handle full rank matrices when used as function bases, which do not scale well for larger problems. Due to the depth of this matter RBFs will not be investigated further in this thesis.

3. Empirical Mode Decomposition Model and Analysis

As already introduced in Chapter 1 we may consider one step of the empirical mode decomposition as an optimization problem over the set of intrinsic mode functions. For a given signal s the cost function might relate to the amount of residual $r := s - u$ left for a given candidate function u , yielding for instance a problem of the form

$$\begin{aligned} \inf_u \quad & \|s - u\|_2^2 \\ \text{s.t.} \quad & u \text{ IMF.} \end{aligned} \tag{3.1}$$

In this chapter, we will only focus on optimization problems of this kind, namely the extraction of a single IMF (that we formally introduce later) from an input signal using a cost function of some kind. The EMD method follows by iteratively using the residual of the previous step as the input signal for the next step.

The objective of this chapter is to clarify what the set of intrinsic mode functions is. During this process we generalize the concept for arbitrary cost functions satisfying convex-likeness, which is a weaker form of convexity. Our goal is to find useful properties for this underlying optimization problem. This could bring useful results and be a step forward for the theoretical analysis of the empirical mode decomposition and be a guide for the development of new heuristic methods.

3.1. Intrinsic Mode Functions

The fundamental building blocks of the empirical mode decomposition are intrinsic mode functions (IMFs) $u(t)$ of the form

$$u(t) := a(t) \cos(\phi(t)), \tag{3.2}$$

where $a(t)$ and $\phi(t)$ satisfy certain conditions we will lay out later. One can imagine an intrinsic mode function to be a wave of varying frequency that is enveloped by a varying amplitude, as shown in Figure 3.1. We can see that for given $a(t)$ and $\phi(t)$ the intrinsic mode function $u(t)$ in Equation (3.2) is fully described. It follows that the real objects of interest are $a(t)$ and $\phi(t)$, especially in regard to conditions we want them to satisfy such that the corresponding IMF has meaningful properties.

The approach we take in this thesis is novel: We represent an IMF as a function pair $(a(t), \phi(t))$ satisfying a set of IMF conditions instead of defining an IMF as a function of analytical form $a(t) \cdot \cos(\phi(t))$, where $a(t)$ and $\phi(t)$ have certain properties. The crucial

3. Empirical Mode Decomposition Model and Analysis

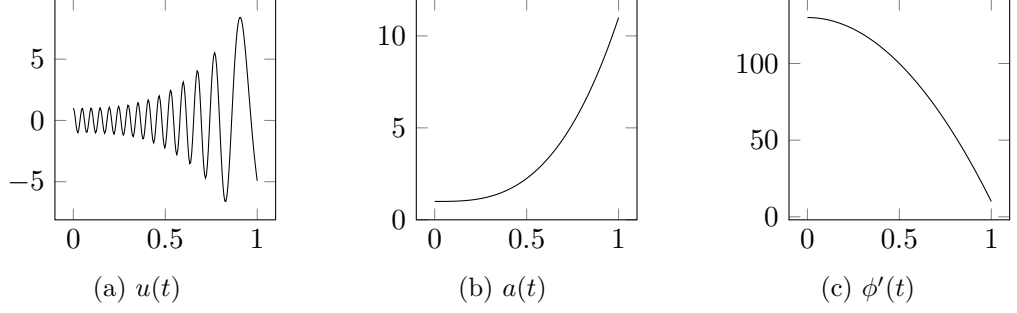


Figure 3.1.: An intrinsic mode function $u(t) := a(t) \cdot \cos(\phi(t))$ with its instantaneous amplitude $a(t)$ and frequency $\phi'(t)$.

advantage of the new approach compared to the classic one is that the components $a(t)$ and $\phi(t)$ are ‘graspable’ rather than hidden within the IMF itself. A central objective of this chapter is thus to find a way to extract $a(t)$ and ϕ from an IMF $u(t)$. As we consider optimization problems over IMFs we need to enforce the IMF conditions in some way, which requires knowledge of $a(t)$ and $\phi(t)$. This should not be dependent on such an extraction process until later.

Given the central role of the pair $(a(t), \phi(t))$ for an IMF $u(t)$ we call it the ‘soul’ of the intrinsic mode function and define it as follows.

Definition 3.1 (Intrinsic mode function soul (IMFS)). *Let $\mu_0, \mu_1, \mu_2 > 0$. The pair $(a, \phi) \in \mathcal{C}^1(\mathbb{R}, \mathbb{R}) \times \mathcal{C}^2(\mathbb{R}, \mathbb{R})$ is an intrinsic mode function soul (IMFS) with characteristic (μ_0, μ_1, μ_2) if and only if*

$$0 \preceq a \tag{3.3}$$

$$\mu_0 \preceq \phi' \tag{3.4}$$

$$|a'| \preceq \mu_1 \cdot |\phi'| \tag{3.5}$$

$$|\phi''| \preceq \mu_2 \cdot |\phi'| \tag{3.6}$$

hold. We define the set of IMFSs as $\mathcal{S}_{\mu_0, \mu_1, \mu_2}$ and call a the instantaneous amplitude, ϕ the instantaneous phase and ϕ' the instantaneous frequency.

The above definition is not arbitrary. To put it into context with physical reality and other publications, we give the following remarks.

Remark 3.2 (Constraint motivations). *The motivations for Equations (3.3) and (3.4) are to ensure that both instantaneous amplitude and phase have physical meaning, i.e. no negative amplitude and strictly positive frequency (as the derivative of the phase is the frequency). We introduce μ_0 rather than demanding $0 \preceq \phi'$ so we are only dealing with non-strict inequality constraints (i.e. \preceq instead of \prec).*

Equations (3.5) and (3.6) are there to ensure a slowly varying instantaneous amplitude and frequency respectively, as we want each intrinsic mode function that is extracted to remain within a certain scope. The exact nature of this scope depends on the type of application and can be shaped with the parameters.

Remark 3.3 (relationship with [DLW11]). *Definition 3.1 is based on [DLW11, Definition 3.1], but generalizes it in certain aspects by introducing an arbitrary lower bound μ_0 for the frequency and generalizing the single parameter ϵ (called ‘accuracy’) in [DLW11] into two separate parameters μ_1 and μ_2 that are part of the characteristic. The latter generalization allows a more fine-grained control of the rate of change of the amplitude and frequency respectively over time without any trade-offs, which is further elaborated in Remark 3.8.*

One part of the definition, namely that the infimum of ϕ' shall be bounded, was left out given there is no practical reason for this condition. Given $\phi \in \mathcal{C}^2(\mathbb{R}, \mathbb{R})$ this would imply that $\phi'(t)$ should have finite limits for $t \rightarrow \pm\infty$. As we can see for instance with the IMF $\cos(t^2)$ with soul $(a, \phi) = (1, t^2)$, and $\phi'(t) = 2t$ in particular, there would be no such simple way to represent this simple case with the definition given in [DLW11].

Remark 3.4 (use of modulus). *Equations (3.5) and (3.6) state $|\phi'|$ instead of ϕ' , even though $\phi' \preceq \mu_0 < 0$ is guaranteed by Equation (3.4). This is for reasons of consistency with the literature (e.g. [DLW11]) that chooses the same form despite the guarantee.*

For examples and further motivation on the IMF characteristic, which is more fitting in the chapters on application, see Subsection 5.4.7 and Section 5.5.

The pair (a, ϕ) itself may perfectly represent the IMF properties, but we also need to evaluate the IMF to, for instance, assess how much residual $r(t) = s(t) - u(t)$ is left with a given candidate pair (a, ϕ) . For this purpose, we define the evaluation as an operator on $\mathcal{S}_{\mu_0, \mu_1, \mu_2}$ as follows.

Definition 3.5 (Intrinsic mode function operator). *Let $\mu_0, \mu_1, \mu_2 > 0$ and $(a, \phi) \in \mathcal{S}_{\mu_0, \mu_1, \mu_2}$. The intrinsic mode function operator is defined as*

$$\mathcal{I}[a, \phi](t) := a(t) \cdot \cos(\phi(t)).$$

One has to keep in mind that for a given IMF, there may be multiple souls that can generate it. This is elaborated in the following

Remark 3.6 (IMF soul non-uniqueness). *Consider the IMF*

$$u(t) := (1 + 2t) \cdot \cos(2\pi t) \cdot \cos(4\pi t)$$

on the interval $[0, 1]$. This can either be interpreted as $u = \mathcal{I}[a, \phi]$ with

$$\begin{aligned} a(t) &:= (1 + 2t) \cdot \cos(2\pi t), \\ \phi(t) &:= 4\pi t, \end{aligned}$$

or as $u = \mathcal{I}[\tilde{a}, \tilde{\phi}]$ with

$$\begin{aligned} \tilde{a} &:= (1 + 2t) \cdot \cos(4\pi t), \\ \tilde{\phi} &:= 2\pi t. \end{aligned}$$

One can possibly exclude such double cases by varying the parameters μ_0 , μ_1 and μ_2 of the IMFS set (see Definition 3.1), excluding possible other candidates by varying the boundaries, but this is a heuristical approach and won't be further elaborated here.

3. Empirical Mode Decomposition Model and Analysis

Another important aspect is one of information theoretical nature.

Remark 3.7 (Information theory). *If you consider the information content going from (a, ϕ) to the IMF $\mathcal{I}(a, \phi)$, the IMF operator may present cases where information is destroyed. In other words, in such a case it becomes impossible to reconstruct a or ϕ from an IMF that was previously generated from them. Two examples of such cases can be found in Figure 3.2. They are almost exclusively due to the fact that amplitude and phase vary almost equally fast.*

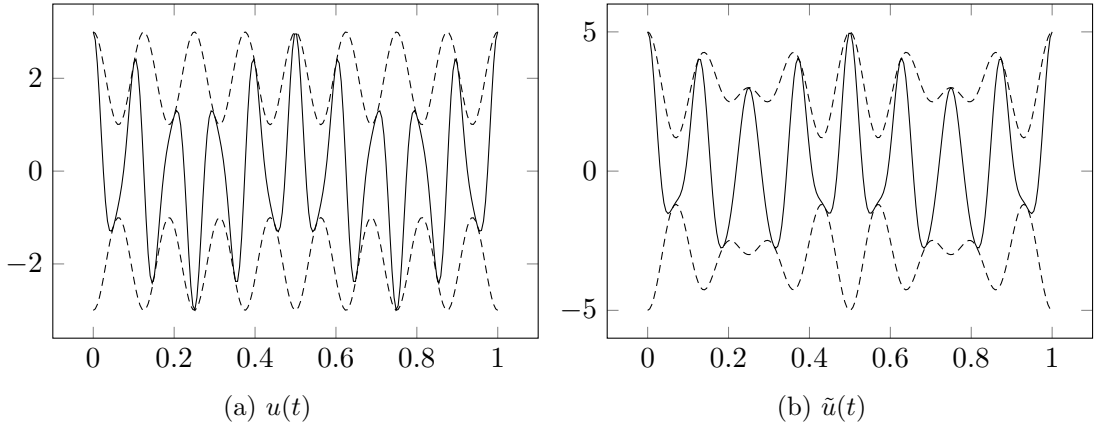


Figure 3.2.: Two intrinsic mode functions u and \tilde{u} (solid), where each is unable to reflect its instantaneous amplitude (dashed) because its rate of change is almost equal to the instantaneous frequency. This example was adapted from [HYY15, Figure 2].

One can deduce from this observation that when extracting a and ϕ from an IMF, it is likely that $\mu_1 \ll 1$ and $\mu_2 \ll 1$ hold, i.e. that amplitude and phase vary slowly relative to each other (and not destroy each other's information content). However, as given in the example in Figure 3.2, the ground truth can of course still contain more information than what remains after applying the intrinsic mode function operator to it. For natural inputs, the ground truth is not known. Thus, such cases are more of a philosophical aspect of this derivation and reflect the analytical nature of the set of IMF souls compared to the practical nature of the IMF itself.

See [HYY15] for a discussion of more of such pathological cases and [DLW11, Definition 3.1] for further reading. We note here though that any attempt to 'fix' such cases makes little sense given one can not create information from nothing.

We will now focus on the parameters μ_0 , μ_1 and μ_2 of the set of IMF souls and the role they play when judging the quality of an extracted IMF.

Remark 3.8 (Characteristic). *The IMFS characteristic defined in Definition 3.1 is a generalization of the IMF accuracy introduced in [DLW11, Definition 3.1], which only employs a single parameter $\varepsilon > 0$ for both μ_1 and μ_2 . This is a disadvantageous limitation for approaches aiming to only have slowly varying amplitude or frequency while*

3.1. Intrinsic Mode Functions

not particularly limiting the behaviour of the respective other. The parameter μ_0 was added as a lower frequency bound. This conveniently eliminates the strict inequality constraint $0 \prec \phi'$ from the original definition, which would complicate the theoretical analysis unnecessarily with no added benefit.

Naturally, for a given IMFS we can calculate the characteristic (μ_0, μ_1, μ_2) with

$$\begin{aligned}\mu_0 &= \inf_{t \in \mathbb{R}} \phi'(t), \\ \mu_1 &= \sup_{t \in \mathbb{R}} \left| \frac{a'(t)}{\phi'(t)} \right|, \\ \mu_2 &= \sup_{t \in \mathbb{R}} \left| \frac{\phi''(t)}{\phi'(t)} \right|.\end{aligned}$$

This makes it possible to assess its relative quality and ascertain conditions on its characteristic. This idea is later further explored in the toolbox (see Subsection 5.4.7).

Now that we have formally defined intrinsic mode functions and put them into the context of physical reality and [DLW11], we return to our original optimization problem in Equation (3.1) and express it in terms of our newly defined set of IMFSs. We obtain the following optimization problem.

$$\begin{aligned}\min_u \quad & \|s - \mathcal{I}[a, \phi]\|_2^2 \\ \text{s.t.} \quad & (a, \phi) \in \mathcal{S}_{\mu_0, \mu_1, \mu_2}\end{aligned}\tag{3.7}$$

In the ideal case this would be a convex optimization problem. This means that both the cost function and the candidate set are convex (according to Definitions B.2 and B.1) and we have a global minimum. Given we will later look at cost functions the first step is to see if our candidate set is convex. We show that in the following

Theorem 3.9. *Let $\mu_0, \mu_1, \mu_2 \geq 0$. $\mathcal{S}_{\mu_0, \mu_1, \mu_2}$ is convex according to Definition B.1.*

Proof. Let $(a_1, \phi_1), (a_2, \phi_2) \in \mathcal{S}_{\mu_0, \mu_1, \mu_2}$ and $q \in [0, 1]$. We define an element on the path between (a_1, ϕ_1) and (a_2, ϕ_2) as

$$(a_\star, \phi_\star) := (a_1, \phi_1) + q \cdot [(a_2, \phi_2) - (a_1, \phi_1)] = (1 - q) \cdot (a_1, \phi_1) + q \cdot (a_2, \phi_2).$$

Component-wise, we obtain

$$a_\star = (1 - q) \cdot a_1 + q \cdot a_2$$

and

$$\phi_\star = (1 - q) \cdot \phi_1 + q \cdot \phi_2.$$

We now show that (a_\star, ϕ_\star) satisfies the conditions from Definition 3.1:

1. We note from Equation (3.3) that $a_1 \succeq 0$ and $a_2 \succeq 0$ and follow $a_\star = (1 - q) \cdot a_1 + q \cdot a_2 \succeq (1 - q) \cdot 0 + q \cdot 0 = 0$.

3. Empirical Mode Decomposition Model and Analysis

2. We note from Equation (3.4) that $\phi'_1 \succeq \mu_0$ and $\phi'_2 \succeq \mu_0$ and follow

$$\phi'_\star = (1 - q) \cdot \phi'_1 + q \cdot \phi'_2 \succeq (1 - q) \cdot \mu_0 + q \cdot \mu_0 = \mu_0$$
3. We note from Equations (3.4) and (3.5) that $\phi'_1 \succeq \mu_0 \succeq 0$, $\phi'_2 \succeq \mu_0 \succeq 0$, $|a'_1| \preceq \mu_1 \cdot |\phi'_1|$ and $|a'_2| \preceq \mu_1 \cdot |\phi'_2|$ and follow

$$|a'_\star| = |(1 - q) \cdot a'_1 + q \cdot a'_2| \preceq (1 - q) \cdot |a'_1| + q \cdot |a'_2| \preceq \mu_1 \cdot ((1 - q) \cdot |\phi'_1| + q \cdot |\phi'_2|) \preceq \mu_1 \cdot |(1 - q) \cdot \phi'_1 + q \cdot \phi'_2| = \mu_1 \cdot |\phi'_\star|$$
4. We note from Equations (3.4) and (3.6) that $\phi'_1 \succeq \mu_0 \succeq 0$, $\phi'_2 \succeq \mu_0 \succeq 0$, $|\phi''_1| \preceq \mu_2 \cdot |\phi'_1|$ and $|\phi''_2| \preceq \mu_2 \cdot |\phi'_2|$ and follow

$$|\phi''_\star| = |(1 - q) \cdot \phi''_1 + q \cdot \phi''_2| \preceq (1 - q) \cdot |\phi''_1| + q \cdot |\phi''_2| \preceq \mu_2 \cdot ((1 - q) \cdot |\phi'_1| + q \cdot |\phi'_2|) = \mu_2 \cdot |(1 - q) \cdot \phi'_1 + q \cdot \phi'_2| = \mu_2 \cdot |\phi'_\star|$$

It follows that $(a_\star, \phi_\star) \in \mathcal{S}_{\mu_0, \mu_1, \mu_2}$ and thus $\mathcal{S}_{\mu_0, \mu_1, \mu_2}$ is convex. \square

Up to this point we have defined $\mathcal{S}_{\mu_0, \mu_1, \mu_2}$ as a set of function pairs. Let us reconsider the results of Chapters 2 and A: We introduced a way to relate functions to each other and showed that the one-to-one relation of spline functions and their B-spline basis coefficients preserves that order. It thus becomes logical to use this relation and express intrinsic mode function souls as a set of pairs of vectors in \mathbb{R}^n . Their entries correspond to B-spline basis coefficients of the spline functions describing instantaneous amplitude and phase.

Definition 3.10 (Intrinsic mode spline function soul (IMSpFS)). *Let $\mu_0, \mu_1, \mu_2 > 0$ and $k \geq 4$ (for derivability). The pair $(\mathbf{a}, \phi) \in \mathbb{R}^n \times \mathbb{R}^n$ is an intrinsic mode spline function soul (IMSpFS) if and only if*

$$0 \preceq \mathbb{B}_k(\mathbf{a}) \tag{3.8}$$

$$\mu_0 \preceq \mathbb{B}'_k(\phi) \tag{3.9}$$

$$|\mathbb{B}'_k(\mathbf{a})| \preceq \mu_1 \cdot |\mathbb{B}'_k(\phi)| \tag{3.10}$$

$$|\mathbb{B}''_k(\phi)| \preceq \mu_2 \cdot |\mathbb{B}'_k(\phi)| \tag{3.11}$$

hold. We define the set of IMSpFSs as $\mathcal{S}_{\mu_0, \mu_1, \mu_2}$.

It becomes apparent that by using this reformulation the handling of IMF souls merely as vectors instead of function pairs is much simpler. What follows from Theorem 3.9 is that, given the relation between B-splines and their coefficients is order-preserving, the set of IMSpFS's is also convex.

3.2. Cost Functions

Having obtained the result in Theorem 3.9, if we now find a convex cost function that meaningfully judges an intrinsic mode function soul relative to an input signal we would have solved the problem of building a convex EMD optimization problem. This is because we have already shown that the set of IMF souls is convex. Together with a convex cost

function we would then obtain a convex optimization problem. The search for such a convex cost function will not be within the scope of this thesis as it might require adding more constraints to the set of IMFSs or a completely different approach altogether. Instead, we will take a look at cost functions from [PH08] and [PH10] that are well-established and have a strong footing within the classic EMD theory.

We have until now only looked at the nature of intrinsic mode functions and not how we can actually express which fits our input signal the best. Each step of the empirical mode decomposition applies to an input signal $s(t)$, which we want to split up into an intrinsic mode function $u(t)$ and residual function $r(t)$. To determine the split we want to minimize the ‘cost’ a split-up of a signal $s(t)$ into an IMF $u(t)$ and residual $r(t)$ has. This cost should be relative to the quality of extraction. There are obviously many possible ways to define such an EMD cost function and we will explore this topic in the following section.

The final goal is to generalize the optimization problem in Equation 3.7 for an arbitrary cost function later.

3.2.1. Canonical

The simplest idea for an EMD cost function is to look at the residual, as it corresponds to the classic EMD approach proposed in [HSL⁺98] and is formally used in [PH08] and [PH10]. This makes the residual approach the most common idea for an EMD cost function in the literature. The smaller the difference between the signal and intrinsic mode function, the less the cost. That is because we have then extracted as much from the signal as possible. Additionally, as we will later see in Section 3.2.2, it is the basis for derived EMD cost functions in the context of more advanced separation techniques.

Definition 3.11 (Canonical EMD cost function). *Let $\mu_0, \mu_1, \mu_2 > 0$ and $s \in \mathcal{C}^0(\mathbb{R}, \mathbb{R})$. The canonical EMD cost function $c_1[s]: \mathcal{S}_{\mu_0, \mu_1, \mu_2} \rightarrow \mathbb{R}$ is defined as*

$$c_1[s](a, \phi) := \|s - \mathcal{I}(a, \phi)\|_2^2 = \|s - a \cdot \cos(\phi)\|_2^2.$$

Just as with the set of IMFSs we can also formulate the EMD cost function in terms of B-splines. We do that by expressing it as a function over $\mathcal{S}_{\mu_0, \mu_1, \mu_2}$ (see Definition 3.10) instead of $\mathcal{S}_{\mu_0, \mu_1, \mu_2}$. This makes it possible to examine its convexity as introduced in Chapter B.

Definition 3.12 (Canonical spline EMD cost function). *Let $\mu_0, \mu_1, \mu_2 > 0$, $k \geq 4$ (for derivability) and $\mathbf{s} \in \mathbb{R}^n$. The canonical spline EMD cost function $\mathbf{c}_1[\mathbf{s}]: \mathcal{S}_{\mu_0, \mu_1, \mu_2} \rightarrow \mathbb{R}$ is defined as*

$$\mathbf{c}_1[\mathbf{s}](\mathbf{a}, \phi) := c_1[\mathbb{B}_k(\mathbf{s})](\mathbb{B}_k(\mathbf{a}), \mathbb{B}_k(\phi)).$$

According to the motivation laid out earlier, we want this cost function to be convex.

Proposition 3.13. *The canonical spline EMD cost function $\mathbf{c}_1[\mathbf{s}]$ is not convex in (\mathbf{a}, ϕ) according to Definition B.2.*

3. Empirical Mode Decomposition Model and Analysis

Proof. We approach this proof by checking if the requirements of Theorem B.7 hold for distinct partial derivatives for entries of \mathbf{a} and $\boldsymbol{\phi}$. We begin with \mathbf{a} and first calculate the entries of the Hessian matrix $H_{\mathbf{c}_1[\mathbf{s}]}(\mathbf{a})$, which means that we consider $\mathbf{c}_1[\mathbf{s}](\mathbf{a}, \boldsymbol{\phi})$ to only vary in \mathbf{a} . We first note that it holds

$$\begin{aligned} \mathbf{c}_1[\mathbf{s}](\mathbf{a}, \boldsymbol{\phi}) &= c_1[\mathbb{B}_k(\mathbf{s})](\mathbb{B}_k(\mathbf{a}), \mathbb{B}_k(\boldsymbol{\phi})) \\ &= \|\mathbb{B}_k(\mathbf{s}) - \mathcal{I}(\mathbb{B}_k(\mathbf{a}), \mathbb{B}_k(\boldsymbol{\phi}))\|_2^2 \\ &= \|\mathbb{B}_k(\mathbf{s}) - \mathbb{B}_k(\mathbf{a}) \cdot \cos(\mathbb{B}_k(\boldsymbol{\phi}))\|_2^2 \\ &= \int_{-\infty}^{\infty} \left[\mathbb{B}_k(\mathbf{s}) - \left(\sum_{i=0}^{n-1} a_i \cdot B_{i,k}(t) \right) \cdot \cos \left(\sum_{i=0}^{n-1} \phi_i \cdot B_{i,k}(t) \right) \right]^2 dt \end{aligned}$$

and can deduce for $m, p \in \{0, \dots, n-1\}$

$$\begin{aligned} \frac{\partial \mathbf{c}_1[\mathbf{s}]}{\partial a_m}(\mathbf{a}, \boldsymbol{\phi}) &= \int_{-\infty}^{\infty} (-2) \cdot \left[\mathbb{B}_k(\mathbf{s}) - \left(\sum_{i=0}^{n-1} a_i \cdot B_{i,k}(t) \right) \cdot \cos(\mathbb{B}_k(\boldsymbol{\phi})(t)) \right] \cdot \\ &\quad B_{m,k}(t) \cdot \cos(\mathbb{B}_k(\boldsymbol{\phi})(t)) dt \\ &= \int_{-\infty}^{\infty} (-2) \cdot B_{m,k}(t) \cdot \cos(\mathbb{B}_k(\boldsymbol{\phi})(t)) \cdot \\ &\quad \left[\mathbb{B}_k(\mathbf{s}) - \left(\sum_{i=0}^{n-1} a_i \cdot B_{i,k}(t) \right) \cdot \cos(\mathbb{B}_k(\boldsymbol{\phi})(t)) \right] dt, \end{aligned}$$

and consequently as $\forall i \in \{0, \dots, n-1\} : B_{i,k} \succeq 0$

$$\frac{\partial^2 \mathbf{c}_1[\mathbf{s}]}{\partial a_m \partial a_p}(\mathbf{a}, \boldsymbol{\phi}) = \int_{-\infty}^{\infty} 2 \cdot B_{m,k}(t) \cdot B_{p,k}(t) \cdot \cos^2(\mathbb{B}_k(\boldsymbol{\phi})(t)) dt \geq 0. \quad (3.12)$$

Our Hessian matrix is of the form

$$H_{\mathbf{c}_1[\mathbf{s}]}(\mathbf{a}, \boldsymbol{\phi}) = \left(\frac{\partial^2 \mathbf{c}_1[\mathbf{s}]}{\partial a_m \partial a_p}(\mathbf{a}, \boldsymbol{\phi}) \right)_{(m,p) \in \{1, \dots, n\}^2},$$

and we now check the conditions for Theorem B.7. Symmetry follows immediately because the order of partial differentiation does not matter for continuously-differentiable functions. What is left to show for convexity is that the diagonal entries are strictly positive and the matrix is diagonally dominant. We know from Equation (3.12) that

$$\frac{\partial^2 \mathbf{c}_1[\mathbf{s}]}{\partial a_m \partial a_m}(\mathbf{a}, \boldsymbol{\phi}) = \int_{-\infty}^{\infty} 2 \cdot B_{m,k}^2(t) \cdot \cos^2(\mathbb{B}_k(\boldsymbol{\phi})(t)) dt > 0,$$

which means that the diagonal entries are positive. To show that the matrix is diagonally dominant, we first note that Equation (3.12) shows that all entries of the Hessian matrix

are positive and we thus only have to consider the sum of non-diagonal entries without applying the modulus. It holds due to Proposition 2.13

$$\begin{aligned}
 \sum_{\substack{p=0 \\ p \neq m}}^{n-1} \frac{\partial^2 \mathbf{c}_1[\mathbf{s}]}{\partial a_m \partial a_p}(\mathbf{a}, \phi) &= \sum_{\substack{p=0 \\ p \neq m}}^{n-1} \int_{-\infty}^{\infty} 2 \cdot B_{m,k}(t) \cdot B_{p,k}(t) \cdot \cos^2(\mathbb{B}_k(\phi)(t)) dt \\
 &= \int_{-\infty}^{\infty} 2 \cdot B_{m,k}(t) \cdot \left(\sum_{\substack{p=0 \\ p \neq m}}^{n-1} B_{p,k}(t) \right) \cdot \cos^2(\mathbb{B}_k(\phi)(t)) dt \\
 &= \int_{-\infty}^{\infty} 2 \cdot B_{m,k}(t) \cdot (1 - B_{m,k}(t)) \cdot \cos^2(\mathbb{B}_k(\phi)(t)) dt \\
 &\not\leq \int_{-\infty}^{\infty} 2 \cdot B_{m,k}(t) \cdot B_{m,k}(t) \cdot \cos^2(\mathbb{B}_k(\phi)(t)) dt \\
 &= \sum_{\substack{p=0 \\ p \neq m}}^{n-1} \frac{\partial^2 \mathbf{c}_1[\mathbf{s}]}{\partial a_m \partial a_m}(\mathbf{a}, \phi).
 \end{aligned}$$

We have shown that the Hessian matrix is symmetric and has strictly positive diagonal elements, however, it is not diagonally dominant. With Theorem B.7 alone we can thus not conclude that the Hessian matrix is positive definite. The Theorem of GERŠGORIN-HADAMARD is by no means exhaustive, but one of the most precise methods for this task, which means that the assumption that this matrix is not positive definite is well-founded and we can state that the canonical cost function is not convex in \mathbf{a} .

We now proceed with ϕ . Using the cosine sum formula we obtain

$$\begin{aligned}
 \frac{\partial \mathbf{c}_1[\mathbf{s}]}{\partial \phi_m}(\mathbf{a}, \phi) &= \int_{-\infty}^{\infty} (-2) \cdot \left[\mathbb{B}_k(\mathbf{s}) - \mathbb{B}_k(\mathbf{a})(t) \cdot \cos\left(\sum_{i=0}^{n-1} \phi_i \cdot B_{i,k}(t)\right) \right] \cdot \\
 &\quad \mathbb{B}_k(\mathbf{a})(t) \cdot B_{m,k}(t) \cdot (-1) \cdot \sin\left(\sum_{i=0}^{n-1} \phi_i \cdot B_{i,k}(t)\right) dt \\
 &= \int_{-\infty}^{\infty} 2 \cdot \mathbb{B}_k(\mathbf{a})(t) \cdot B_{m,k}(t) \cdot \sin\left(\sum_{i=0}^{n-1} \phi_i \cdot B_{i,k}(t)\right) \cdot \\
 &\quad \left[\mathbb{B}_k(\mathbf{s}) - \mathbb{B}_k(\mathbf{a})(t) \cdot \cos\left(\sum_{i=0}^{n-1} \phi_i \cdot B_{i,k}(t)\right) \right] dt,
 \end{aligned}$$

3. Empirical Mode Decomposition Model and Analysis

and consequently

$$\begin{aligned} \frac{\partial^2 \mathbf{c}_1[\mathbf{s}]}{\partial \phi_m \partial \phi_p}(\mathbf{a}, \phi) &= \int_{-\infty}^{\infty} 2 \cdot \mathbb{B}_k(\mathbf{a})(t) \cdot B_{m,k}(t) \cdot B_{p,k}(t) \cdot \cos\left(\sum_{i=0}^{n-1} \phi_i \cdot B_{i,k}(t)\right) \cdot \\ &\quad \left[\mathbb{B}_k(\mathbf{s}) - \mathbb{B}_k(\mathbf{a})(t) \cdot \cos\left(\sum_{i=0}^{n-1} \phi_i \cdot B_{i,k}(t)\right) \right] + \\ &\quad 2 \cdot \mathbb{B}_k(\mathbf{a})(t)^2 \cdot B_{m,k}(t) \cdot B_{p,k}(t) \cdot \sin^2\left(\sum_{i=0}^{n-1} \phi_i \cdot B_{i,k}(t)\right) dt. \end{aligned}$$

As we can see in this expression, especially if we look at diagonal entries with $p = m$, they are not strictly positive given the oscillating cosine terms and we can not apply Theorem B.7. Granted, only because we can not apply it does not mean that the Hessian matrix corresponding to ϕ is not positive semidefinite. The critical argument that leads to this conclusion though is that the sign is arbitrarily controlled by the unrelated parameter \mathbf{a} such that there is always a way to find a counterexample for some \mathbf{a} such that the Hessian matrix for ϕ is not positive definite. In total, we thus find no general convexity property for ϕ . \square

The result of this proposition clearly shows that, at least with this class of cost functions, the search for a truly convex optimization problem leads to a dead end. Convexity only makes sense if it applies to the entire function for all mixed second partial derivatives (even between amplitude and phase). Only showing it for a subset of the parameters, in our case the amplitude \mathbf{a} , is not of much use. However, it shows the approach that must be taken to analyze future candidates for such cost functions. Considering what we've seen in the last proof and how close we were to convexity, we can imply that such candidates will also yield diagonally dominant symmetric Hessian matrices, and the only real aspect that will matter is the strict positivity of the diagonal entries.

However, not all is lost only because we have not shown convexity, and we will go an alternative path in Section 3.4 using the theory of convex-likeness to show some useful properties. In the long run though, the residual-approach might have to be overthought and completely novel approaches developed, for instance ones making use of information theory with the goal of maximum information extraction in each step.

Unfortunately, this is not easy and probably even impossible, given we actually need to evaluate the intrinsic mode function itself to assess the relation of a candidate IMF in regard to the input signal. One cannot directly do that with just the soul of the IMF. The reason for the problem is that the IMF evaluation from its soul

$$\mathcal{I}[a, \phi](t) = a(t) \cdot \cos(\phi(t)),$$

or analogously in spline formulation

$$\mathcal{I}[\mathbb{B}_k(\mathbf{a}), \mathbb{B}_k(\phi)](t) = \left(\sum_{i=0}^{n-1} a_i \cdot B_{i,k}(t) \right) \cdot \cos\left(\sum_{i=0}^{n-1} \phi_i \cdot B_{i,k}(t) \right)$$

‘moves’ ϕ from frequency to signal space, which makes any expression containing it non-convex. If one manages to find a convex EMD cost function which in some way circumvents this problem, one has in an instance solved a central part of the previously discussed problem in regard to the empirical mode decomposition on an analytical level. A consequence would be a convex analytical optimization problem and a strong theoretical footing for EMD, which would have far-reaching effects. From the current standpoint, though, this feat seems to be impossible to achieve.

3.2.2. Leakage Factor

We have already seen the canonical EMD cost function in Definition 3.11 in the previous subsection. The motivation behind it is that we want to leave as little residual as possible and strive for the first IMFs to make up the biggest part of the signal. However, serving as a small outlook, what if we do not want to extract as much as possible in each step and want to control the extraction degree? This has been discussed in [PH10] and can be achieved heuristically by putting a penalty on the norm of the extracted IMF and scaling this penalty with a so-called ‘leakage factor’.

Definition 3.14 (Leakage factor EMD cost function [PH10, (16)]). *Let $\mu_0, \mu_1, \mu_2 > 0$, $\gamma \geq 0$ and $s \in \mathcal{C}^0(\mathbb{R}, \mathbb{R})$. The leakage factor EMD cost function $c_\ell[s]: \mathcal{S}_{\mu_0, \mu_1, \mu_2} \rightarrow \mathbb{R}$ is defined as*

$$c_\ell[s](a, \phi) := \|s - \mathcal{I}(a, \phi)\|_2^2 + \gamma \cdot \|\mathcal{I}(a, \phi)\|_2^2.$$

The higher the leakage factor γ is chosen, the more we punish the extraction of ‘large’ IMFs and let it slip through for one of the next EMD extraction steps. Analogous to the canonical spline EMD cost function, we can define a leakage factor spline EMD cost function as follows.

Definition 3.15 (Leakage factor spline EMD cost function). *Let $\mu_0, \mu_1, \mu_2 > 0$, $\gamma \geq 0$, $k \geq 4$ (for derivability) and $\mathbf{s} \in \mathbb{R}^n$. The leakage factor spline EMD cost function $c_\ell[\mathbf{s}]: \mathcal{S}_{\mu_0, \mu_1, \mu_2} \rightarrow \mathbb{R}$ is defined as*

$$c_\ell[\mathbf{s}](\mathbf{a}, \phi) := c_\ell[\mathbb{B}_k(\mathbf{s})](\mathbb{B}_k(\mathbf{a}), \mathbb{B}_k(\phi)).$$

Looking at the equation, we can make an interesting observation that relates the leakage factor cost function to our canonical cost function.

Remark 3.16. *We can directly see that*

$$c_\ell[s](a, \phi) = c_1[s](a, \phi) + \gamma \cdot c_1[0](a, \phi), \quad (3.13)$$

which means that the leakage factor EMD cost function, as $\gamma \geq 0$, is a positive linear combination of the canonical EMD cost function.

This thesis will not further investigate the advantages or disadvantages of the leakage factor approach itself. However, what we can see is that it integrates well into the canonical approach and any results we obtain as follows apply to both the canonical and leakage factor cost functions. This is especially useful considering the final results in terms of convex-like functions, as with the above remark we have shown that if the canonical cost function is convex-like, the leakage-factor cost function is so as well.

3.3. General Optimization Problem

Having discussed the nature of intrinsic mode and EMD cost functions, we can now formulate the general optimization problem that is the core of each empirical mode decomposition step. As already laid out previously we are constructing an optimization problem

$$\begin{aligned} \inf_u \quad & \|s - u\|_2^2 \\ \text{s.t.} \quad & u \text{ IMF.} \end{aligned}$$

for an input signal $s(t)$ and candidate IMFs $u(t)$. Based on our IMF construction in Section 3.1 we have noted that looking at IMF souls $(a(t), \phi(t))$ is much more useful and the only direct way to theorize the IMF constraints properly, given we have to explicitly work with a and ϕ to steer the extraction process. Consequently, instead of the fixed $\|s - u\|_2^2$ in the sketch in Equation (3.7) we consider arbitrary EMD cost functions operating on our set of IMF souls $\mathcal{S}_{\mu_0, \mu_1, \mu_2}$, two of which we presented in Section 3.2.

Definition 3.17 (EMDOP). *Let $\mu_0, \mu_1, \mu_2 > 0$, $s \in \mathcal{C}^0(\mathbb{R}, \mathbb{R})$ the input signal function and $c[s]: \mathcal{S}_{\mu_0, \mu_1, \mu_2} \rightarrow \mathbb{R}$ an EMD cost function. The EMD optimization problem (EMDOP) for the input signal s is defined as*

$$\begin{aligned} \min_{(a, \phi)} \quad & c[s](a, \phi) \\ \text{s.t.} \quad & (a, \phi) \in \mathcal{S}_{\mu_0, \mu_1, \mu_2}. \end{aligned}$$

As previously done, we can also express the optimization problem in terms of B-spline coefficients rather than functions based on the theoretical groundwork in Chapter A.

Definition 3.18 (SpEMDOP). *Let $\mu_0, \mu_1, \mu_2 > 0$, $\mathbf{s} \in \mathbb{R}^n$ B-spline coefficients of the spline input signal function and $\mathbf{c}[\mathbf{s}]: \mathcal{S}_{\mu_0, \mu_1, \mu_2} \rightarrow \mathbb{R}$ a spline EMD cost function. The spline EMD optimization problem (SpEMDOP) for input signal s is defined as*

$$\begin{aligned} \min_{(\mathbf{a}, \phi)} \quad & \mathbf{c}[\mathbf{s}](\mathbf{a}, \phi) \\ \text{s.t.} \quad & (\mathbf{a}, \phi) \in \mathcal{S}_{\mu_0, \mu_1, \mu_2}. \end{aligned}$$

As we have seen in Theorem 3.9, the set of intrinsic mode function souls $\mathcal{S}_{\mu_0, \mu_1, \mu_2}$ and its analogue $\mathcal{S}_{\mu_0, \mu_1, \mu_2} \subset \mathbb{R}^n \times \mathbb{R}^n$ are convex sets. However, the canonical and leakage factor EMD cost functions are not convex in (a, ϕ) , which is a big downside, as we would otherwise have a strong guarantee that an obtained local minimum is also a global minimum and each EMD extraction step unique. The positive aspect of this analysis is that, using the B-spline relation, we are able to examine this problem at all using this novel formulation.

Given the empirically good results observed with regard to the empirical mode decomposition in previous publications, it makes one still wonder why it still works so well

despite the non-convexity of the underlying optimization problem. Given we now have the tools to theoretically examine this at the root and because we are not trying to go into the theory of the search for a convex EMD cost function, we will work with what is given and instead of convexity focus on the regularity of the optimization problem.

3.4. Regularity

We have shown that the SpEMDOP (which is equivalent to the EMDOP) is not a convex optimization problem, but we can still examine its regularity. To explain what regularity is, we take a look at the EMDOP from Definition 3.17, which was defined as

$$\begin{aligned} \min_{(a,\phi)} \quad & c[s](a, \phi) \\ \text{s.t.} \quad & (a, \phi) \in \mathcal{S}_{\mu_0, \mu_1, \mu_2} \end{aligned}$$

for an EMD cost function $c[s]$. s , a and ϕ relate to the input signal $s(t)$ and candidate IMF soul pair $(a(t), \phi(t))$. When approaching this problem, we vary a and ϕ such that the EMD cost function is minimized, under the condition that $(a(t), \phi(t))$ are within our set $\mathcal{S}_{\mu_0, \mu_1, \mu_2}$ of IMF souls. However, it is difficult to enforce the latter condition as this set is too ‘large’ to check as a whole, making it necessary to find other ways to ‘steer’ the candidates $(a(t), \phi(t))$ in a direction where they in fact are IMF souls.

The approach that can be taken is to modify the cost function and add a so-called regularization term $R(a, \phi): (\mathcal{C}^0(\mathbb{R}, \mathbb{R}))^2 \rightarrow \mathbb{R}$. This term is designed such that it is exactly 0 when its arguments satisfy the constraints and a positive value when they violate them, preferably corresponding in size to the violation. Given we are aiming to minimize the cost function of the optimization problem, adding a term to punish violation of the constraints will, in the best case, enforce them. The advantage of this regularization approach is that we obtain an unconstrained optimization problem of the form

$$\min_{(a,\phi) \in (\mathcal{C}^0(\mathbb{R}, \mathbb{R}))^2} \quad c[s](a, \phi) + R(a, \phi)$$

that is relatively simple to model and implement numerically using the equivalent B-spline formulation. A trivial way to define the regularization term is as the so-called ‘characteristic function’ of convex analysis as

$$R(a, \phi) = \begin{cases} 0 & (a, \phi) \in \mathcal{S}_{\mu_0, \mu_1, \mu_2} \\ \infty & (a, \phi) \notin \mathcal{S}_{\mu_0, \mu_1, \mu_2}, \end{cases}$$

but for obvious reasons other choices for $R(a, \phi)$ are much better-suited. This is because the characteristic function does not distinguish between candidates close to or far away from the target set $\mathcal{S}_{\mu_0, \mu_1, \mu_2}$ and for numerical approaches we would want to be able to calculate a ‘slope’ of the cost function to be able to steer into the optimum in some way.

3. Empirical Mode Decomposition Model and Analysis

If we take a look at our constraint for our candidates to be intrinsic mode spline function souls we notice that (using Definition 3.1 and brackets to group conditions)

$$(a, \phi) \in \mathcal{S}_{\mu_0, \mu_1, \mu_2} \Leftrightarrow \begin{cases} 0 \preceq a \\ \mu_0 \preceq \phi' \\ |a'| \preceq \mu_1 \cdot |\phi'| \\ |\phi''| \preceq \mu_2 \cdot |\phi'| \end{cases} \Leftrightarrow \begin{cases} g_1(a, \phi) := -a \preceq 0 \\ g_2(a, \phi) := \mu_0 - \phi' \preceq 0 \\ g_3(a, \phi) := |a'| - \mu_1 \cdot |\phi'| \preceq 0 \\ g_4(a, \phi) := |\phi''| - \mu_2 \cdot |\phi'| \preceq 0. \end{cases}$$

So we see that we can formulate four functions g_1, \dots, g_4 which are negative if and only if their parameters are IMF souls. These functions correspond to four inequality constraints of the underlying optimization problem. These can be used in the method of LAGRANGE multipliers, that is introduced later, to find a ‘perfect’ regularization of the problem based on these functions that are each ‘weighted’ and ‘added’ to the cost function. The optimization problem then is a two-step process of first finding the optimal parameters (a, ϕ) and then the optimal ‘weights’ applied to the constraint functions. It is called the ‘dual problem’ as opposed to the constrained ‘primal problem’ we started with in Definition 3.17.

It can be shown that under certain conditions this dual problem yields the same optimal value as the constrained (primal) optimization problem. This is known as strong duality and the conditions are called regularity conditions. One particular sufficient condition for strong duality is the ‘Slater’ condition that is presented later, and we will show that it applies to the spline formulation SpEMDOP (and EMDOP respectively). This may be a surprising result, as it is commonly assumed that the ‘Slater’ condition can only be shown for convex optimization problems. This is a wrong assumption, as the requirements for ‘Slater’ regularity are weaker than convexity and only require so-called ‘convex-like’ functions we will introduce later.

The main result of this section and one of the central results of this thesis is strong duality for the SpEMDOP (see Theorem 3.41) and EMDOP respectively, as they are equivalent. The formalism introduced as follows though is inconsequential for the thesis and can be skipped up to the conclusion in Section 3.5, which gives a thematic classification of strong duality of the EMDOP within the operator-based regularization methods we introduce in Chapter 4.

3.4.1. Convex-Like Optimization

The theory of convex-like functions and consequently convex-like optimization problems presented here is based on [Jah07] that formulates constrained optimization problems as cone optimization problems and constructs the theory of convex-like optimization problems on top of that. The goal of this subsection is to introduce the necessary definitions for cone optimization problems and convex-likeness. To map the results from [Jah07] to the SpEMDOP we reformulate it as a cone optimization problem for which we then show that it is a convex-like optimization problem. It shall be noted here that we should remind ourselves of the definitions given in Chapter A.

First we begin with the introduction of cone optimization, which is an elegant way to express constrained optimization problems of higher dimensions and with non-standard orderings. This is necessary in our case as our constraints do not have a scalar order \leq but a function order \preceq , for which the classic notation fails.

Definition 3.19 (Cone [Jah07, Definition 4.1]). *Let V be a vector space and $C \subseteq V$. C is a cone in V if and only if*

$$\forall x \in C: \forall \alpha \in \mathbb{R}_+: \alpha \cdot x \in C.$$

As we can see, a cone is a set which contains all positive scalar multiplications of a vector. Consequently we can make the following

Definition 3.20 (Convex cone [Jah07, Theorem 4.3]). *Let V be a vector space and C a cone in V . C is a convex cone in V if and only if C is a convex set.*

We use cone optimization to handle non-standard orders, in our case the function order \preceq that was introduced in Chapter A. Central to this concept is the concept of a positive cone, which contains all positive elements of a vector space.

Definition 3.21 (Positive cone [SW99, Chapter V, §1]). *Let (V, \leq_V) be a preordered vector space. The positive cone of V is defined as*

$$V^+ := \{x \in V \mid 0 \leq_V x\}.$$

Proposition 3.22. *Let (V, \leq_V) be a preordered vector space. V^+ is a convex cone.*

Proof. Let $x, y \in V^+$ and $\alpha, \beta \in \mathbb{R}_+$. It holds because of the scalar multiplication compatibility of the preordered vector space that $\alpha \cdot x \geq_V 0$ and $\beta \cdot y \geq_V 0$ and thus it follows with the addition compatibility of the preordered vector space that $\alpha \cdot x + \beta \cdot y \geq_V 0$. \square

Before we can express what convex-likeness means, we first define a few aspects of notation.

Definition 3.23 (MINKOWSKI sum). *Let $(G, +)$ be a group and $A, B \subseteq G$ be sets. The MINKOWSKI sum of A and B is defined as*

$$A + B := \{a + b \mid a \in A \wedge b \in B\}.$$

We can see that the MINKOWSKI sum is just the set of all pairwise additions of all elements in both sets.

Definition 3.24 (set evaluation). *Let A, B be sets and $f: A \rightarrow B$. The set evaluation of f in A is defined as*

$$f(A) := \{f(a) \mid a \in A\}$$

The set evaluation of a function is thus just the set of all evaluations of the function in all elements of the set. Making use of the MINKOWSKI sum and the set evaluation, we can now define what a convex-like function is.

3. Empirical Mode Decomposition Model and Analysis

Definition 3.25 (Convex-like function [Jah07, Definition 6.3]). *Let $(V, \leq_V), (W, \leq_W)$ be real ordered vector spaces, $S \subseteq V$ and $f: S \rightarrow W$. f is a convex-like function in relation to W^+ if and only if the set*

$$M := f(S) + W^+$$

is convex.

As we can see, the idea behind a convex-like function is to say that if we take the domain of a function f within a vector space W and do a set-addition of all positive elements in W (which is W^+) and find that the resulting set is convex, then the function f is convex-like. In particular, every convex function is also convex-like in relation to \mathbb{R}_+ (all positive numbers including 0) as we know that the epigraph (the set of points lying on or above its graph) of a convex function is also convex. However, not all convex-like functions in relation to \mathbb{R}_+ are also convex, which we can see in the following example.

Example 3.26. *Consider the function $f: \mathbb{R} \rightarrow \mathbb{R}$ with*

$$f(t) := \sin(t).$$

We know that $f(t)$ is not convex, but it is convex-like in relation to \mathbb{R}_+ , the positive cone of (\mathbb{R}, \leq) , because

$$M := \sin(\mathbb{R}) + \mathbb{R}_+ = [-1, 1] + [0, \infty) = [-1, \infty)$$

is a convex set.

The next logical step is to take a look at the canonical spline EMD cost function and see if it is a convex-like function. This is true as we can see in the following

Proposition 3.27. *The canonical spline EMD cost function (see Definition 3.12) is a convex-like function in relation to \mathbb{R}_+ .*

Proof. We defined the canonical spline EMD cost function $\mathbf{c}_1: \mathcal{S}_{\mu_0, \mu_1, \mu_2} \rightarrow \mathbb{R}$ with fixed $\mathbf{s} \in \mathbb{R}^n$ as

$$\begin{aligned} \mathbf{c}_1[\mathbf{s}](\mathbf{a}, \phi) &= c_1[\mathbb{B}_k(\mathbf{s})](\mathbb{B}_k(\mathbf{a}), \mathbb{B}_k(\phi)) \\ &= \|\mathbb{B}_k(\mathbf{s}) - \mathcal{I}(\mathbb{B}_k(\mathbf{a}), \mathbb{B}_k(\phi))\|_2^2 \\ &= \|\mathbb{B}_k(\mathbf{s}) - \mathbb{B}_k(\mathbf{a}) \cdot \cos(\mathbb{B}_k(\phi))\|_2^2 \end{aligned}$$

If we, according to Definition 3.25, take $(V, \leq_V) = (\mathbb{R}^n \times \mathbb{R}^n, \leq)$ and $(W, \leq_W) = (\mathbb{R}, \leq)$ (i.e. use the canonical orders) and note that in this case the domain of our cost function is $S = \mathcal{S}_{\mu_0, \mu_1, \mu_2} \subset \mathbb{R}^n \times \mathbb{R}^n$, we obtain

$$\begin{aligned} M &= \mathbf{c}_1[\mathbf{s}](S) + W^+ \\ &= \mathbf{c}_1[\mathbf{s}](\mathcal{S}_{\mu_0, \mu_1, \mu_2}) + \mathbb{R}_+ \\ &= \left\{ \left\| \mathbb{B}_k(\mathbf{s}) - \left(\sum_{i=0}^{n-1} a_i \cdot B_{i,k} \right) \cdot \cos \left(\sum_{i=0}^{n-1} \phi_i \cdot B_{i,k} \right) \right\|_2^2 \mid (\mathbf{a}, \phi) \in \mathcal{S}_{\mu_0, \mu_1, \mu_2} \right\} + \mathbb{R}_+. \end{aligned}$$

The vector \mathbf{s} is fixed, so the matter of interest is the right hand side of the subtraction within the norm. Fundamentally, we subtract all possible IMFs from the input signal $\mathbb{B}_k(\mathbf{s})$ and thus construct all residuals and determine their norm. Of all norms that we obtain, the minimal norm determines the lower bound of the set. In the ideal case, if the residual vanishes for a certain IMF, the lower bound is 0, but it usually is a positive constant $q(\mathbf{s}, \mu_0, \mu_1, \mu_2)$ that only depends on \mathbf{s} and the predetermined IMF characteristic $\mu_0, \mu_1, \mu_2 > 0$. The upper bound of this set does not matter, as we add \mathbb{R}_+ later, and can be set to a constant $r(\mathbf{s}, \mu_0, \mu_1, \mu_2)$ corresponding to the norm of the ‘worst’ residual. It follows that

$$\begin{aligned} M &= [q(\mathbf{s}, \mu_0, \mu_1, \mu_2), r(\mathbf{s}, \mu_0, \mu_1, \mu_2)) + \mathbb{R}_+ \\ &= [q(\mathbf{s}, \mu_0, \mu_1, \mu_2), r(\mathbf{s}, \mu_0, \mu_1, \mu_2)) + [0, \infty) \\ &= [q(\mathbf{s}, \mu_0, \mu_1, \mu_2), \infty), \end{aligned}$$

which is a convex set. □

Consequently, we can also consider our leakage factor spline EMD cost function, for which the proof is simpler, based on previous results.

Corollary 3.28. *The leakage factor spline EMD cost function (see Definition 3.15) is a convex-like function in relation to \mathbb{R}_+ .*

Proof. This follows directly from Proposition 3.27 and Remark 3.16. □

We have now shown that our two classic cost functions are convex-like and are now interested in the definition of the convex-like optimization problem. This is given as follows.

Definition 3.29 (Convex-like optimization problem [Jah07, (6.2)]). *Let $(V, \leq_V), (W, \leq_W)$ be normed ordered vector spaces, $W^+ \neq \emptyset$, $c: V \rightarrow \mathbb{R}$ a cost function, $g: V \rightarrow W$ and $\emptyset \neq S \subseteq V$. The optimization problem*

$$\begin{aligned} \min_x \quad & c(x) \\ \text{s.t.} \quad & g(x) \in -W^+ \\ & x \in S \end{aligned}$$

is a convex-like optimization problem if and only if $K: V \rightarrow \mathbb{R} \times W$ defined as

$$K(x) := (c(x), g(x))$$

is a convex-like function in relation to $\mathbb{R}_+ \times W^+$.

What we can see is that an optimization problem is a convex-like optimization problem when the cost function is convex-like and the constraints can be expressed as a convex-like function $g(x) \in -W^+$ (which means that the candidate x satisfies the constraints when $g(x)$ is in the negative cone of W , written as the negation of the positive cone

3. Empirical Mode Decomposition Model and Analysis

W^+). The set S can just be chosen as V , unless it also needs to reflect some conditions that did not fit into g as it would violate convex-likeness.

To prove that our SpEMDOP is a convex-like optimization problem we need the following lemma. It will be later used because the set $\mathcal{S}_{\mu_0, \mu_1, \mu_2}$ cannot be directly expressed using a convex-like function. We need to consider the superset $\mathcal{S}_{0, \mu_1, \mu_2}$ (which is a convex cone) of $\mathcal{S}_{\mu_0, \mu_1, \mu_2}$ and move the remaining conditions into our set S .

Lemma 3.30. *Let $\mu_1, \mu_2 > 0$. $\mathcal{S}_{0, \mu_1, \mu_2}$ is a convex cone.*

Proof. We have already shown in Theorem 3.9 that $\mathcal{S}_{0, \mu_1, \mu_2}$ is convex. What is left to show is that $\mathcal{S}_{0, \mu_1, \mu_2}$ is a cone (see Definition 3.19).

Let $\alpha > 0$, $(a, \phi) \in \mathcal{S}_{0, \mu_1, \mu_2}$ and define

$$(a_\star, \phi_\star) := \alpha \cdot (a, \phi) = (\alpha \cdot a, \alpha \cdot \phi).$$

We now show that (a_\star, ϕ_\star) satisfies the conditions from Definition 3.1.

1. $a_\star = \alpha \cdot a \succeq \alpha \cdot 0 = 0$
2. $\phi'_\star = \alpha \cdot \phi' \succeq \alpha \cdot 0 = 0$
3. $|a'_\star| = |\alpha \cdot a'| = \alpha \cdot |a'| \preceq \alpha \cdot \mu_1 \cdot |\phi'| = \mu_1 \cdot |\alpha \cdot \phi'| = \mu_1 \cdot |\phi'_\star|$
4. $|\phi''_\star| = |\alpha \cdot \phi''| = \alpha \cdot |\phi''| \preceq \alpha \cdot \mu_2 \cdot |\phi'| = \mu_2 \cdot |\alpha \cdot \phi'| = \mu_2 \cdot |\phi'_\star|$

It follows that $(a_\star, \phi_\star) \in \mathcal{S}_{0, \mu_1, \mu_2}$ and thus $\mathcal{S}_{0, \mu_1, \mu_2}$ is a convex cone. □

Remark 3.31. *One important consequence seen in this proof is that $\mathcal{S}_{\mu_0, \mu_1, \mu_2}$ is not a convex cone. This is because in general it holds*

$$\phi'_\star = \alpha \cdot \phi' \succeq \alpha \cdot \mu_0 \not\preceq \mu_0.$$

and thus not all scalar multiplications of elements in $\mathcal{S}_{\mu_0, \mu_1, \mu_2}$ are within $\mathcal{S}_{\mu_0, \mu_1, \mu_2}$

With this lemma shown we can go ahead and formulate the first central theorem of this section, namely that the SpEMDOP is a convex-like optimization problem.

Theorem 3.32. *Let $\mu_0, \mu_1, \mu_2 > 0$ and $k \geq 4$ (for derivability). The SpEMDOP (see Definition 3.18) with a convex-like spline EMD cost function $\mathbf{c}[\mathbf{s}]: \mathcal{S}_{0, \mu_1, \mu_2} \rightarrow \mathbb{R}$ in relation to \mathbb{R}_+ is a convex-like optimization problem of the form*

$$\begin{aligned} \min_{(\mathbf{a}, \phi)} \quad & \mathbf{c}[\mathbf{s}](\mathbf{a}, \phi) \\ \text{s.t.} \quad & g(\mathbf{a}, \phi) \in -(\mathcal{C}^0(\mathbb{R}, \mathbb{R})^4)^+ \\ & (\mathbf{a}, \phi) \in S \end{aligned}$$

with $g: \mathbb{R}^n \times \mathbb{R}^n \rightarrow \mathcal{C}^0(\mathbb{R}, \mathbb{R})^4$ defined as

$$g(\mathbf{a}, \boldsymbol{\phi}) := \begin{pmatrix} -\mathbb{B}_k(\mathbf{a}) \\ -\mathbb{B}'_k(\boldsymbol{\phi}) \\ |\mathbb{B}'_k(\mathbf{a})| - \mu_1 \cdot |\mathbb{B}'_k(\boldsymbol{\phi})| \\ |\mathbb{B}''_k(\boldsymbol{\phi})| - \mu_2 \cdot |\mathbb{B}'_k(\boldsymbol{\phi})| \end{pmatrix}$$

and

$$S := \{(\mathbf{a}, \boldsymbol{\phi}) \in \mathbb{R}^n \times \mathbb{R}^n \mid \mathbb{B}'_k(\boldsymbol{\phi}) \succeq \mu_0\}.$$

Proof. According to Definition 3.29 we can take $(V, \leq_V) = (\mathbb{R}^n \times \mathbb{R}^n, \leq)$ and $(W, \leq_W) = (\mathcal{C}^0(\mathbb{R}, \mathbb{R})^4, \preceq)$ (in both cases using the canonical orders) and note that the cost function $\mathbf{c}[\mathbf{s}]$ is already convex-like in relation to \mathbb{R}_+ by precondition.

What is left to do is to split up the set $\mathcal{S}_{\mu_0, \mu_1, \mu_2}$ into a ‘cone-component’ and a residual set S . The former is characterized by a mapping $g: \mathbb{R}^n \times \mathbb{R}^n \rightarrow \mathcal{C}^0(\mathbb{R}, \mathbb{R})^4$ such that

$$(\mathbf{a}, \boldsymbol{\phi}) \in \mathcal{S}_{\mu_0, \mu_1, \mu_2} \Leftrightarrow \begin{cases} g(\mathbf{a}, \boldsymbol{\phi}) \in -W^+ \\ (\mathbf{a}, \boldsymbol{\phi}) \in S. \end{cases}$$

We know from Remark 3.31 that $\mathcal{S}_{\mu_0, \mu_1, \mu_2}$ is not a convex cone. However, we know from Lemma 3.30 that $\mathcal{S}_{0, \mu_1, \mu_2}$ is a convex cone, and we want to bring them into relation in some way. It holds (by Definition 3.10) that (using brackets to group conditions)

$$(\mathbf{a}, \boldsymbol{\phi}) \in \mathcal{S}_{\mu_0, \mu_1, \mu_2} \Leftrightarrow \begin{cases} (\mathbf{a}, \boldsymbol{\phi}) \in \mathcal{S}_{0, \mu_1, \mu_2} \\ \mathbb{B}'_k(\boldsymbol{\phi}) \succeq \mu_0 \end{cases} \Leftrightarrow \begin{cases} \begin{cases} -\mathbb{B}_k(\mathbf{a}) \preceq 0 \\ -\mathbb{B}'_k(\boldsymbol{\phi}) \preceq 0 \\ |\mathbb{B}'_k(\mathbf{a})| - \mu_1 \cdot |\mathbb{B}'_k(\boldsymbol{\phi})| \preceq 0 \\ |\mathbb{B}''_k(\boldsymbol{\phi})| - \mu_2 \cdot |\mathbb{B}'_k(\boldsymbol{\phi})| \preceq 0 \end{cases} \\ \mathbb{B}'_k(\boldsymbol{\phi}) \succeq \mu_0 \end{cases}$$

and thus, as $\mathcal{S}_{0, \mu_1, \mu_2}$ is a convex cone by Lemma 3.30 and using the canonical spline isomorphism, we can define

$$g(\mathbf{a}, \boldsymbol{\phi}) := \begin{pmatrix} -\mathbb{B}_k(\mathbf{a}) \\ -\mathbb{B}'_k(\boldsymbol{\phi}) \\ |\mathbb{B}'_k(\mathbf{a})| - \mu_1 \cdot |\mathbb{B}'_k(\boldsymbol{\phi})| \\ |\mathbb{B}''_k(\boldsymbol{\phi})| - \mu_2 \cdot |\mathbb{B}'_k(\boldsymbol{\phi})| \end{pmatrix}$$

and

$$(\mathbf{a}, \boldsymbol{\phi}) \in S \Leftrightarrow \mathbb{B}'_k(\boldsymbol{\phi}) \succeq \mu_0.$$

If a candidate $(\mathbf{a}, \boldsymbol{\phi})$ satisfies $g(\mathbf{a}, \boldsymbol{\phi}) \preceq 0 \in \mathcal{C}(\mathbb{R}, \mathbb{R})^4$ and $(\mathbf{a}, \boldsymbol{\phi}) \in S$ this means that $(\mathbf{a}, \boldsymbol{\phi}) \in \mathcal{S}_{\mu_0, \mu_1, \mu_2}$, our constraint set.

As $\mathcal{S}_{0, \mu_1, \mu_2}$ is a convex cone it follows by construction that g is a convex-like function in relation to W^+ . Consequently, $K: \mathbb{R}^n \times \mathbb{R}^n \rightarrow \mathbb{R} \times \mathcal{C}^0(\mathbb{R}, \mathbb{R})^4$ defined as

$$K(\mathbf{a}, \boldsymbol{\phi}) := (\mathbf{c}[\mathbf{s}](\mathbf{a}, \boldsymbol{\phi}), g(\mathbf{a}, \boldsymbol{\phi}))$$

is a convex-like function in relation to $\mathbb{R}_+ \times W^+$. □

3. Empirical Mode Decomposition Model and Analysis

Up to this point we have successfully shown that the SpEMDOP is a convex-like optimization problem. It was not possible to fit the entire set $\mathcal{S}_{\mu_0, \mu_1, \mu_2}$ into the function g , as it is not a convex cone, and there remained a property to be put into S . However, this remaining property, namely that $\mathbb{B}'_k(\phi) \succeq \mu_0$, is simple enough.

3.4.2. Slater Condition and Strong Duality

Our next point of interest is to examine the regularity of the SpEMDOP. With convex-likeness shown what remains to be seen is if it also satisfies the SLATER condition, which is defined as follows

Definition 3.33 (SLATER condition [Jah07, Lemma 5.9]). *Let $(V, \leq_V), (W, \leq_W)$ be normed ordered vector spaces, $W^+ \neq \emptyset$, $c: V \rightarrow \mathbb{R}$ a cost function, $g: V \rightarrow W$ and $\emptyset \neq S \subseteq V$. The convex-like optimization problem*

$$\begin{aligned} \min_x \quad & c(x) \\ \text{s.t.} \quad & g(x) \in -W^+ \\ & x \in S \end{aligned}$$

satisfies the SLATER condition if and only if

$$\exists \tilde{x} \in V: \begin{cases} g(\tilde{x}) \in -W^+ \\ \tilde{x} \in S \end{cases} : g(\tilde{x}) \in \text{int}(-W^+).$$

The big advantage of the SLATER condition over other regularity conditions (for strong duality) is that it is sufficient to find one point that strictly satisfies the constraints. Even though it will not be further elaborated here, most other regularity conditions require an examination on a case-by-case basis for a given candidate. In our case, finding a single intrinsic mode spline function soul that is strictly satisfying the constraints is enough to show it for all cases and candidates. We prove that such a point exists in the following

Theorem 3.34. *Let $k \geq 4$ (for derivability). The SpEMDOP (see Definition 3.18) with the canonical spline EMD cost function (see Definition 3.12) satisfies the SLATER condition.*

Proof. Let $\mu_0, \mu_1, \mu_2 > 0$. We have already shown in Theorem 3.32 that the SpEMDOP is a convex-like optimization problem of the form

$$\begin{aligned} \min_{(\mathbf{a}, \phi)} \quad & c_1[\mathbf{s}](\mathbf{a}, \phi) \\ \text{s.t.} \quad & g(\mathbf{a}, \phi) \in -(\mathcal{C}^0(\mathbb{R}, \mathbb{R})^4)^+ \\ & (\mathbf{a}, \phi) \in S \end{aligned}$$

with $g: \mathbb{R}^n \times \mathbb{R}^n \rightarrow \mathcal{C}^0(\mathbb{R}, \mathbb{R})^4$ defined as

$$g(\mathbf{a}, \phi) := \begin{pmatrix} -\mathbb{B}_k(\mathbf{a}) \\ -\mathbb{B}'_k(\phi) \\ |\mathbb{B}'_k(\mathbf{a})| - \mu_1 \cdot |\mathbb{B}'_k(\phi)| \\ |\mathbb{B}''_k(\phi)| - \mu_2 \cdot |\mathbb{B}'_k(\phi)| \end{pmatrix}$$

and

$$S := \left\{ (\mathbf{a}, \phi) \in \mathbb{R}^n \times \mathbb{R}^n \mid \mathbb{B}'_k(\phi) \succeq \mu_0 \right\}.$$

Let $(\mathbf{a}, \phi) \in \mathbb{R}^n \times \mathbb{R}^n$. We can see, considering the approach taken in the proof of Theorem 3.32, that (using brackets to group conditions)

$$\begin{cases} g(\mathbf{a}, \phi) \in -(\mathcal{C}^0(\mathbb{R}, \mathbb{R}^4))^+ \\ (\mathbf{a}, \phi) \in S \end{cases} \Leftrightarrow \begin{cases} (\mathbf{a}, \phi) \in \mathcal{S}_{0, \mu_1, \mu_2} \\ (\mathbf{a}, \phi) \in S. \end{cases}$$

As (using brackets to group conditions)

$$g(\mathbf{a}, \phi) \in \text{int} \left(-(\mathcal{C}^0(\mathbb{R}, \mathbb{R}^4))^+ \right) \Leftrightarrow (\mathbf{a}, \phi) \in \text{int}(\mathcal{S}_{0, \mu_1, \mu_2}) \Leftrightarrow \begin{cases} \mathbb{B}_k(\mathbf{a}) \succ 0 \\ \mathbb{B}'_k(\phi) \succ 0 \\ |\mathbb{B}'_k(\mathbf{a})| \prec \mu_1 \cdot |\mathbb{B}'_k(\phi)| \\ |\mathbb{B}''_k(\phi)| \prec \mu_2 \cdot |\mathbb{B}'_k(\phi)| \end{cases}$$

holds,

$$\begin{cases} g(\mathbf{a}, \phi) \in -\text{int} \left(\mathcal{C}^0(\mathbb{R}, \mathbb{R}^4) \right)^+ \\ (\mathbf{a}, \phi) \in S \end{cases} \Leftrightarrow \begin{cases} \mathbb{B}_k(\mathbf{a}) \succ 0 \\ \mathbb{B}'_k(\phi) \succeq \mu_0 \\ |\mathbb{B}'_k(\mathbf{a})| \prec \mu_1 \cdot |\mathbb{B}'_k(\phi)| \\ |\mathbb{B}''_k(\phi)| \prec \mu_2 \cdot |\mathbb{B}'_k(\phi)| \end{cases} \quad (3.14)$$

follows with the definition of S . Let $c > 0$ and $\tilde{a}, \tilde{\phi}: \mathbb{R} \rightarrow \mathbb{R}$ defined as

$$\begin{aligned} \tilde{a}(t) &:= c, \\ \tilde{\phi}(t) &:= \mu_0 \cdot t. \end{aligned}$$

We can immediately see that $\tilde{a}, \tilde{\phi} \in \Sigma_k$ and

$$\begin{aligned} \tilde{a} &\succ 0, \\ \tilde{\phi}' &= \mu_0 \succeq \mu_0, \\ |\tilde{a}'| &= 0 \prec \mu_1 \cdot \mu_0 = \mu_1 \cdot |\tilde{\phi}'|, \\ |\tilde{\phi}''| &= 0 \prec \mu_2 \cdot \mu_0 = \mu_2 \cdot |\tilde{\phi}'|. \end{aligned}$$

Thus, using the canonical spline isomorphism, we obtain $(\tilde{\mathbf{a}}, \tilde{\phi}) := (\mathbb{B}_k^{\text{inv}}(\tilde{a}), \mathbb{B}_k^{\text{inv}}(\tilde{\phi}))$ satisfying the conditions in Equation (3.14), and thus we have shown that the SpEMDOP satisfies the SLATER condition. \square

The pair $(\tilde{a}(t), \tilde{\phi}(t)) = (c, \mu_0 \cdot t)$ always strictly satisfies the constraints and is thus the strictly interior point we have been looking for.

What remains to be seen is what we can deduce from the result that our SpEMDOP is SLATER regular. To do that, we have to introduce the duality theory on cone optimization problems. This is the part that was left vague in the introduction of this section and will now be properly defined, especially in regard to the LAGRANGE multiplier method.

3. Empirical Mode Decomposition Model and Analysis

Definition 3.35 (Dual cone [Jah07, Definition D.6]). *Let (V, \leq_V) be a normed ordered vector space and $V^* := \{\ell: V \rightarrow \mathbb{R} \mid \ell \text{ linear}\}$ its dual space. The dual cone of V is defined as*

$$V' := \{\ell \in V^* \mid \forall_{x \in V^+}: \ell(x) \geq 0\}.$$

The dual cone is thus the set of linear functions ℓ on V that map positive elements in V to positive numbers in \mathbb{R} , building a bridge from the concept of positiveness in cones to positive numbers. In other words, when we take any element in the positive cone V^+ of a vector space V and apply ℓ to it, it is mapped to a positive number. Conversely, any element in the negative cone $-V^+$ is mapped to a negative number.

Having defined the dual cone, we can now define the LAGRANGE functional that has already been introduced at the beginning of Section 3.4.

Definition 3.36 (LAGRANGE functional [Jah07, Definition 6.8]). *Let $(V, \leq_V), (W, \leq_W)$ be normed ordered vector spaces, $W^+ \neq \emptyset$, $c: V \rightarrow \mathbb{R}$ a cost function, $g: V \rightarrow W$ and $\emptyset \neq S \subseteq V$. The LAGRANGE functional $\Lambda: S \times W' \rightarrow \mathbb{R}$ associated with the optimization problem*

$$\begin{aligned} \min_x \quad & c(x) \\ \text{s.t.} \quad & g(x) \in -W^+ \\ & x \in S \end{aligned}$$

is defined as

$$\Lambda(x, \lambda) := c(x) + \lambda(g(x)).$$

The function $W' \ni \lambda: W \rightarrow \mathbb{R}$ is called the dual variable.

As we can see, the dual variable λ is taken from the dual cone, such that the ‘sign’ of $g(x)$ is preserved. By varying λ , we specify how much each subcomponent of $g(x)$ influences the cost function $\Lambda(X, \lambda)$. With this in mind, we take the idea further and make the following

Definition 3.37 (LAGRANGE dual functional). *Let $(V, \leq_V), (W, \leq_W)$ be normed ordered vector spaces, $W^+ \neq \emptyset$, $c: V \rightarrow \mathbb{R}$ a cost function, $g: V \rightarrow W$ and $\emptyset \neq S \subseteq V$. The LAGRANGE dual functional $\underline{\Lambda}: W' \rightarrow \mathbb{R}$ associated with the optimization problem*

$$\begin{aligned} \min_x \quad & c(x) \\ \text{s.t.} \quad & g(x) \in -W^+ \\ & x \in S \end{aligned}$$

is defined as

$$\underline{\Lambda}(\lambda) := \inf_{x \in S} \Lambda(x, \lambda).$$

In the LAGRANGE dual functional, we take the LAGRANGE functional from earlier and optimize it over the set of candidates within set S . Thus, the only variable left of this problem is the choice of λ , so to say the weights applied to each component of $g(x)$. Consequently, as described at the beginning of the section, we can define the dual optimization problem as this optimization over λ .

Definition 3.38 (Dual optimization problem [Jah07, (6.4)]). *Let $(V, \leq_V), (W, \leq_W)$ be normed ordered vector spaces, $W^+ \neq \emptyset$, $c: V \rightarrow \mathbb{R}$ a cost function, $g: V \rightarrow W$ and $\emptyset \neq S \subseteq V$. The dual optimization problem associated with the (primal) optimization problem*

$$\begin{aligned} \min_x \quad & c(x) \\ \text{s.t.} \quad & g(x) \in -W^+ \\ & x \in S \end{aligned}$$

is defined as

$$\begin{aligned} \max_\lambda \quad & \underline{\Lambda}(\lambda) \\ \text{s.t.} \quad & \lambda \in W'. \end{aligned}$$

We see that now the set of candidates is the dual cone W' of W and thus we are optimizing over linear functions on W . In the classical optimization theory, the λ is a set of scalars (the LAGRANGE multipliers), one for each constraint function that already maps to \mathbb{R} . Given we map to positive cones of general vector spaces, we have to take the little detour and define the λ as a linear function like above. Consistent with the introduced theory, we can now define the concept of strong duality as it has already been explained in the beginning.

Definition 3.39 (Strong duality [Jah07, Theorem 6.7]). *Let $(V, \leq_V), (W, \leq_W)$ be normed ordered vector spaces, $W^+ \neq \emptyset$, $c: V \rightarrow \mathbb{R}$ a cost function, $g: V \rightarrow W$ and $\emptyset \neq S \subseteq V$. The optimization problem*

$$\begin{aligned} \min_x \quad & c(x) \\ \text{s.t.} \quad & g(x) \in -W^+ \\ & x \in S \end{aligned}$$

satisfies strong duality if and only if the cost functions of the primal and dual optimization problems attain the same value in optimality.

It has to be clear here that this does not mean that both optimization problems yield the same solution. It just means that if we solve both optimization problems, the respective cost functions have the same value. To bring duality and convex-likeness together, we make the following observations.

Proposition 3.40. *A convex-like optimization problem (see Definition 3.29) satisfies strong duality if it satisfies the SLATER condition (see Definition 3.33).*

Proof. See [Jah07, Theorem 7.12]. □

Theorem 3.41. *The SpEMDOP (see Definition 3.18) with a convex-like spline EMD cost function $\mathbf{c}[\mathbf{s}]: \mathcal{S}_{0, \mu_1, \mu_2} \rightarrow \mathbb{R}$ in relation to \mathbb{R}_+ satisfies strong duality.*

3. Empirical Mode Decomposition Model and Analysis

Proof. We have shown in Theorem 3.32 that the SpEMDOP is a convex-like optimization problem with a convex-like spline EMD cost function and in Theorem 3.34 that it satisfies the SLATER condition. It follows directly with Proposition 3.27 that the SpEMDOP satisfies strong duality. \square

3.5. Conclusion

The main result of this chapter is that the newly introduced EMD optimization problem (EMDOP)

$$\begin{aligned} \min_{(a, \phi)} \quad & c[s](a, \phi) \\ \text{s.t.} \quad & (a, \phi) \in \mathcal{S}_{\mu_0, \mu_1, \mu_2}. \end{aligned}$$

with an EMD cost function $c[s]$ (see Definition 3.11 for the definition of the canonical cost function) over the set $\mathcal{S}_{\mu_0, \mu_1, \mu_2}$ of IMF souls (IMFS) (see Definition 3.1) satisfies strong duality, which has been shown using its equivalent B-spline formulation. The only condition is that the cost function is convex-like (see Definition 3.25). In particular, if we find a convex EMD cost function, given every convex function is also convex-like, we will also have automatically shown strong duality as well. In general, the model is thus a good object to further study the EMD from a theoretical perspective, as the only variable is the cost function, for which only simple properties have to be shown to obtain strong results for the entire EMD optimization problem. This is also the reason why the cost function has been kept as general as possible in the theoretical derivation.

It is the author's impression that there are only two avenues to further formalize the empirical mode decomposition, and none of them is the development of more informal heuristics. The first one is to find a convex cost function for the entire set of IMF souls, which would be the optimal scenario. The second one is to add more constraints to the set of IMF souls, such that an EMD cost function is convex on this restricted set. This would require an adaption of the proof in this section and might make some aspects much more difficult. It remains to be seen which direction will be taken.

In terms of regularization and the role of strong duality, which at first sight 'only' applies to the method of LAGRANGE multipliers, in terms of general regularization schemes we can make the following remark: One can imagine the LAGRANGE multipliers to be the most perfect regularization term possible. If we look at it intuitively, it finds a feasible solution and optimally assigns weights to each constraint such that the cost function is as minimal as possible. We have shown that strong duality holds and thus that the LAGRANGE multiplier method yields the same optimal cost function value, no matter if one considers the constrained primal problem or the dual LAGRANGE problem. Thus it follows that considering regularization terms (refer to $R(\mathbf{a}, \phi)$ at the beginning of Section 3.4) is a valid approach. If we could not have shown strong duality, even a very good regularization term, which comes close to the LAGRANGE term, would not have the chance to properly 'represent' the constraints.

Consequently, as the approach outlined in Chapter 4 examines one regularization term approach using operators, and with the results of this chapter, we can assume that it is

3.5. Conclusion

not wrong to approach the empirical mode decomposition like this. In broader terms, the strong duality shown in this chapter might even explain why many of the heuristic EMD methods work as well as they do.

4. Operator-Based Analysis of Intrinsic Mode Functions

Let us again consider the EMD optimization problem (EMDOP) that we defined in the previous chapter as

$$\begin{aligned} \min_{(a,\phi)} \quad & c[s](a,\phi) \\ \text{s.t.} \quad & (a,\phi) \in \mathcal{S}_{\mu_0,\mu_1,\mu_2} \end{aligned}$$

with an EMD cost function $c[s](a,\phi)$ (for instance the canonical cost function from Definition 3.11) and the set of IMF souls $\mathcal{S}_{\mu_0,\mu_1,\mu_2}$. At the beginning of Section 3.4 we looked at the approach of adding a regularization term $R(a,\phi)$ to the cost function of the optimization problem. This regularization term punishes violations of the constraints given by the IMF soul set and, in the ideal case, ‘steers’ arbitrary candidate function pairs $(a,\phi) \in (\mathcal{C}^0(\mathbb{R},\mathbb{R}))^2$ into the desired constraints. The resulting regularized optimization problem

$$\min_{(a,\phi) \in (\mathcal{C}^0(\mathbb{R},\mathbb{R}))^2} c[s](a,\phi) + R(a,\phi)$$

is unconstrained and easier to handle than the original constrained optimization problem. We have examined the regularity of the EMDOP in Section 3.4 and found out that if we find a ‘perfect’ regularization operator that behaves equivalently to the regularization of the LAGRANGE multiplier method, we can minimize the cost function just as well as with the constrained optimization problem. Up to this point though, we have not yet seen a non-trivial definition of a regularization term for the EMD optimization problem.

The motivation of this chapter is to examine one such approach for defining a regularization term that is called the null-space-pursuit (NSP) (see [PH08] and [PH10]) which is classified as a so-called operator-based signal-separation (OSS) method. It is based on so-called ‘adaptive operators’ that have been introduced with an example in Chapter 1. The fundamental idea is as follows: Suppose that we have a function $h(t)$ that ‘contains’ a function $\phi(t)$, for example $h(t) = \cos(\phi(t))$. It is our interest to extract $\phi(t)$ from it. To approach this problem, we can define an operator $\mathcal{D}_{\tilde{\phi}}$ with a parameter function $\tilde{\phi}(t)$ as

$$\left(\mathcal{D}_{\tilde{\phi}}h\right)(t) := \frac{\partial^2 h(t)}{\partial t^2} - \frac{\tilde{\phi}''(t)}{\tilde{\phi}'(t)} \cdot \frac{\partial h(t)}{\partial t} + (\tilde{\phi}'(t))^2 \cdot h(t),$$

for which it holds (see Equation (1.11)) that

$$\mathcal{D}_{\phi}h \equiv 0.$$

4. Operator-Based Analysis of Intrinsic Mode Functions

Adapting it to the EMD optimization problem, our goal is to find an adaptive operator $\mathcal{D}_{(\tilde{a}, \tilde{\phi})}$ such that for an intrinsic mode function (IMF) $u(t)$ of the form $u(t) := a(t) \cdot \cos(\phi(t))$ with instantaneous amplitude $a(t)$ and phase $\phi(t)$, it holds that

$$\mathcal{D}_{(a, \phi)} u \equiv 0.$$

Given any norm is positive definite, this is equivalent to the norm of the operator vanishing, namely

$$\|\mathcal{D}_{(a, \phi)} u\|_2^2 = 0.$$

In the ideal case that the operator does not match (i.e. vanishes for) other functions, we can make the following observation: If a function is ‘annihilated’ by the operator $\mathcal{D}_{(a, \phi)}$, we can assume that the function is of the IMF form $a(t) \cdot \cos(\phi(t))$. We can use that to our advantage by reminding ourselves how we defined the regularization operator $R(a, \phi)$. We want it to be exactly zero when the constraints are satisfied and non-zero otherwise. This corresponds to the norm of our adaptive operator and it is justified to set the regularization of our EMDOP to

$$R(a, \phi) := \|\mathcal{D}_{(a, \phi)} u\|_2^2.$$

If a function is annihilated by the operator we can equivalently say that the function is in the kernel of this operator. Another name for the kernel is the ‘null-space’, and thus it becomes clear why this regularization method is called the null-space-pursuit, as we aim to vary the operator parameters $(\tilde{a}, \tilde{\phi})$ until the operator itself vanishes. This tells us that the input function is an IMF and what the underlying instantaneous amplitude and phase look like.

4.1. IMF Differential Operator

Up to this point we have only described the properties we would like to see from an adaptive operator $\mathcal{D}_{(\tilde{a}, \tilde{\phi})}$ for the EMD optimization problem, which we will from now on call ‘IMF differential operator’. We have not yet defined one and will do that in this section.

The operator we are going to examine is a natural generalization of the complex-valued differential operator presented in [GPHX17] from a first order to a second order differential operator, which will be elaborated later. Before we define it we first define two operators that are used in the expression of the IMF operator itself and will become more important later.

Definition 4.1 (Instantaneous envelope derivation operator). *The instantaneous envelope derivation operator is defined as*

$$A[a] := \frac{a'}{a}.$$

Definition 4.2 (Inverse square continuous frequency operator). *The inverse square continuous frequency operator is defined as*

$$\Omega[\phi] := \frac{1}{(\phi')^2}.$$

We can think of the instantaneous envelope derivation and inverse square continuous frequency operators as derived expressions of a and ϕ . Using the notation from Definition A.8 we define our operator as follows.

Definition 4.3 (IMF differential operator [GPHX17]). *The IMF differential operator is defined as*

$$\begin{aligned} \mathcal{D}_{(a,\phi)} := & \Omega[\phi] \cdot D^2 + \\ & \left[-2 \cdot \Omega[\phi] \cdot A[a] + \frac{1}{2} \cdot \Omega'[\phi] \right] \cdot D^1 + \\ & \left[\Omega[\phi] \cdot \left(A^2[a] - A'[a] \right) - \frac{1}{2} \cdot \Omega'[\phi] \cdot A[a] + 1 \right] \cdot D^0. \end{aligned}$$

As we can see, the IMF differential operator contains derivative operators of up to order two, which is why we call it a second order differential operator.

4.1.1. Properties

We will now show that it is in fact an operator that annihilates IMFs when its parameters match the soul of the input IMF. For that, we remind ourselves of the IMF operator from Definition 3.5.

Proposition 4.4. *Let $(a, \phi) \in \mathcal{S}_{\mu_0, \mu_1, \mu_2}$. It holds*

$$\mathcal{D}_{(a,\phi)} \mathcal{I}[a, \phi] = 0.$$

Proof. We first prepare some results of derivatives for different expressions that will occur later. The two operators defined earlier behave as follows:

$$\begin{aligned} \Omega'[\phi] &= \left(\frac{1}{(\phi')^2} \right)' = (-2) \cdot \frac{\phi''}{(\phi')^3}, \\ A'[a] &= \left(\frac{a'}{a} \right)' = \frac{a''}{a} - \frac{(a')^2}{a^2} = \frac{a'' \cdot a - (a')^2}{a^2}. \end{aligned}$$

Additionally, we determine the second derivative of an IMF as

$$\begin{aligned} D^2(a \cdot \cos(\phi)) &= (a \cdot \cos(\phi))'' = (a' \cdot \cos(\phi) - a \cdot \phi' \cdot \sin(\phi))' \\ &= a'' \cdot \cos(\phi) - 2 \cdot a' \cdot \phi' \cdot \sin(\phi) - a \cdot \phi'' \cdot \sin(\phi) - a \cdot (\phi')^2 \cos(\phi) \\ &= [-2 \cdot a' \cdot \phi' - a \cdot \phi''] \cdot \sin(\phi) + [a'' - a \cdot (\phi')^2] \cdot \cos(\phi). \end{aligned}$$

4. Operator-Based Analysis of Intrinsic Mode Functions

With these results we can look at the differential operator itself and expand the derivations accordingly by applying the differential operators:

$$\begin{aligned}\mathcal{D}_{(a,\phi)}\mathcal{I}[a,\phi] &= \mathcal{D}_{(a,\phi)}(a \cdot \cos(\phi)) \\ &= \Omega[\phi] \cdot (a \cdot \cos(\phi))'' + \\ &\quad \left[-2 \cdot \Omega[\phi] \cdot A[a] + \frac{1}{2} \cdot \Omega'[\phi] \right] \cdot (a \cdot \cos(\phi))' + \\ &\quad \left[\Omega[\phi] \cdot (A^2[a] - A'[a]) - \frac{1}{2} \cdot \Omega'[\phi] \cdot A[a] + 1 \right] \cdot (a \cdot \cos(\phi)).\end{aligned}$$

To show the proposition we now calculate the derivatives making use of the chain rule and simplify:

$$\begin{aligned}\mathcal{D}_{(a,\phi)}\mathcal{I}[a,\phi] &= \left(\frac{1}{(\phi')^2} \right) \cdot \left\{ [-2 \cdot a' \cdot \phi' - a \cdot \phi''] \cdot \sin(\phi) + [a'' - a \cdot (\phi')^2] \cdot \cos(\phi) \right\} + \\ &\quad \left[\frac{-2 \cdot a'}{a \cdot (\phi')^2} + \frac{1}{2} \cdot (-2) \cdot \frac{\phi''}{(\phi')^3} \right] \cdot (a' \cdot \cos(\phi) - a \cdot \phi' \cdot \sin(\phi)) + \\ &\quad \left[\left(\frac{1}{(\phi')^2} \right) \cdot \left(\frac{(a')^2}{a^2} - \frac{a \cdot a'' - (a')^2}{a^2} \right) - \frac{1}{2} \cdot (-2) \cdot \frac{a' \cdot \phi''}{a \cdot (\phi')^3} + 1 \right] \cdot (a \cdot \cos(\phi)) \\ &= \frac{-2 \cdot a' \cdot \phi' - a \cdot \phi''}{(\phi')^2} \cdot \sin(\phi) + \frac{a'' - a \cdot (\phi')^2}{(\phi')^2} \cdot \cos(\phi) + \\ &\quad \left[\frac{-2 \cdot a'}{a \cdot (\phi')^2} - \frac{\phi''}{(\phi')^3} \right] \cdot (a' \cdot \cos(\phi) - a \cdot \phi' \cdot \sin(\phi)) + \\ &\quad \left[\frac{2 \cdot (a')^2 - a \cdot a''}{a^2 \cdot (\phi')^2} + \frac{a' \cdot \phi''}{a \cdot (\phi')^3} + 1 \right] \cdot (a \cdot \cos(\phi)).\end{aligned}$$

Sine and cosine are separated and we show that their coefficients are zero, implying that the entire expression is zero, as follows:

$$\begin{aligned}\mathcal{D}_{(a,\phi)}\mathcal{I}[a,\phi] &= \left[\frac{-2 \cdot a'}{\phi'} - \frac{a \cdot \phi''}{(\phi')^2} \right] \cdot \sin(\phi) + \left[\frac{a''}{(\phi')^2} - a \right] \cdot \cos(\phi) + \\ &\quad \left[\frac{2 \cdot a'}{\phi'} + \frac{a \cdot \phi''}{(\phi')^2} \right] \cdot \sin(\phi) + \left[\frac{-2 \cdot (a')^2}{a \cdot (\phi')^2} - \frac{a' \cdot \phi''}{(\phi')^3} \right] \cdot \cos(\phi) + \\ &\quad \left[\frac{2 \cdot (a')^2}{a \cdot (\phi')^2} - \frac{a''}{(\phi')^2} + \frac{a' \cdot \phi''}{(\phi')^3} + a \right] \cdot \cos(\phi) \\ &= \left[\frac{-2 \cdot a'}{\phi'} - \frac{a \cdot \phi''}{(\phi')^2} + \frac{2 \cdot a'}{\phi'} + \frac{a \cdot \phi''}{(\phi')^2} \right] \cdot \sin(\phi) + \\ &\quad \left[\frac{a''}{(\phi')^2} - a + \frac{-2 \cdot (a')^2}{a \cdot (\phi')^2} - \frac{a' \cdot \phi''}{(\phi')^3} + \frac{2 \cdot (a')^2}{a \cdot (\phi')^2} - \frac{a''}{(\phi')^2} + \frac{a' \cdot \phi''}{(\phi')^3} + a \right] \cdot \cos(\phi) \\ &= 0. \quad \square\end{aligned}$$

This shows that $\mathcal{D}_{(a,\phi)}$ is in fact an annihilating operator. When considering the IMF differential operator from Definition 4.3 again, one can observe that the only way the a and ϕ ‘interface’ with the operator is through instantaneous envelope derivation operator $A[a]$ and inverse square continuous frequency operator $\Omega[\phi]$. Given both are functions just like a and ϕ , we can express the operator parametrized by A and Ω instead of a and ϕ and call it the modified IMF operator.

Definition 4.5 (Modified IMF operator). *The modified IMF operator is defined as*

$$\begin{aligned} \tilde{\mathcal{D}}_{(A,\Omega)} := & \Omega \cdot D^2 + \\ & \left[-2 \cdot \Omega \cdot A + \frac{1}{2} \cdot \Omega' \right] \cdot D^1 + \\ & \left[\Omega \cdot (A^2 - A') - \frac{1}{2} \cdot \Omega' \cdot A + 1 \right] \cdot D^0. \end{aligned}$$

How to determine a from A and ϕ from Ω shall not yet be of concern here, but for instance in the case of Ω , the inverse square root of Ω yields ϕ' directly (compare Definition 4.2).

It is now in our interest to examine the behaviour of the differential operator under its parameters. As we vary A and Ω , we want to know that if we found an annihilating pair we really obtained a unique solution or not. We will approach this question just like the cost functions in Section 3.2 and consider the A and Ω to be spline functions that vary over their B-spline basis coefficients $\mathbf{A} \in \mathbb{R}^n$ and $\mathbf{\Omega} \in \mathbb{R}^n$. To give an example, we consider A to be the spline function (using Definitions 2.5 and 2.10)

$$\mathbb{B}_k(\mathbf{A}) = \sum_{i=0}^{n-1} A_i \cdot B_{i,k}$$

that varies over the vector entries A_i of \mathbf{A} . If we consider the norm of this function, we can for instance calculate its partial derivative in A_m for $m \in \{0, \dots, n-1\}$ using the chain rule as

$$\frac{\partial \|\mathbb{B}_k(\mathbf{A})\|_2^2}{\partial A_m} = \frac{\partial}{\partial A_m} \left(\int_{-\infty}^{\infty} (\mathbb{B}_k(\mathbf{A}))^2 dt \right) = \int_{-\infty}^{\infty} \frac{\partial (\mathbb{B}_k(\mathbf{A}))^2}{\partial A_m} dt = \int_{-\infty}^{\infty} 2 \cdot \mathbb{B}_k(\mathbf{A}) \cdot B_{m,k}(t) dt.$$

To go even further, we can of course also partially derive again, this time in A_p for $p \in \{0, \dots, n-1\}$. We obtain

$$\frac{\partial^2 \|\mathbb{B}_k(\mathbf{A})\|_2^2}{\partial A_m \partial A_p} = \frac{\partial}{\partial A_m} \left(\int_{-\infty}^{\infty} 2 \cdot \mathbb{B}_k(\mathbf{A}) \cdot B_{m,k}(t) dt \right) = \int_{-\infty}^{\infty} 2 \cdot B_{m,k}(t) \cdot B_{p,k}(t) dt.$$

The result of this particular observation is that the covariation of $\|\mathbb{B}_k(\mathbf{A})\|_2^2$ in A_m and A_p is directly related to the orthogonality of $B_{m,k}$ and $B_{p,k}$. If the B-spline basis were truly orthogonal, the final integral will always be zero. However, the B-spline basis is not orthogonal. Thus, if m and p are ‘close’ to each other or even equal, the integral will be positive. Another interpretation is to consider the Hessian matrix in partial derivatives

4. Operator-Based Analysis of Intrinsic Mode Functions

in A_i , which can be used to prove that a function is convex in multiple variables. After all, the function $\|\mathbb{B}_k(\mathbf{A})\|_2^2$ is a mapping $\mathbb{R}^n \rightarrow \mathbb{R}$. Making use of this general technique, we prove the following

Theorem 4.6. *Let $f \in \mathcal{C}^2(\mathbb{R}, \mathbb{R})$ and $k \geq 4$ (for derivability). $\|\tilde{\mathcal{D}}_{(\mathbb{B}_k(\mathbf{A}), \mathbb{B}_k(\mathbf{\Omega}))} f\|_2^2$ is strictly convex in $\mathbf{\Omega}$ but not convex in \mathbf{A} .*

Proof. By definition we obtain that

$$\|\tilde{\mathcal{D}}_{(\mathbb{B}_k(\mathbf{A}), \mathbb{B}_k(\mathbf{\Omega}))} f\|_2^2 = \int_{-\infty}^{\infty} \left(\tilde{\mathcal{D}}_{(\mathbb{B}_k(\mathbf{A}), \mathbb{B}_k(\mathbf{\Omega}))} f \right)^2 dt.$$

In particular we first consider the term within the norm itself and expand it from its definition (see Definition 4.5)

$$\begin{aligned} \tilde{\mathcal{D}}_{(\mathbb{B}_k(\mathbf{A}), \mathbb{B}_k(\mathbf{\Omega}))} f &= \mathbb{B}_k(\mathbf{\Omega}) \cdot f'' + \\ &\left[-2 \cdot \mathbb{B}_k(\mathbf{\Omega}) \cdot \mathbb{B}_k(\mathbf{A}) + \frac{1}{2} \cdot (\mathbb{B}_k(\mathbf{\Omega}))' \right] \cdot f' + \\ &\left[\mathbb{B}_k(\mathbf{\Omega}) \cdot \left((\mathbb{B}_k(\mathbf{A}))^2 - (\mathbb{B}_k(\mathbf{A}))' \right) - \frac{1}{2} \cdot (\mathbb{B}_k(\mathbf{\Omega}))' \cdot \mathbb{B}_k(\mathbf{A}) + 1 \right] \cdot f. \end{aligned}$$

Making use of Definition 2.10 to expand the spline functions into B-spline expressions it follows

$$\begin{aligned} \tilde{\mathcal{D}}_{(\mathbb{B}_k(\mathbf{A}), \mathbb{B}_k(\mathbf{\Omega}))} f &= \left(\sum_{i=0}^{n-1} \Omega_i \cdot B_{i,k} \right) \cdot f'' + \\ &\left[-2 \cdot \left(\sum_{i=0}^{n-1} \Omega_i \cdot B_{i,k} \right) \cdot \left(\sum_{i=0}^{n-1} A_i \cdot B_{i,k} \right) + \right. \\ &\left. \frac{1}{2} \cdot \left(\sum_{i=0}^{n-1} \Omega_i \cdot B'_{i,k} \right) \right] \cdot f' + \\ &\left[\left(\sum_{i=0}^{n-1} \Omega_i \cdot B_{i,k} \right) \cdot \left(\left(\sum_{i=0}^{n-1} A_i \cdot B_{i,k} \right)^2 - \left(\sum_{i=0}^{n-1} A_i \cdot B'_{i,k} \right) \right) - \right. \\ &\left. \frac{1}{2} \cdot \left(\sum_{i=0}^{n-1} \Omega_i \cdot B'_{i,k} \right) \cdot \left(\sum_{i=0}^{n-1} A_i \cdot B_{i,k} \right) + 1 \right] \cdot f. \end{aligned}$$

We approach this proof checking if the requirements of Theorem B.7 hold for distinct partial derivatives for entries of \mathbf{A} and $\mathbf{\Omega}$. By applying partial derivatives we obtain

that for $m, p \in \{0, \dots, n-1\}$ it holds with the chain rule for partial derivatives in \mathbf{A}

$$\begin{aligned} \frac{\partial^2 \left\| \tilde{\mathcal{D}}_{(\mathbb{B}_k(\mathbf{A}), \mathbb{B}_k(\boldsymbol{\Omega}))} f \right\|_2^2}{\partial A_m \partial A_p}(\mathbf{A}, \boldsymbol{\Omega}) &= \frac{\partial}{\partial A_p} \left(\int_{-\infty}^{\infty} 2 \cdot \tilde{\mathcal{D}}_{(\mathbb{B}_k(\mathbf{A}), \mathbb{B}_k(\boldsymbol{\Omega}))} f \cdot \frac{\partial \tilde{\mathcal{D}}_{(\mathbb{B}_k(\mathbf{A}), \mathbb{B}_k(\boldsymbol{\Omega}))} f}{\partial A_m} dt \right) \\ &= \int_{-\infty}^{\infty} 2 \cdot \frac{\partial \tilde{\mathcal{D}}_{(\mathbb{B}_k(\mathbf{A}), \mathbb{B}_k(\boldsymbol{\Omega}))} f}{\partial A_m} \cdot \frac{\partial \tilde{\mathcal{D}}_{(\mathbb{B}_k(\mathbf{A}), \mathbb{B}_k(\boldsymbol{\Omega}))} f}{\partial A_p} + \\ &\quad 2 \cdot \tilde{\mathcal{D}}_{(\mathbb{B}_k(\mathbf{A}), \mathbb{B}_k(\boldsymbol{\Omega}))} f \cdot \frac{\partial^2 \tilde{\mathcal{D}}_{(\mathbb{B}_k(\mathbf{A}), \mathbb{B}_k(\boldsymbol{\Omega}))} f}{\partial A_m \partial A_p} dt \end{aligned} \quad (4.1)$$

and analogously for partial derivatives in $\boldsymbol{\Omega}$

$$\begin{aligned} \frac{\partial^2 \left\| \tilde{\mathcal{D}}_{(\mathbb{B}_k(\mathbf{A}), \mathbb{B}_k(\boldsymbol{\Omega}))} f \right\|_2^2}{\partial \Omega_m \partial \Omega_p}(\mathbf{A}, \boldsymbol{\Omega}) &= \int_{-\infty}^{\infty} 2 \cdot \frac{\partial \tilde{\mathcal{D}}_{(\mathbb{B}_k(\mathbf{A}), \mathbb{B}_k(\boldsymbol{\Omega}))} f}{\partial \Omega_m} \cdot \frac{\partial \tilde{\mathcal{D}}_{(\mathbb{B}_k(\mathbf{A}), \mathbb{B}_k(\boldsymbol{\Omega}))} f}{\partial \Omega_p} + \\ &\quad 2 \cdot \tilde{\mathcal{D}}_{(\mathbb{B}_k(\mathbf{A}), \mathbb{B}_k(\boldsymbol{\Omega}))} f \cdot \frac{\partial^2 \tilde{\mathcal{D}}_{(\mathbb{B}_k(\mathbf{A}), \mathbb{B}_k(\boldsymbol{\Omega}))} f}{\partial \Omega_m \partial \Omega_p} dt. \end{aligned} \quad (4.2)$$

First for partial derivatives in \mathbf{A} , we consider the bare derivatives of the operator (without the norm) that we found within the derivative expressions of the operator within the norm. For the first order we find that

$$\begin{aligned} \frac{\partial \tilde{\mathcal{D}}_{(\mathbb{B}_k(\mathbf{A}), \mathbb{B}_k(\boldsymbol{\Omega}))} f}{\partial A_m}(\mathbf{A}, \boldsymbol{\Omega}) &= [-2 \cdot \mathbb{B}_k(\boldsymbol{\Omega}) \cdot B_{m,k}] \cdot f' + \\ &\quad \left[\mathbb{B}_k(\boldsymbol{\Omega}) \cdot \left(2 \cdot \mathbb{B}_k(\mathbf{A}) \cdot B_{m,k} - B'_{m,k} \right) - \frac{1}{2} \cdot (\mathbb{B}_k(\boldsymbol{\Omega}))' \cdot B_{m,k} \right] \cdot f \\ &= [-2 \cdot \mathbb{B}_k(\boldsymbol{\Omega}) \cdot B_{m,k}] \cdot f' + \\ &\quad \left[\mathbb{B}_k(\boldsymbol{\Omega}) \cdot \left(2 \cdot \left(\sum_{i=0}^{n-1} A_i \cdot B_{i,k} \right) \cdot B_{m,k} - B'_{m,k} \right) - \right. \\ &\quad \left. \frac{1}{2} \cdot (\mathbb{B}_k(\boldsymbol{\Omega}))' \cdot B_{m,k} \right] \cdot f, \end{aligned}$$

and for the second order we finally obtain

$$\frac{\partial^2 \tilde{\mathcal{D}}_{(\mathbb{B}_k(\mathbf{A}), \mathbb{B}_k(\boldsymbol{\Omega}))} f}{\partial A_m \partial A_p}(\mathbf{A}, \boldsymbol{\Omega}) = 2 \cdot \mathbb{B}_k(\boldsymbol{\Omega}) \cdot B_{m,k} \cdot B_{p,k} \cdot f \neq 0.$$

This implies that for $m = p$ the sign of the term in Equation (4.1) is not positive, as the bare operator is not zeroed out in the second summand. Thus the necessary condition in Theorem B.7 that all diagonal elements of the Hessian matrix must be positive is violated. It follows that we can not show convexity for partial derivatives in \mathbf{A} , as the Hessian matrix for derivatives in \mathbf{A} can not be shown to be positive semidefinite.

4. Operator-Based Analysis of Intrinsic Mode Functions

For partial derivatives of the bare operator in Ω we find for the first order that

$$\begin{aligned} \frac{\partial \tilde{\mathcal{D}}_{(\mathbb{B}_k(\mathbf{A}), \mathbb{B}_k(\Omega))} f}{\partial \Omega_m}(\mathbf{A}, \Omega) &= B_{m,k} \cdot f'' + \\ &\quad \left[-2 \cdot \mathbb{B}_k(\mathbf{A}) \cdot B_{m,k} + \frac{1}{2} \cdot B'_{m,k} \right] \cdot f' + \\ &\quad \left[B_{m,k} \cdot \left((\mathbb{B}_k(\mathbf{A}))^2 - (\mathbb{B}_k(\mathbf{A}))' \right) - \frac{1}{2} \cdot \mathbb{B}_k(\mathbf{A}) \cdot B'_{m,k} \right] \cdot f \end{aligned}$$

which yields for the second order that

$$\frac{\partial^2 \tilde{\mathcal{D}}_{(\mathbb{B}_k(\mathbf{A}), \mathbb{B}_k(\Omega))} f}{\partial \Omega_m \partial \Omega_p}(\mathbf{A}, \Omega) \equiv 0.$$

We obtain from this result that the second summand in the integral in Equation (4.2) is zero and it holds that

$$\frac{\partial^2 \left\| \tilde{\mathcal{D}}_{(\mathbb{B}_k(\mathbf{A}), \mathbb{B}_k(\Omega))} f \right\|_2^2}{\partial \Omega_m \partial \Omega_p}(\mathbf{A}, \Omega) = \int_{-\infty}^{\infty} 2 \cdot \frac{\partial \tilde{\mathcal{D}}_{(\mathbb{B}_k(\mathbf{A}), \mathbb{B}_k(\Omega))} f}{\partial \Omega_m} \cdot \frac{\partial \tilde{\mathcal{D}}_{(\mathbb{B}_k(\mathbf{A}), \mathbb{B}_k(\Omega))} f}{\partial \Omega_p} dt.$$

We can immediately see that the Hessian matrix of $\left\| \tilde{\mathcal{D}}_{(\mathbb{B}_k(\mathbf{A}), \mathbb{B}_k(\Omega))} f \right\|_2^2$ for derivatives in Ω is symmetric. In particular, for $m = p$, it also holds

$$\frac{\partial^2 \left\| \tilde{\mathcal{D}}_{(\mathbb{B}_k(\mathbf{A}), \mathbb{B}_k(\Omega))} f \right\|_2^2}{\partial \Omega_m^2}(\mathbf{A}, \Omega) = \int_{-\infty}^{\infty} 2 \cdot \left(\frac{\partial \tilde{\mathcal{D}}_{(\mathbb{B}_k(\mathbf{A}), \mathbb{B}_k(\Omega))} f}{\partial \Omega_m} \right)^2 dt > 0,$$

which means that the diagonal entries of the Hessian matrix for Ω are strictly positive. It is also diagonally dominant with the same argument as in the proof of Proposition 3.13, namely due to the compact support and partial orthogonality of the B-spline basis functions. It follows with Theorem B.7 that the Hessian matrix for derivatives in Ω is positive definite and by Proposition B.5 that $\left\| \tilde{\mathcal{D}}_{(\mathbb{B}_k(\mathbf{A}), \mathbb{B}_k(\Omega))} f \right\|_2^2$ is strictly convex in Ω . \square

Given this result we do not have the theoretical guarantee that our operator gives us a unique and minimal solution, as it is not generally convex. This is obviously undesirable as our primary motivation is to find and examine methods that have a stronger theoretical foundation than the classic heuristic EMD methods.

4.1.2. Simplification

The reassuring part of the result in Theorem 4.6 is that the function is strictly convex if we reduce the variation to Ω and keep \mathbf{A} constant. Without loss of generality, if we know that our input IMF has constant amplitude 1, namely that it only has the form $\cos(\phi)$, we can apply a simplified differential operator to it of which we know that it is

strictly convex. This assumption may sound a bit too extravagant, but we will show in Chapter 5 that it is meaningful and use the results of the following subsection to extract the instantaneous phase from IMFs with constant amplitude 1.

If we know that our input IMFs will have the form $\cos(\phi)$, we might wonder how our IMF differential operator changes under this assumption.

Proposition 4.7. *It holds*

$$\mathcal{D}_{(1,\phi)} = \Omega[\phi] \cdot D^2 + \frac{1}{2} \cdot \Omega'[\phi] \cdot D^1 + D^0.$$

Proof. It follows directly from Definition 4.3 and observing that

$$A[1] = \frac{(1)'}{1} = 0. \quad \square$$

The great simplification of the operator is apparent. We now wonder how the modified IMF operator behaves under the assumption that $a \equiv 1$. Making the observation that the instantaneous envelope derivation operator $A[a]$ (see Definition 4.1) vanishes for $a \equiv 1$, as $A[1] = (1)'/1 = 0$, we can see that the parametrization for the modified IMF operator is $(0, \Omega)$ and we can formulate the following

Corollary 4.8. *Let $f \in \mathcal{C}^2(\mathbb{R}, \mathbb{R})$ and $k \geq 4$ (for derivability). $\left\| \tilde{\mathcal{D}}_{(0, \mathbb{B}_k(\Omega))} f \right\|_2^2$ is strictly convex in Ω .*

Proof. This follows directly from Theorem 4.6. □

Given this convexity property, we have a theoretical guarantee that we reach a global minimum for a given input IMF and a unique Ω . As already mentioned earlier, we obtain the desired instantaneous frequency from Ω by inversely applying the inverse square continuous frequency operator in Definition 4.2. This equates to inverting and taking the square root of Ω , which is a relatively simple operation.

4.1.3. Discretization

Given the results from this chapter and especially Theorem 4.6 we will as follows only consider the simple case with constant amplitude $a \equiv 1$ for discretization, as this will also be the only relevant case for the toolbox presented in Chapter 5 given we can't use the differential operator to extract the amplitude anyway.

We have shown in Proposition 4.8 that $\left\| \tilde{\mathcal{D}}_{(0, \mathbb{B}_k(\Omega))} f \right\|_2^2$ is strictly convex in Ω , however, for the discretization we can make two observations to simplify it: The first is that given $\Omega \in \mathbb{R}^n$ we need a system of at least n samples and additional boundary conditions to solve the problem. The second is that given we have a uniform grid we can, instead of minimizing an integral function, minimize at least n samples $\left(\tilde{\mathcal{D}}_{(0, \mathbb{B}_k(\Omega))} f \right) (t_i)$ over Ω . We take this detour as we can see that $\tilde{\mathcal{D}}_{(0, \mathbb{B}_k(\Omega))} f$ is linear in Ω , yielding a least squares problem of the form

$$\|A \cdot \Omega - b\|^2,$$

4. Operator-Based Analysis of Intrinsic Mode Functions

where A is the matrix representing $\tilde{\mathcal{D}}_{(0, \mathbb{B}_k(\Omega))}$ and b is the vector of samples in t_i . This is better than the nonlinear problem we would obtain by just using the squared integral.

Given the precomputation-concepts of the toolbox we make use of the precomputed ‘extended grid’ (see Section 5.4) and evaluate $\tilde{\mathcal{D}}_{(0, \mathbb{B}_k(\Omega))}f$ on the extended grid, obtaining more than n equations, one for each point on the extended grid. This way we obtain implicit boundary conditions, saving us from proposing possibly wrong or ill-chosen ones in the process. See Subsection 5.4.3 for more reflexions on boundary effects.

The instantaneous frequency is calculated from Ω by evaluating $\mathbb{B}_k(\Omega)$, applying an inversion and square root and running a B-splines-fit on the resulting data. Given the nature of the transformation the inverse square continuous frequency operator in Definition 4.2 specifies it is most likely impossible to exploit any B-spline property to circumvent this step and directly work with the B-spline coefficient vector Ω .

4.2. Examples

Following the previous theoretical perspective, this section gives a few examples on the numerical behaviour of the simplified IMF differential operator. For this purpose we restrict ourselves to IMFs with constant instantaneous amplitude $a \equiv 1$ and known analytical form and apply our operator to them. The question is how well we manage to extract the instantaneous phase ϕ , which we can assess by comparing the results to the ground truth. The examples were implemented using the ETHOS-toolbox and can be found in Listing D.2.3.

The parameters (k, q, n) given in the figure captions refer to the spline order k , in-fill-count q (see Section 5.4) and number of B-spline basis functions n . See Subsection 5.4.3 for a discussion on the boundary effects of these examples in the context of information theory and other literature.

Example 4.9 (Constant frequency). *As an introduction consider the simple IMF*

$$u_0(t) := \cos(\phi_0(t)) := \cos(40 \cdot t), \quad (4.3)$$

on the interval $[0, 1]$ (see Figure 4.1). The analytical instantaneous frequency ϕ'_0 is 40, i.e. the IMF is of constant frequency.

Given the instantaneous amplitude is constantly 1, we can use the toolbox to fit the simple IMF differential operator to u_0 to calculate the numerical instantaneous frequency $\tilde{\phi}'_0$.

The difference between ϕ'_0 and $\tilde{\phi}'_0$ is too small to be visible in a normal plot and thus we examine the semi-log plot of the relative error (see Figure 4.2). We can see that the relative error is at most 0.1% briefly at the beginning and stays below 10^{-4} on the remaining interval.

Example 4.10 (Harmonic peaks). *Consider the simple IMF*

$$u_1(t) := \cos(\phi_1(t)) := \cos(3 \cdot \sin(3 \cdot \pi \cdot t) + 16 \cdot \pi \cdot t), \quad (4.4)$$

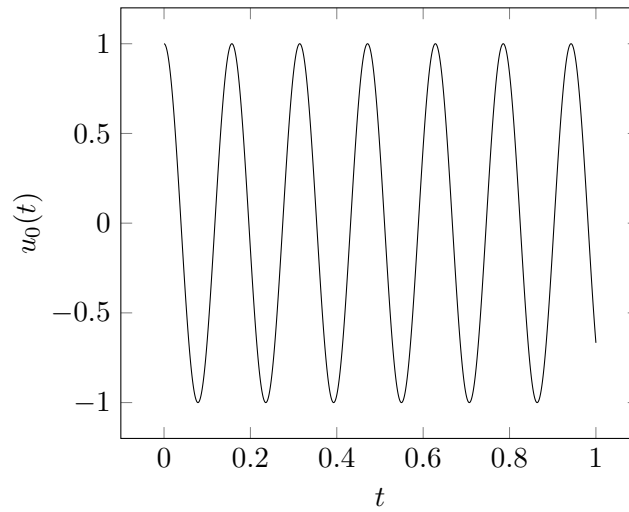


Figure 4.1.: Plot of the IMF u_0 (see (4.3)) from Example 4.9.

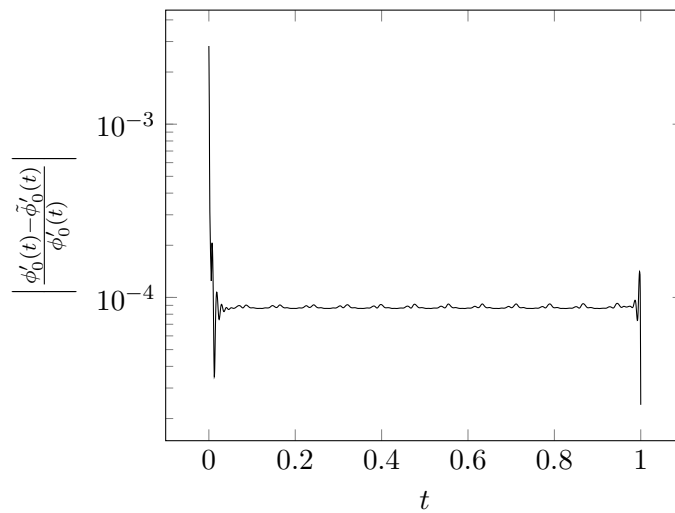


Figure 4.2.: Semi-log plot of the relative error between the analytical instantaneous frequency $\phi'_0 = 40$ and the solution $\tilde{\phi}'_0$, obtained using the IMF differential operator for $(k, q, n) = (4, 4, 180)$, from Example 4.9.

4. Operator-Based Analysis of Intrinsic Mode Functions

on the interval $[0, 1]$ (see Figure 4.3). It is easy to analytically obtain the instantaneous frequency ϕ'_1 of the signal by calculation, namely

$$\phi'_1(t) = 9 \cdot \pi \cdot \cos(3 \cdot \pi \cdot t) + 16 \cdot \pi, \quad (4.5)$$

which you can find pictured in Figure 4.4.

Given the IMF has constant instantaneous amplitude 1 we can use the toolbox to fit the simple IMF differential operator to u_1 to calculate the numerical instantaneous frequency $\tilde{\phi}'_1$. As can be seen the instantaneous frequency itself is a wave function too, explaining the irregular shape of the IMF.

The difference between ϕ'_1 and $\tilde{\phi}'_1$ is too small to be visible in a normal plot and we thus examine the semi-log plot of the relative error (see Figure 4.5). We can see that the relative error is at most 1% briefly at the beginning and between 1 and 4 orders of magnitude lower on the remaining interval.

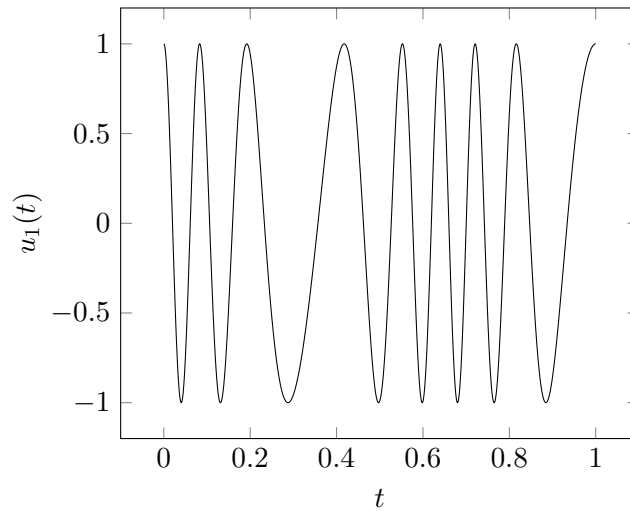


Figure 4.3.: Plot of the IMF u_1 (see (4.4)) from Example 4.10.

Example 4.11 (Sigmoid up-chirp). *An aspect of interest is an IMF with rapidly increasing frequency in a short timeframe. We want to know how well our differential operator handles such a case.*

A signal whose frequency changes over time is called a ‘chirp’, and one with increasing frequency over time an ‘up-chirp’. Even with a rapid increase, as with all natural phenomena, we can reasonably expect our frequency to still be smooth. This is best illustrated if we compare the frequency with velocity. We can not have sudden changes in velocity of an object either, as it would imply infinite acceleration in that moment. To take the idea further, we can not have sudden changes in the acceleration either, as it would imply infinite jerk (rate of change of acceleration) in that moment, et cetera.

A good modelling function for this is a sigmoid function, more precisely the logistic

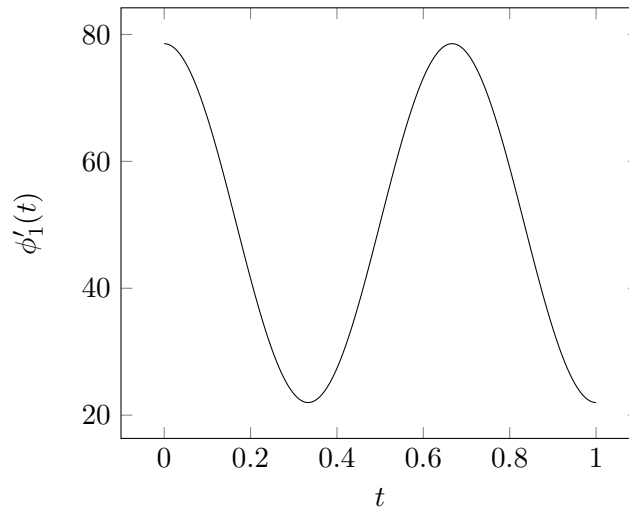


Figure 4.4.: Plot of the analytical instantaneous frequency ϕ'_1 (see (4.5)) from Example 4.10.

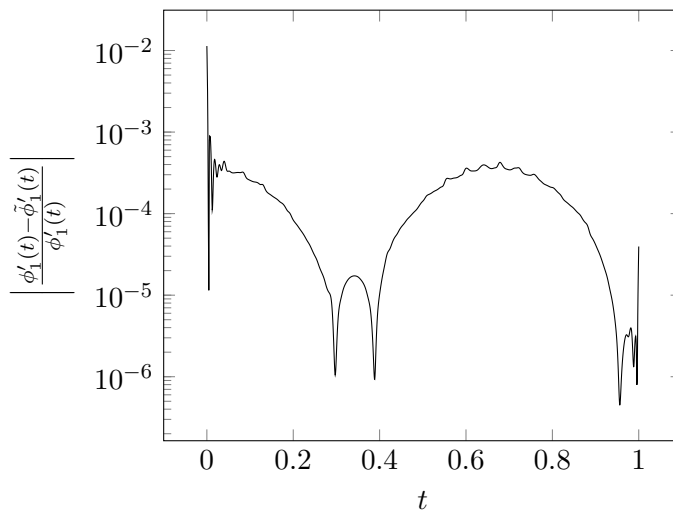


Figure 4.5.: Semi-log plot of the relative error between the analytical instantaneous frequency ϕ'_1 (see (4.5)) and the solution $\tilde{\phi}'_1$, obtained using the IMF differential operator for $(k, q, n) = (4, 4, 180)$, from Example 4.10.

4. Operator-Based Analysis of Intrinsic Mode Functions

function, which we will make use of in this example. Consider the simple IMF

$$u_2(t) := \cos(\phi_2(t)) := \cos\left(40 \cdot t + \frac{100}{90} \cdot \ln(1 + \exp(90 \cdot (t - 0.5)))\right) \quad (4.6)$$

on the interval $[0, 1]$ (see Figure 4.6). We calculate the instantaneous frequency ϕ_2' , which happens to be a transformation of the logistic function, analytically as

$$\phi_2'(t) = 40 + \frac{100}{1 + \exp(-90 \cdot (t - 0.5))}. \quad (4.7)$$

You can find it pictured in Figure 4.7. It represents a sudden frequency increase from 40 to 140 in a very short timeframe around the middle of the interval $[0, 1]$.

As in Example 4.10, given the instantaneous amplitude is constantly 1, we can use the toolbox to fit the simple IMF differential operator to u_2 to calculate the numerical instantaneous frequency $\tilde{\phi}_2'$.

The difference between ϕ_2' and $\tilde{\phi}_2'$ is too small to be visible in a normal plot and thus we examine the semi-log plot of the relative error (see Figure 4.8). We can see that the relative error is at most roughly 0.1% and ranges between around 2 orders of magnitude below that.

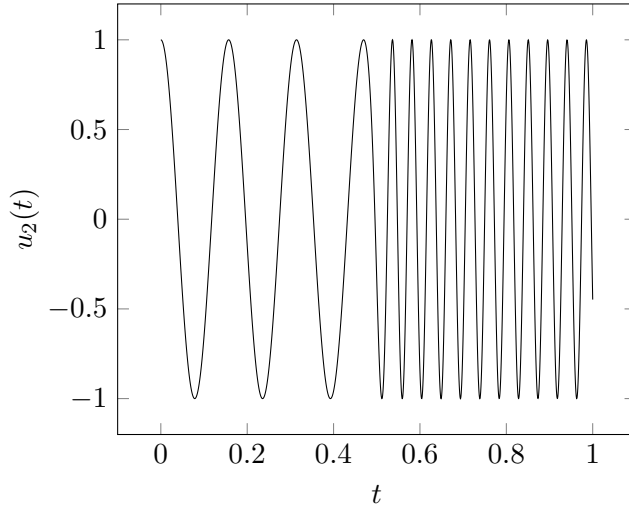


Figure 4.6.: Plot of the IMF u_2 (see (4.6)) from Example 4.11.

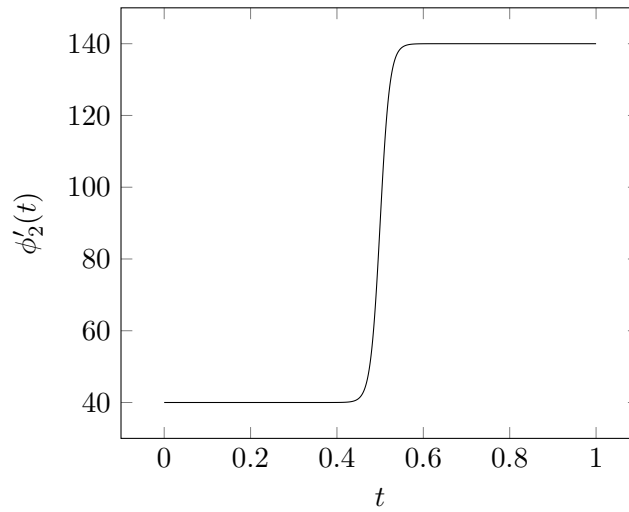


Figure 4.7.: Plot of the analytical instantaneous frequency ϕ'_2 (see (4.7)) from Example 4.11.

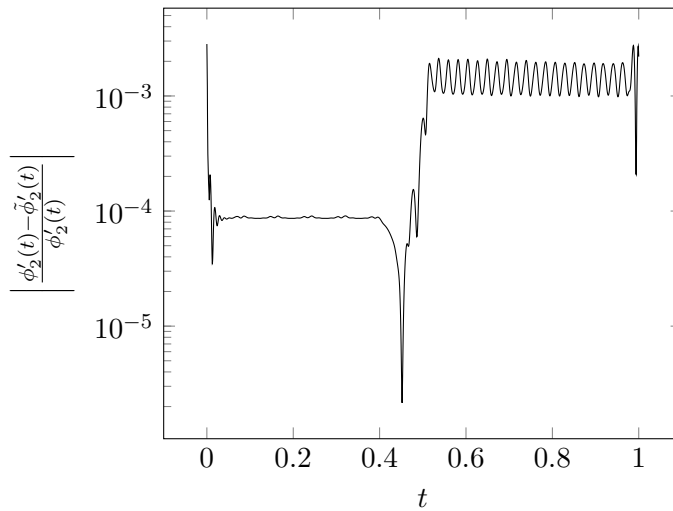


Figure 4.8.: Semi-log plot of the relative error between the analytical instantaneous frequency ϕ'_2 (see (4.7)) and the solution $\tilde{\phi}'_2$, obtained using the IMF differential operator for $(k, q, n) = (4, 4, 180)$, from Example 4.11.

4.3. Discussion

In this chapter we have examined the IMF differential operator (see Definition 4.3) as a possible means to extract instantaneous amplitude and frequency from an IMF and to regularize the EMD optimization problem introduced in Definition 3.17. What we noticed in Theorem 4.6 is that the IMF differential operator is not convex in the parameters corresponding to amplitude and frequency, which is why we modified it in Definition 4.5 to work only on IMFs with constant amplitude 1 and only extract the frequency, which we proved in Corollary 4.8. Consequently, we showed in the examples in Section 4.2 that the operator, as expected, successfully extracts the frequency from given IMFs with constant amplitude 1.

The limitation to IMFs with constant amplitude 1 appears to be a drastic limitation, but we show in Chapter 5 how to work around it and extract the amplitude already during the EMD sifting process. However, when considering the EMD optimization problem from Definition 3.17 the general differential operator from Definition 4.3 is unsuitable as a general regularization term $R(a, \phi)$ from a theoretical perspective. Given we have shown that it is not convex, one can even consider it to be more of a heuristic tool.

5. Hybrid Operator-Based Methods

This chapter is the culmination of the results obtained in the previous chapters. In Chapter 3 we formulated and analyzed the optimization problem (see Equation (3.7))

$$\begin{aligned} \min_u \quad & \|s - \mathcal{I}[a, \phi]\|_2^2 \\ \text{s.t.} \quad & (a, \phi) \in \mathcal{S}_{\mu_0, \mu_1, \mu_2} \end{aligned}$$

In particular we have shown that this optimization problem can also be expressed as a regularized optimization problem (see Section 3.4)

$$\min_{(a, \phi) \in (\mathcal{C}^0(\mathbb{R}, \mathbb{R}))^2} c[s](a, \phi) + R(a, \phi).$$

$R(a, \phi)$ is a regularization term that punishes solution candidates of the optimization problem that are not an IMF soul (see Definition 3.1).

In Chapter 4 we introduced one possible way to define this regularization term. We made use of a differential operator $\mathcal{D}_{(\tilde{a}, \tilde{\phi})}$ with parameters \tilde{a} and $\tilde{\phi}$ that annihilates IMF functions $u(t) := a(t) \cdot \cos(\phi(t))$ when $\tilde{a} = a$ and $\tilde{\phi} = \phi$. Unfortunately, this operator does not yield unique results for a given input IMF (see Theorem 4.6) and thus is highly reliant on heuristics to work.

However, when reduced to input IMFs with constant amplitude 1, the differential operator is convex and the resulting frequency for an IMF is unique (see Corollary 4.8). This result does not look very useful, but can be leveraged when combined with the classic EMD method proposed by [HSL⁺98]. The result of this combination is a hybrid of classic and modern methods and will be introduced later in this chapter. Before considering this approach, we first introduce the classic EMD method.

5.1. Classic EMD method

The classic EMD method was first proposed in [HSL⁺98] and will be described as follows. The EMD is a multistep method, but we will without loss of generality only consider a single extraction step. In this step we separate a given multicomponent signal $s(t)$ into an IMF $u(t)$ and a residual $r(t)$. This is without loss of generality, as subsequent extraction steps are realized by considering the residual of the previous step as the input signal for the current step. Continuing this process, we sooner or later obtain a residual that does not contain any more IMFs. The stopping criterion might for instance be when the residual has no or at most one local extremum, but this is not within the scope of this thesis.

5. Hybrid Operator-Based Methods

After the separation of $s(t)$ into $u(t)$ and $r(t)$, one can determine the instantaneous amplitude $a(t)$ and phase $\phi(t)$ of $u(t) := a(t) \cdot \cos(\phi(t))$ by complexification of $u(t)$ using the HILBERT transform, which will not be further elaborated here. We note here though that this HILBERT transform provides some numerical challenges. In particular, it requires heuristics to work properly in the numerical context, which is why alternatives to this approach are desired and presented in this thesis.

The process of separation is called ‘sifting’ in the original paper [HSL⁺98] and commonly referred to as the empirical mode decomposition (EMD). The extraction of $a(t)$ and $\phi(t)$ from $u(t)$ is called the ‘HILBERT spectral-analysis’ (HSA). The complete process of EMD and HSA is referred to as the ‘HILBERT-HUANG-transform’ (HHT). Of note here is though that because the HHT describes a very specific approach using the HILBERT transform, one finds that the term ‘EMD’ is often used to also include the spectral analysis part that makes use of some other method.

The sifting method of separating the signal $s(t)$ into an IMF $u(t)$ and residual $r(t)$ can be separated into three steps, illustrated in Figure 5.1 and given in Algorithm 5.1. The

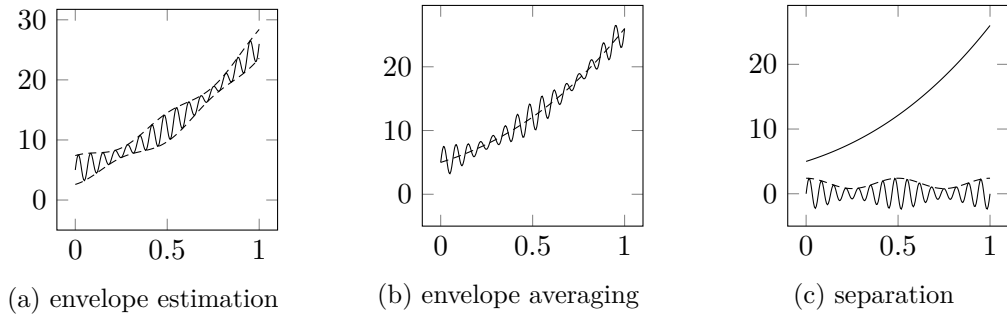


Figure 5.1.: Visualization of the EMD sifting process of a 1-component signal.

input : multicomponent signal $s \in \mathcal{C}^2(\mathbb{R}, \mathbb{R})$
output: intrinsic mode function $u \in \mathcal{C}^2(\mathbb{R}, \mathbb{R})$
instantaneous amplitude $a \in \mathcal{C}^2(\mathbb{R}, \mathbb{R})$
residual $r \in \mathcal{C}^2(\mathbb{R}, \mathbb{R})$

```

 $\underline{a} \leftarrow \text{LowerEnvelope}(s);$ 
 $\bar{a} \leftarrow \text{UpperEnvelope}(s);$ 
 $r \leftarrow \frac{1}{2} \cdot (\underline{a} + \bar{a});$ 
 $u \leftarrow s - r;$ 
 $a \leftarrow \bar{a} - r;$ 

```

Algorithm 5.1.: EMD sifting algorithm.

first step is to estimate the lower and upper envelopes $\underline{a}(t)$ and $\bar{a}(t)$ of the input signal. What an envelope is exactly will be defined later. The second is to take the average of $\underline{a}(t)$ and $\bar{a}(t)$, yielding the residual $r(t)$, and the third is to separate the signal into

residual and IMF $u(t)$ by subtracting $r(t)$ from $s(t)$. The instantaneous amplitude $a(t)$ of $u(t) := a(t) \cdot \cos(\phi(t))$ follows naturally by subtracting r from the upper envelope \bar{a} .

From this observation we can conclude two things: The first is that the envelope estimation is central to the EMD method. The second is that given we obtain the IMF $u(t)$ and its instantaneous amplitude $a(t)$ naturally from the sifting process, we can make use of our differential operator to extract the instantaneous phase $\phi(t)$. This is because the IMF $\tilde{u}(t) := u(t)/a(t)$ has amplitude 1 and makes it possible to use the differential operator introduced in Chapter 4 in a theoretically meaningful way. What is left to do is to analyze the envelope estimation method itself, which we will do as follows.

5.2. Envelope Estimation

An envelope is not uniquely classified, but defined as a function that encloses a function either from above ('upper envelope') or below ('lower envelope').

Definition 5.1 (Lower/upper envelope). *Let $v, f \in C^0(\mathbb{R}, \mathbb{R})$. v is a lower envelope of f if and only if*

$$v \preceq f.$$

v is an upper envelope of f if and only if

$$v \succeq f.$$

As an example, an upper envelope for $\cos(t)$ is the constant function 1 and a lower envelope is the constant function -1 , but we can also choose 2 and -2 or $\cos(t)$ for both as lower and upper amplitudes (see Figure 5.2). We can thus note that by far there

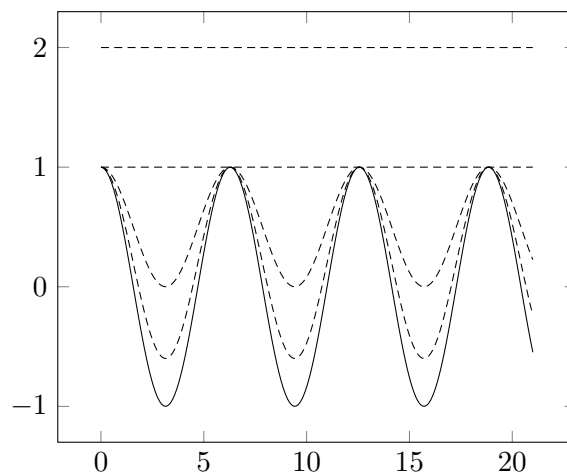


Figure 5.2.: Examples (dashed) for upper envelopes of $\cos(t)$ (solid).

is no unique choice for a lower and upper envelope of a function and we will have to specify more requirements the envelopes have to fulfill. In the context of the empirical

5. Hybrid Operator-Based Methods

mode decomposition, determining the lower and upper envelopes of an input signal is the central step to obtain the residual and IMF, as explained in Section 5.1.

As follows, we will, without loss of generality, only consider the upper envelope estimation. The procedure for the lower envelope follows respectively, given the following

Proposition 5.2. *Let $f \in \mathcal{C}^0(\mathbb{R}, \mathbb{R})$ and $v \in \mathcal{C}^0(\mathbb{R}, \mathbb{R})$ be a lower envelope of s . It holds that $-v$ is an upper envelope of $-f$.*

Proof. It holds by Definition 5.1 that $v \preceq f$ and

$$v \preceq f \Leftrightarrow -v \succeq -f. \quad \square$$

Thus, to determine the lower envelope we simply determine the negated upper envelope of the negated input function.

5.2.1. Classic Envelope Estimation

Knowing the requirements for an upper envelope in the context of the empirical mode decomposition listed previously, we now take a look at the classic envelope estimation proposed in [HSL⁺98, Section 5]. When we reconsider the previous example $\cos(t)$ (which has upper envelope 1) we see that the function assumes the value 1 in its local maxima. Consequently, we can propose that an IMF assumes the value of its upper envelope in its local maxima and we obtain the upper envelope by interpolating them. The corresponding algorithm in pseudocode can be found in Algorithm 5.2.

input : multicomponent signal $s \in \mathcal{C}^2(\mathbb{R}, \mathbb{R})$

output: upper envelope $m \in \mathcal{C}^2(\mathbb{R}, \mathbb{R})$

$P \leftarrow \{(t, s(t)) \in \mathbb{R} \times \mathbb{R} \mid s'(t) = 0 \wedge s''(t) < 0\};$

$m \leftarrow \text{Interpolate}(P);$

Algorithm 5.2.: Classic upper envelope estimation algorithm.

The Interpolate-method in the Algorithm is left out by choice and means the fitting of a B-spline-curve to each point in the set p .

The problem is that with varying amplitude the estimated envelope tends to dip below the signal, thus violating the definition of an envelope not to cut the signal at any moment. This is illustrated in Figure 5.3. As we can see, the classic method of interpolating the local maxima reaches its limits very quickly and is in general not a very good envelope estimation method, given it violates the definition.

5.2.2. Iterative Slope Envelope Estimation

There have been multiple approaches to the problem with the intersection of envelope and signal that we described earlier. [HK13, Subsection 2.3] introduced an optimization scheme to obtain the envelope, strictly enforcing the nature of the envelope definition, but

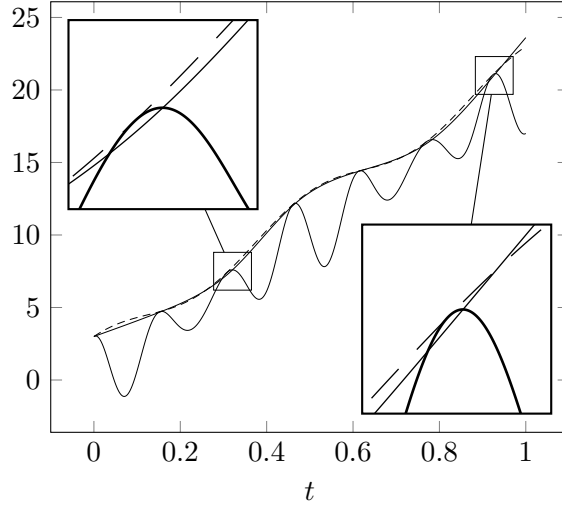


Figure 5.3.: Multicomponent signal s_0 (thick) from Example 5.4 with analytical upper envelope (dashed) and estimated upper envelope using the classic sifting algorithm (thin). Two sections where the latter cuts the signal are enlarged.

at the cost of the smoothness of the resulting amplitude estimation. [HPH12] approached the problem by analytically moving the interpolation points from the local maxima to more fitting spots, with the disadvantage that these approaches only work where it is at least possible to estimate the current frequency. Additionally, it only allows to work with IMFs and not a multicomponent signal, which we are relying on in the sifting process, because it is not possible to easily find analytical results taking the entire multicomponent signal into account.

If we take a step back and think how a human would draw an upper envelope of a signal $s(t)$ by hand, we see that the result $m_0(t)$ of the classic sifting can be considered as a first step toward a better envelope estimation which just needs some refining. We do that by taking $m_0(t)$ and finding every point on the signal $s(t)$ where $m'_0(t) = s'(t)$ (matching slope) and $s''(t) < 0$ (negative curvature) hold. We obtain the upper envelope $m_1(t)$ by interpolating these points. Repeating this process yields a curve with a better fitting, as it becomes by definition a tangential curve.

The algorithm describing this process can be found as pseudocode in Algorithm 5.3. We begin with a multicomponent signal $s(t)$ and a tolerance. Our estimated upper envelope m is first initialized to the zero-function before entering the main loop, in which m is copied to \tilde{m} and m set to the next envelope estimate iterate. If the difference between the previous and current envelope estimate iterate is strictly smaller than our tolerance ε in the supremum norm, we are done.

We make use of the supremum norm given it is easy to calculate a close upper bound of it within the well-conditioned B-spline basis (see 2.12), which amounts to just the supremum norm of the respective vector of B-spline basis coefficients.

Remark 5.3 (Generalization of the classic envelope estimation method). *Let us compare*

5. Hybrid Operator-Based Methods

input : multicomponent signal $s \in \mathcal{C}^2(\mathbb{R}, \mathbb{R})$
 tolerance $\varepsilon > 0$
output: upper envelope $m \in \mathcal{C}^2(\mathbb{R}, \mathbb{R})$
 $m \leftarrow 0 \in \mathcal{C}^0(\mathbb{R}, \mathbb{R});$
repeat
 $\tilde{m} \leftarrow m;$
 $p \leftarrow \{t \in \mathbb{R} \mid s'(t) = \tilde{m}'(t) \wedge s''(t) < 0\};$
 $m \leftarrow \text{Interpolate}(p);$
until $\|m - \tilde{m}\|_\infty < \varepsilon;$

Algorithm 5.3.: Iterative slope upper envelope estimation algorithm.

Algorithms 5.2 and 5.3. We remind ourselves that to determine the upper envelope, the classic method interpolates the local maxima. The slope in the maxima is 0 and the curvature is negative. It is easy to see that the first iteration of the iterative slope envelope algorithm is simply the classic envelope estimation, because the slope of the 0-function is also zero. Thus, all slope matches in the signal are those where the slope is zero.

Forcing the algorithm to finish after the first iteration by setting $\varepsilon = \infty$ we obtain the classic method. We can thus say that the proposed upper envelope estimation algorithm is a generalization of the classic algorithm.

Obtaining the lower envelope of a given input signal s is analogous to Proposition 5.2 by determining the negative upper envelope of the negated input signal $-s$. Given these negations are linear time operations there is no effect on the run-time of the algorithm regardless of whether we estimate the upper or lower envelope.

An advantage of this algorithm over the method presented in [HPH12] is that we do not need to estimate the instantaneous frequency and do not require the input signal to have any special form. Given our new method is a generalization of the classic envelope estimation, it fits more naturally into the existing methods. Moreover, we solve the intersection problem as described in Figure 5.3 and obtain meaningful envelopes that satisfy the definition.

5.2.3. Examples

The following examples were implemented using the ETHOS-toolbox developed in the course of this thesis and can be found in Listing D.2.2. The parameters (k, q, n, ε) given in the figure captions refer to the spline order k , in-fill-count q (see Section 5.4), number of B-spline basis functions n (see Definition 2.5) and envelope extraction tolerance ε (see Algorithm 5.3). See Subsection 5.4.3 for a discussion on the boundary effects of these examples in the context of information theory and other literature.

Example 5.4 (Ladder). *Consider the composite signal*

$$s_0(t) := 40 \cdot t + (20 + 10 \cdot \cos(5 \cdot \pi \cdot t)) \cdot \cos(25 \cdot \pi \cdot t) \quad (5.1)$$

on the interval $[0,1]$. Beginning with the highest frequency component, the first analytical envelope to be extracted by the sifting process is

$$m_0(t) := 40 \cdot t + (20 + 10 \cdot \cos(5 \cdot \pi \cdot t)). \quad (5.2)$$

In Figure 5.4 you can see the result of the proposed iterative slope sifting process compared with the analytical envelope m_0 .

Due to the little differences in most parts we examine the semi-log plot of the relative error (see Figure 5.5) for both the classic and iterative slope sifting processes. We can see that the relative error for the proposed iterative slope method is up to an order of magnitude less in some parts while staying equally good e.g. in the boundary regions, which is more due to an information theoretical reason and not a quality criterion of the sifting algorithm.

What is more important is that the iterative slope envelope is a true envelope in that it does not cut the signal in any location like the envelope obtained with the classic sifting algorithm. This is due to the fact that the iterative slope envelope is a tangent by construction.

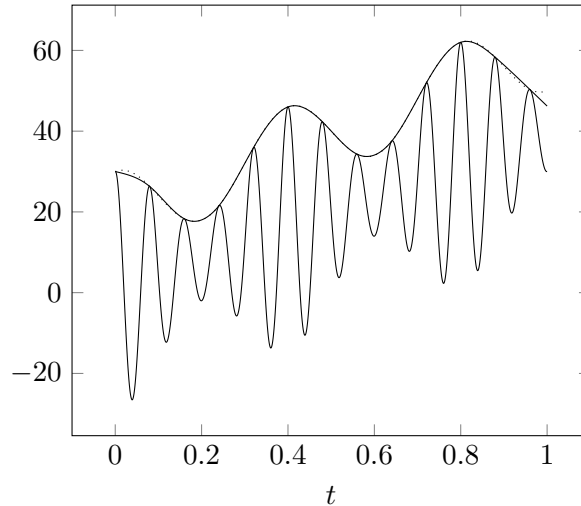


Figure 5.4.: Plot of the multicomponent signal s_0 (see (5.1)), its analytical highest frequency component envelope m_0 (dotted) (see (5.2)) and calculated iterative slope envelope (thin) for $(k, q, n, \varepsilon) = (4, 4, 180, 0.01)$ from Example 5.4.

Example 5.5 ([HPH12, Figure 2]). Consider the IMF

$$s_1(t) := \frac{1}{16} \cdot (t^2 + 2) \cdot \cos(\pi \cdot \sin(8 \cdot t) + \pi) \quad (5.3)$$

on the interval $[-4,4]$. The analytical envelope to be extracted by the sifting process is

$$m_1(t) := t^2 + 2. \quad (5.4)$$

5. Hybrid Operator-Based Methods

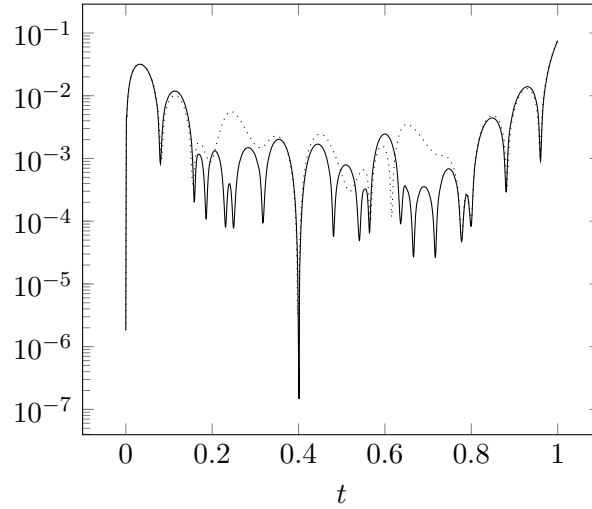


Figure 5.5.: Semi-log plot of the relative errors between the analytical highest frequency component envelope m_0 (see (5.2)) and both the envelopes obtained using the classic (dotted) and iterative slope sifting algorithms for $(k, q, n, \varepsilon) = (4, 4, 180, 0.01)$ from Example 5.4.

In Figure 5.6 you can see the result of the proposed iterative slope sifting process compared with the analytical envelope m_1 .

Due to the little differences in most parts we examine the semi-log plot of the relative error (see Figure 5.7) for both the classic and iterative slope sifting processes. We can see that the relative error for the proposed iterative slope method is equal to that of the classic sifting method and even up to an order of magnitude lower in the increasing branch of s_1 .

The reason the error is not symmetric like that of the classic sifting method is because even though the maxima are symmetrically distributed, s_1 itself is not symmetric. The classic sifting method only considers the maxima though and thus is oblivious to the shape of s_1 itself, unlike the iterative slope method.

What we can clearly see is that the newly presented iterative slope sifting algorithm provides a better envelope estimation than the classic sifting algorithm. Of note is especially the intuition behind it and the fact that it is a generalization of the classic method. For this reason, we will make use of it in our hybrid EMD algorithm presented in the next section.

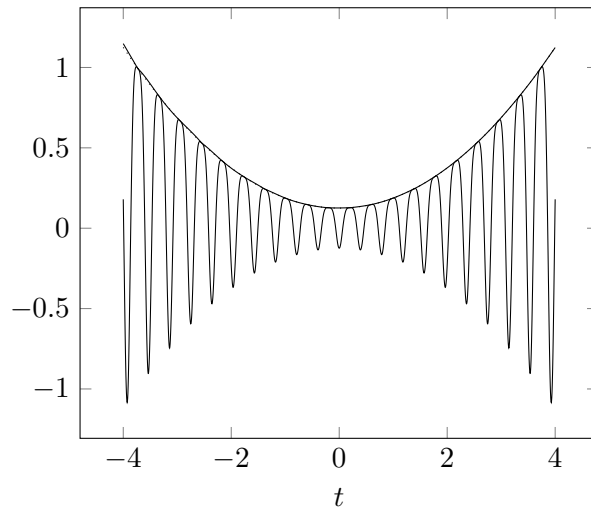


Figure 5.6.: Plot of the multicomponent signal s_1 (see (5.3)), its analytical highest frequency component envelope m_1 (dotted) (see (5.4)) and calculated iterative slope envelope (thin) for $(k, q, n, \varepsilon) = (4, 4, 180, 0.1)$ from Example 5.5.

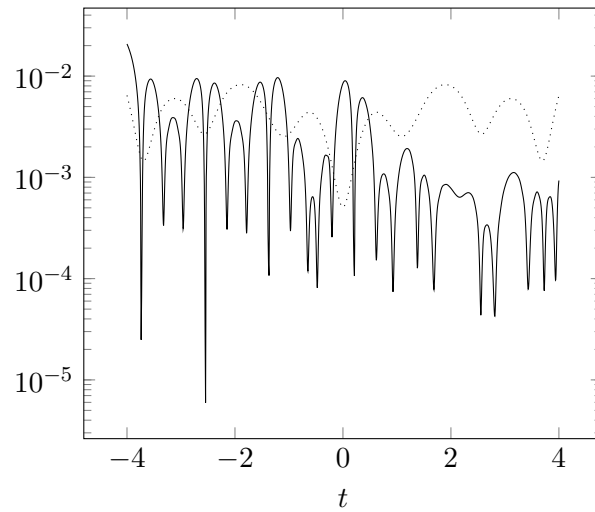


Figure 5.7.: Semi-log plot of the relative errors between the analytical highest frequency component envelope m_1 (see (5.4)) and both the envelopes obtained using the classic (dotted) and iterative slope sifting algorithms for $(k, q, n, \varepsilon) = (4, 4, 180, 0.1)$ from Example 5.5.

5.3. Hybrid EMD Algorithm

This section presents a new EMD algorithm making use of the new iterative slope sifting algorithm and the differential- operator-based method presented earlier. Given the former is considered a more classic approach compared to the operator-based signal-separation and the latter operator-based method is a modern concept it is fitting to call this algorithm a ‘hybrid’ algorithm. The entire procedure for a single step of the decomposition is given in Algorithm 5.4, but we will construct the method step by step in the following section for a given multicomponent signal s . The complete decomposition is obtained by successive runs of the algorithm with the residual subtracted from the signal as the input for the next step.

input : multicomponent signal $s \in \mathcal{C}^2(\mathbb{R}, \mathbb{R})$
 tolerance $\varepsilon > 0$
output: intrinsic mode function $u \in \mathcal{C}^2(\mathbb{R}, \mathbb{R})$
 instantaneous amplitude $a \in \mathcal{C}^2(\mathbb{R}, \mathbb{R})$
 instantaneous frequency $\phi' \in \mathcal{C}^2(\mathbb{R}, \mathbb{R})$
 residual $r \in \mathcal{C}^2(\mathbb{R}, \mathbb{R})$

$\bar{a} \leftarrow \text{UpperEnvelope}(s, \varepsilon);$
 $\underline{a} \leftarrow -\text{UpperEnvelope}(-s, \varepsilon);$
 $r \leftarrow \frac{1}{2} \cdot (\bar{a} + \underline{a});$
 $u \leftarrow s - r;$
 $a \leftarrow \bar{a} - r;$
 $\Omega^* \leftarrow \arg \min_{\Omega \in \mathcal{C}^2(\mathbb{R}, \mathbb{R})} \left(\left\| \tilde{\mathcal{D}}_{(0, \Omega)}(u/a) \right\|_2^2 \right);$
 $\phi' \leftarrow \frac{1}{\sqrt{\Omega^*}};$

Algorithm 5.4.: Hybrid operator-based empirical mode decomposition algorithm.

The first step is to determine the upper and lower envelopes \bar{a} and \underline{a} of s . We make use of the fact that the lower envelope is just the negation of the upper envelope of the negated signal s . This is why we previously only considered the upper envelope estimation, as the lower envelope estimation follows as a corollary.

The idea behind the following steps to obtain r , u and a were first introduced in [HSL⁺98]. Once we’ve determined \bar{a} and \underline{a} we can calculate the residual r as their mean. The intrinsic mode function u is obtained by subtracting r from s and the instantaneous amplitude a is calculated by subtracting r from \bar{a} .

Next we use the simple case (see Subsection 4.1.2) of the modified IMF differential operator (see Definition 4.5) to obtain our instantaneous frequency. We first solve the NSP optimization problem for the inverse square continuous frequency operator $\Omega[\phi]$ (see Definition 4.2) and then calculate the instantaneous frequency directly by applying the inverse square root.

5.4. ETHOS Toolbox

The central numerical piece of this thesis is the ETHOS toolbox. It stands for ‘EMD Toolbox using Hybrid Operator-Based Methods and B-splines’ and has been developed in the course of this thesis to provide an implementation for the new concepts presented in this work, making it possible to do an empirical mode decomposition on a discrete input signal. The implementation language is C99 (see [ISO99]), making use of the GNU Scientific Library (see [GDT⁺18]) for the numerical backend (including B-splines). All examples in this and previous chapters have been realized in this toolbox (see Section D.2) and the entire source code is listed under Section D.1.

The main header exposing the toolbox function is `ethos.h` (see Listing D.1.1) with the main datatype `struct ethos`. Nearly all functions take a `struct ethos` as input and it is the main storage for system parameters and precomputed data.

As follows, we will take a look at the most important functions with regard to the decomposition process. For all exposed functions refer to `ethos.h` (see Listing D.1.1).

5.4.1. Initialization and Precomputation

The main initialization and first step of any program using the ETHOS toolbox is done by `ethos_init()` (see Listing D.1.2). It takes a pointer to an ETHOS-struct `e`, vector `T` of length `N` with spline order `k`, in-fill-count `q`, density `d` and grid-type `g` as input and fills the given ETHOS-struct with the necessary parameters and precomputes data for later use. The parameters are explained as follows.

The vector `T` contains all time-steps of the discrete input signal, or comparable like a superset of multiple possible interpolation areas, and it is our interest to only take a certain subset of these steps for our spline knot-vector. This is controlled by the parameters `d`, controlling the density of the spline knot vector relative to the input vector and residing in the interval $(0, 1)$, and `g`, controlling the way the selection is made (uniformly or adaptively).

When the spline knot-vector is obtained, it is uniformly in-filled with `q` points between each spline knot. The motivation for this process is to be able to pre-evaluate the splines and their derivatives during the initialization step on this ‘extended grid’ (i.e. the in-filled knot-vector). The reason why the knot-vector is not just made denser is because we want to limit the number of basis functions and for the sake of plotting or general evaluation do not need so many basis functions, because B-splines as is provide a great amount of smoothness.

The evaluation happens only for the non-zero parts of each basis function, resulting in linear memory complexity for this precomputation step.

On this extended grid the B-splines and their first and second derivatives are evaluated and the results stored in `dB` within the ETHOS struct, just like the spline knot-vector in `grid` and in-filled form in `extgrid`.

The size of the B-spline basis `n` is of great importance, as each function is stored internally as a vector of this length, corresponding as coefficients of the B-spline basis.

5.4.2. Data Filtering

After initialization, the next step is to filter the discrete input data, with the goal of obtaining the B-spline coefficients for this given function on the initialized grid. The function for this purpose is `ethos_fit()` (see Listing D.1.2) and it takes an arbitrary discrete input signal \mathbf{S} with the time-steps \mathbf{T} , which do not have to agree completely with the \mathbf{T} used in the initialization, but should agree on the start- and endpoints.

During the fitting process, the B-splines of the initialized basis are evaluated on all points in \mathbf{T} and a weighted least-squares system solved with a set of low-weight smoothness-terms of second order besides the interpolation terms for each given data-point. It returns the B-spline coefficients in \mathbf{s} best fitting the given discrete input data as a vector, which is the standard way of handling functions within the toolbox. Even though not explicitly expressed, all of the coefficient vectors have length \mathbf{n} found in the ETHOS struct.

5.4.3. Boundary Effects and Extension

The boundary effects we have seen in the previous examples opens up some questions that will be addressed here. As you can, for example, see in Figure 5.17 the error goes up as it reaches the boundary. A common countermeasure often (silently) employed in the literature is to extend the signal beyond the boundary, either by mirroring or other methods (see [WR10] for further reading). This way, the ‘shock’ the algorithm is exposed to is moved into the mirrored section or dampened, not as heavily affecting the interior part one actually cares about.

When looking at this matter in an information theoretical way this technique of extension is rather dishonest about the performance of such an algorithm and generates information where there is none. It might be forgivable for applications that care about a good representation, but the real challenge is to design robust algorithms and make them comparable among each other without silent tricks like this one. Moreover, there is not a canonical way to extend beyond the boundary and it presents itself more as its own field of research. This is the reason why the author chose not to use boundary extension methods for his examples and keep them honest with regard to the boundary effects.

Despite these ethical concerns, the ETHOS toolbox includes `ethos_extend_boundary()` (see Listing D.1.2) which takes an arbitrary discrete input signal \mathbf{S} with the time-steps \mathbf{T} and length \mathbf{N} and calculates an extended signal \mathbf{Se} with the time-steps \mathbf{Te} and length \mathbf{Ne} by mirroring the signal into the extended area. This extension is parametrized by `ratio` between 0 and 1, extending the signal by this fraction both on the left and right side.

5.4.4. Decomposition

The function to do the signal decomposition itself is `ethos_emd()` (see Listing D.1.2). It takes a pointer to an ETHOS-struct \mathbf{e} , B-spline coefficient vectors \mathbf{u} of the output IMF,

\mathbf{a} of the amplitude of the output IMF, \mathbf{freq} of the frequency of the output IMF and \mathbf{s} of the input signal of length n and tolerance \mathbf{eps} .

The procedure aligns with Algorithm 5.4, filling the input signal vector \mathbf{s} with the residual and \mathbf{u} , \mathbf{a} and \mathbf{freq} with the extracted IMF and its amplitude and frequency respectively. The tolerance \mathbf{eps} is the tolerance for the iterative slope algorithm (see Algorithm 5.3).

Subsequent invocations of `ethos_emd()` yield the complete decomposition.

5.4.5. Plotting

The ETHOS toolbox provides two ways of plotting data, either as a CSV-output or output meant as input for the `graph(1)` command of the GNU plotting utilities. The input to those plotting functions can either be a set of discrete points or a spline function, represented with a coefficient vector. The former is implemented as `ethos_plot_points()`, the latter as `ethos_plot_spline()` (see Listing D.1.2).

5.4.6. Envelope Estimation

The procedure to estimate the envelope is already used in `ethos_emd()` described in Subsection 5.4.4 and not directly part of the decomposition path, however, it might be of interest to test the envelope estimation itself separately.

This estimation is achieved with `ethos_upper_envelope()` (see Listing D.1.2). It takes a pointer to an ETHOS-struct \mathbf{e} , B-spline coefficient vectors \mathbf{m} of the upper envelope and \mathbf{s} of the input signal and tolerance \mathbf{eps} . The procedure aligns with Algorithm 5.3 and stores the upper envelope estimation of \mathbf{s} in \mathbf{m} with the tolerance \mathbf{eps} .

It can also be used to estimate the envelope using the classic method by setting \mathbf{eps} to `INFINITY` (see Remark 5.3), defined in [Cie97, `math.h`] to represent infinity. This allows an easy comparison of both methods, as done in Subsection 5.2.3.

5.4.7. IMF Characteristic

When we defined intrinsic mode functions in Definition 3.1 we parametrized the model with three parameters (μ_0, μ_1, μ_2) with $\mu_0, \mu_1, \mu_2 > 0$, called the characteristic. We also established the connection with the IMF accuracy presented in [DLW11, Definition 3.1] and the role and calculation of each parameter in Remark 3.8. The former especially underlines the relevance of these parameters and makes it interesting to further explore them instead of just treating them as a theoretical tool.

For the purpose of determining the characteristic for a given IMF, the ETHOS toolbox offers the `ethos_characteristic()` (see Listing D.1.2) function. It takes a pointer to an ETHOS-struct \mathbf{e} , vectors \mathbf{a} and \mathbf{freq} of length n and a vector \mathbf{mu} of length 3, filling \mathbf{mu} with the three characteristic values. The vectors \mathbf{a} and \mathbf{freq} are the B-spline coefficients for the amplitude and frequency functions relative to the current spline environment given with \mathbf{e} .

5. Hybrid Operator-Based Methods

Even though it is not possible to control the characteristic of each extracted IMF during the decomposition it is nevertheless possible to ascertain the quality of the extraction afterwards using this tool.

5.5. Examples

These examples were implemented using the ETHOS-toolbox and can be found in Listing D.2.1. The parameters (k, q, n, ε) given in the figure captions refer to the spline order k , in-fill-count q (see Section 5.4), number of B-spline basis functions n and envelope extraction tolerance ε (see Algorithm 5.4). See Subsection 5.4.3 for a discussion on the boundary effects of these examples in the context of information theory and other literature.

Example 5.6. *This example was inspired by [HS11, Example 1]. Consider the multicomponent signal*

$$s_0(t) := u_{0,0}(t) + u_{0,1}(t) + 20 \cdot (t + 1) \quad (5.5)$$

with the first IMF component (characteristic $\sim (6.60 \cdot 10^1, 1.52 \cdot 10^{-2}, 1.43 \cdot 10^0)$)

$$u_{0,0}(t) := a_{0,0} \cdot \cos(\phi_{0,0}(t)) := (t + 1) \cdot \cos((15 \cdot t + 21) \cdot \pi \cdot t)$$

and the second IMF component (characteristic $\sim (1.57 \cdot 10^1, 1.91 \cdot 10^{-1}, 1.88 \cdot 10^{-12})$)

$$u_{0,1}(t) := a_{0,1} \cdot \cos(\phi_{0,1}(t)) := (3 \cdot t + 1) \cdot \cos(5 \cdot \pi \cdot t).$$

We calculate the instantaneous frequencies $\phi'_{0,0}$ and $\phi'_{0,1}$ of both IMF components $u_{0,0}$ and $u_{0,1}$ as

$$\phi'_{0,0} = 15 \cdot \pi \cdot t + (15 \cdot t + 21) \cdot \pi$$

and

$$\phi'_{0,1} = 5 \cdot \pi.$$

Our objective is to run a full EMD on this input signal s_0 , which means that we, in each step, identify an IMF that we will further analyze to obtain its instantaneous amplitude and frequency. Due to the nature of our HOST-EMD algorithm we first extract high-frequency components only to continue to extract successively lower frequency components in subsequent steps, corresponding to the target in this example to extract $u_{0,0}$ first and then $u_{0,1}$.

In the first step we find the IMF $\tilde{u}_{0,0}$ with instantaneous amplitude $\tilde{a}_{0,0}$ and frequency $\tilde{\phi}'_{0,0}$ (see Figure 5.9). Splitting $u_{0,0}$ analytically from the input signal s_0 we obtain our first residual

$$r_{0,1}(t) := s_0 - u_{0,0} \quad (5.6)$$

(see Figure 5.10), whose calculated form $\tilde{r}_{0,1}$ we will use as the input signal for our second step.

Analogously, we find the IMF $\tilde{u}_{0,1}$ with instantaneous amplitude $\tilde{a}_{0,1}$ and frequency $\tilde{\phi}'_{0,1}$ in the second step (see Figure 5.11) and further splitting $u_{0,1}$ from $r_{0,1}$ analytically yields the second residual

$$r_{0,2}(t) := r_{0,1} - u_{0,1} = s_0 - u_{0,0} - u_{0,1} \quad (5.7)$$

(see Figure 5.12) with its calculated form $\tilde{r}_{0,2}$, which we identify as the last residual given it obviously contains no further IMF components.

Discussing errors is more difficult than in the other examples presented in this thesis as we have two algorithms working in concert, namely the proposed iterative slope sifting and differential operator extraction algorithms. Nevertheless, they turn out to be working independently and what we can note is that the only significant errors are visible at the boundaries of the signal, which is to be expected as it is blind for the analytical nature of the input signal. In the ‘interior’ of the signal, the relative errors range between 10^{-2} and 10^{-6} .

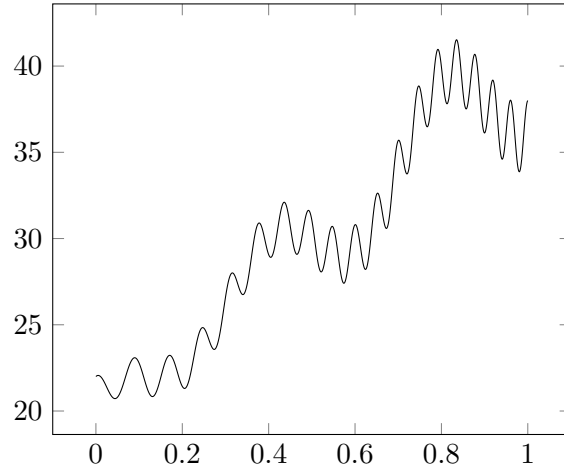


Figure 5.8.: Plot of the multicomponent signal s_0 (see (5.5)) from Example 5.6.

Example 5.7. This example was inspired by [HS11, Example 2]. Consider the multicomponent signal

$$s_1(t) := u_{1,0}(t) + u_{1,1}(t) + 25 \cdot t^3 \quad (5.8)$$

with the first IMF component (characteristic $\sim (2.51 \cdot 10^2, 1.19 \cdot 10^{-2}, 1.88 \cdot 10^{-12})$)

$$u_{1,0}(t) := a_{1,0} \cdot \cos(\phi_{1,0}(t)) := (t + 1) \cdot \cos((15 \cdot t + 21) \cdot \pi \cdot t)$$

and the second IMF component (characteristic $\sim (4.71 \cdot 10^1, 4.24 \cdot 10^{-1}, 2.86 \cdot 10^{-12})$)

$$u_{1,1}(t) := a_{1,1} \cdot \cos(\phi_{1,1}(t)) := (3 \cdot t + 1) \cdot \cos(5 \cdot \pi \cdot t).$$

We calculate the instantaneous frequencies $\phi'_{1,0}$ and $\phi'_{1,1}$ of both IMF components $u_{1,0}$ and $u_{1,1}$ as

$$\phi'_{1,0} = 15 \cdot \pi \cdot t + (15 \cdot t + 21) \cdot \pi$$

5. Hybrid Operator-Based Methods

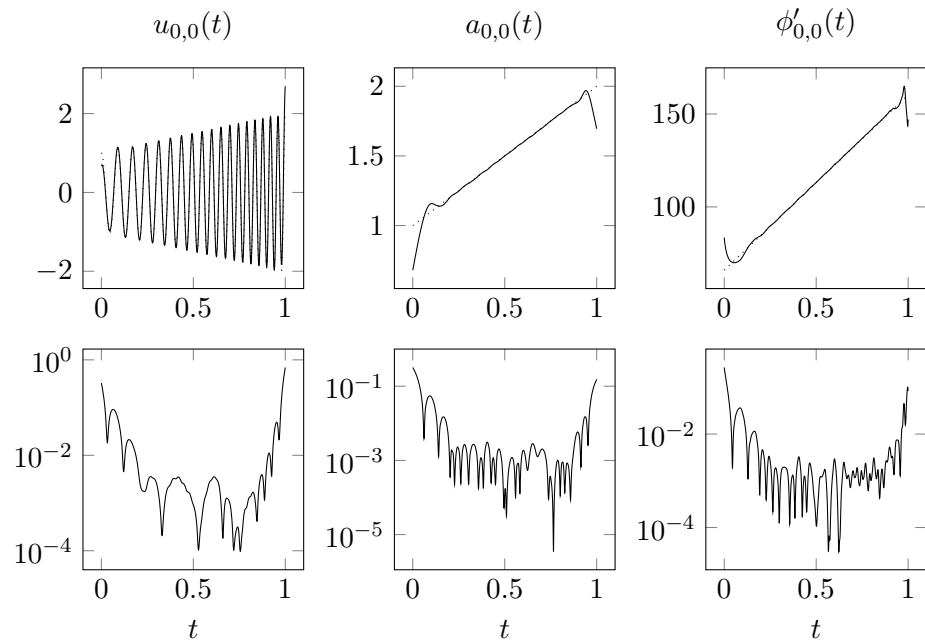


Figure 5.9.: Plots of the first extracted IMF-component $\tilde{u}_{0,0}$ of s_0 (see (5.5)) and its respective instantaneous amplitude $\tilde{a}_{0,0}$ and frequency $\tilde{\phi}'_{0,0}$ in the first row (with analytical solutions $u_{0,0}$, $a_{0,0}$ and $\phi'_{0,0}$ (dotted)) with semi-log plots of the absolute (for $u_{0,0}(t)$) and relative errors (for $a_{0,0}(t)$ and $\phi'_{0,0}(t)$) compared to the analytical solutions in the second row for $(k, q, n, \varepsilon) = (4, 4, 180, 0.01)$ from Example 5.6.

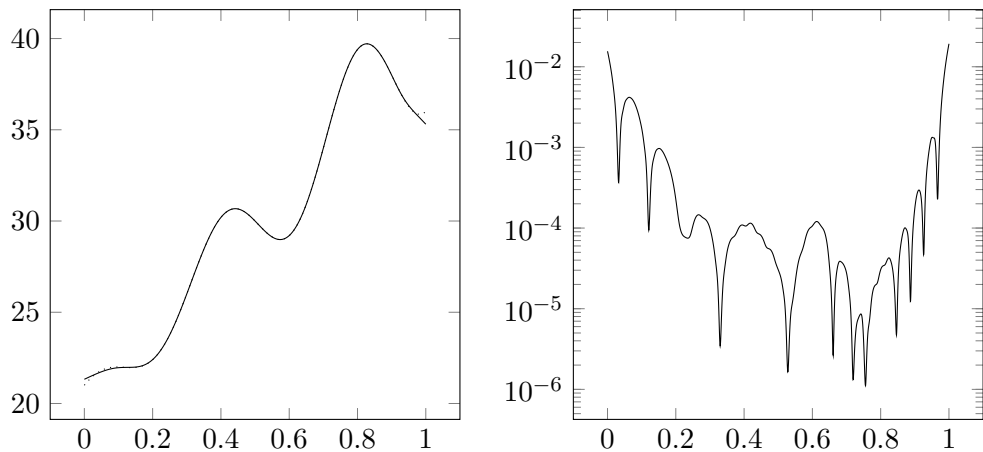


Figure 5.10.: Plots of the calculated first residual $\tilde{r}_{0,1}$ (see (5.6)) and its analytical solution $r_{0,1}$ (dotted) on the left and a semi-log plot of the relative error between both on the right for $(k, q, n, \varepsilon) = (4, 4, 180, 0.01)$ from Example 5.6.

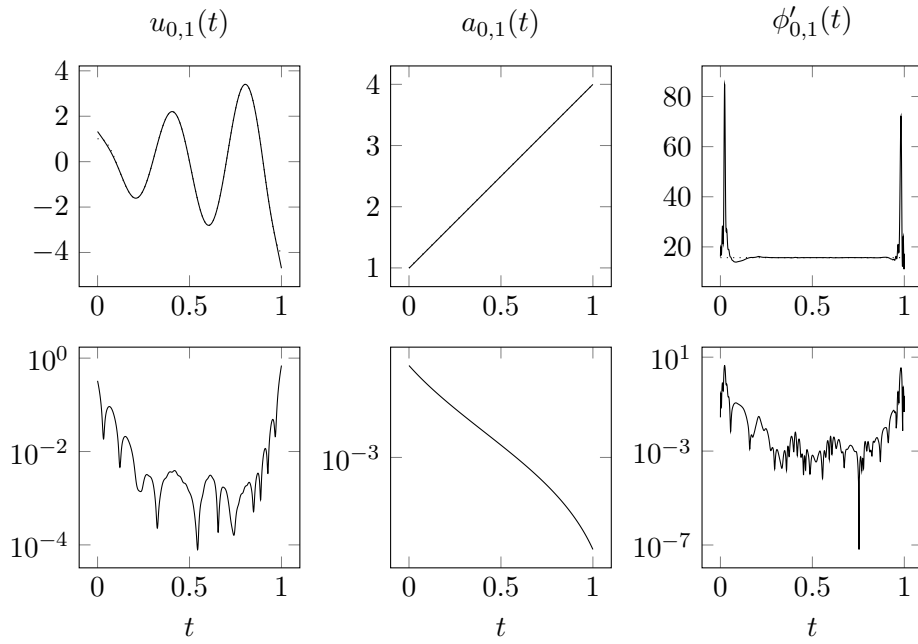


Figure 5.11.: Plots of the second extracted IMF-component $\tilde{u}_{0,1}$ of s_0 (see (5.5)) and its respective instantaneous amplitude $\tilde{a}_{0,1}$ and frequency $\tilde{\phi}'_{0,1}$ in the first row (with analytical solutions $u_{0,1}$, $a_{0,1}$ and $\phi'_{0,1}$ (dotted)) with semi-log plots of the absolute (for $u_{0,1}(t)$) and relative errors (for $a_{0,1}(t)$ and $\phi'_{0,1}(t)$) compared to the analytical solutions in the second row for $(k, q, n, \varepsilon) = (4, 4, 180, 0.01)$ from Example 5.6.

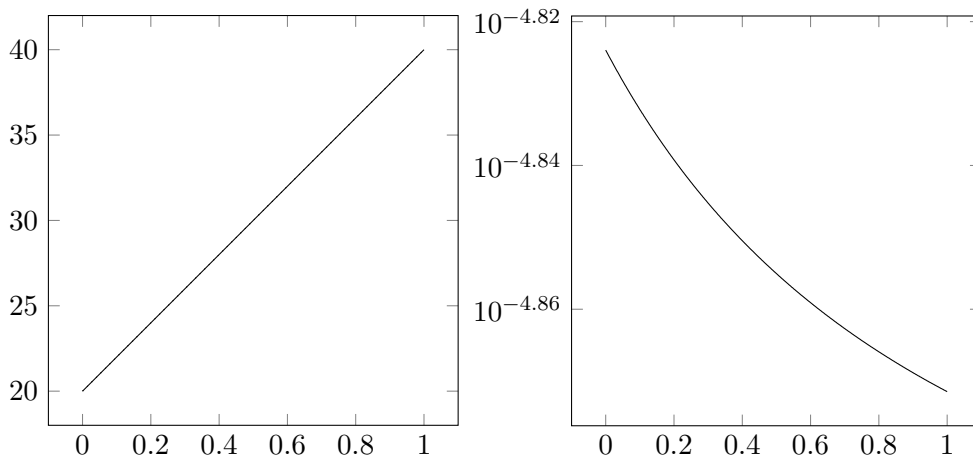


Figure 5.12.: Plots of the calculated second residual $\tilde{r}_{0,2}$ (see (5.7)) and its analytical solution $r_{0,2}$ (dotted) on the left and a semi-log plot of the relative error between both on the right for $(k, q, n, \varepsilon) = (4, 4, 180, 0.01)$ from Example 5.6.

5. Hybrid Operator-Based Methods

and

$$\phi'_{1,1} = 5 \cdot \pi.$$

Our objective is to run a full EMD on this input signal s_0 , which means that we, in each step, identify an IMF that we will further analyze to obtain its instantaneous amplitude and frequency. Due to the nature of our HOST-EMD algorithm we first extract high-frequency components only to continue to extract successively lower frequency components in subsequent steps, corresponding to the target in this example to extract $u_{1,0}$ first and then $u_{1,1}$.

In the first step we find the IMF $\tilde{u}_{1,0}$ with instantaneous amplitude $\tilde{a}_{1,0}$ and frequency $\tilde{\phi}'_{1,0}$ (see Figure 5.14). Splitting $u_{1,0}$ analytically from the input signal s_1 we obtain our first residual

$$r_{1,1}(t) := s_1 - u_{1,0} \quad (5.9)$$

(see Figure 5.15), whose calculated form $\tilde{r}_{1,1}$ we will use as the input signal for our second step.

Analogously, we find the IMF $\tilde{u}_{1,1}$ with instantaneous amplitude $\tilde{a}_{1,1}$ and frequency $\tilde{\phi}'_{1,1}$ in the second step (see Figure 5.16) and further splitting $u_{1,1}$ from $r_{1,1}$ analytically yields the second residual

$$r_{1,2}(t) := r_{1,1} - u_{1,1} = s_1 - u_{1,0} - u_{1,1} \quad (5.10)$$

(see Figure 5.17) with its calculated form $\tilde{r}_{1,2}$, which we identify as the last residual given it obviously contains no further IMF components.

Discussing errors is more difficult than in the other examples presented in this thesis as we have two algorithms working in concert, namely the proposed iterative slope sifting and differential operator extraction algorithms. Nevertheless, they turn out to be working independently and what we can note is that the only significant errors are visible at the boundaries of the signal, which is to be expected as it is blind for the analytical nature of the input signal. In the ‘interior’ of the signal, the relative errors range between 10^{-2} and 10^{-6} .

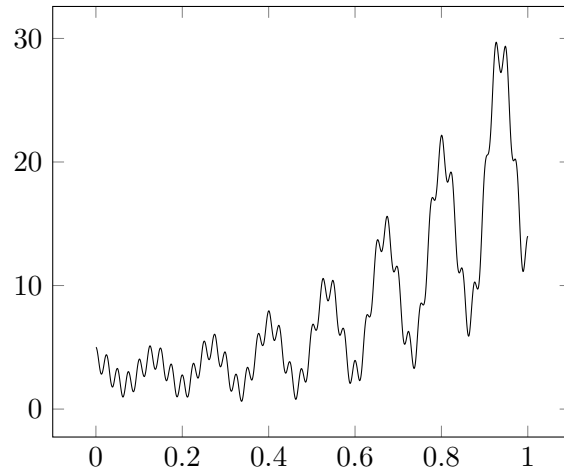


Figure 5.13.: Plot of the multicomponent signal s_1 (see (5.8)) from Example 5.7.

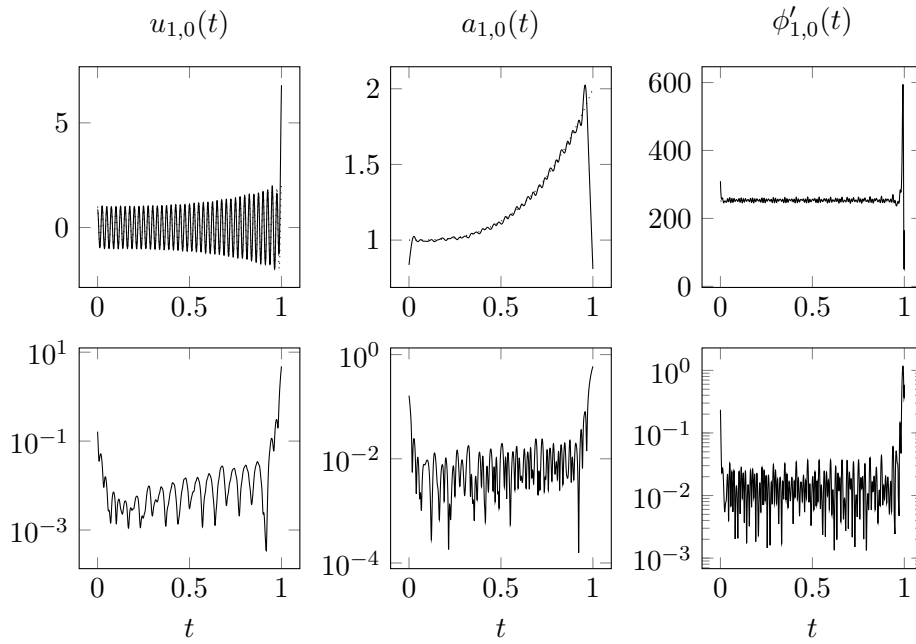


Figure 5.14.: Plots of the first extracted IMF-component $\tilde{u}_{1,0}$ of s_1 (see (5.8)) and its respective instantaneous amplitude $\tilde{a}_{1,0}$ and frequency $\tilde{\phi}'_{1,0}$ in the first row (with analytical solutions $u_{1,0}$, $a_{1,0}$ and $\phi'_{1,0}$ (dotted)) with semi-log plots of the absolute (for $u_{1,0}(t)$) and relative errors (for $a_{1,0}(t)$ and $\phi'_{1,0}(t)$) compared to the analytical solutions in the second row for $(k, q, n, \varepsilon) = (4, 4, 180, 0.01)$ from Example 5.7.

5. Hybrid Operator-Based Methods

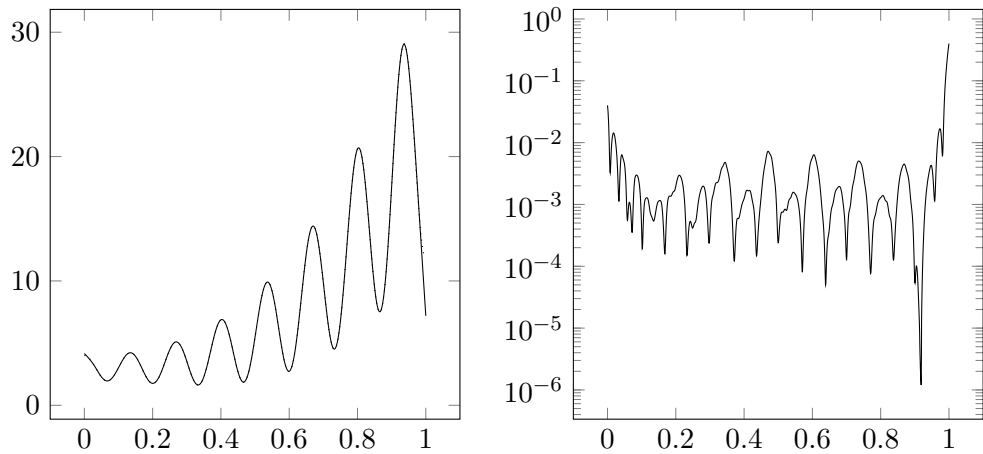


Figure 5.15.: Plots of the calculated first residual $\tilde{r}_{1,1}$ (see (5.9)) and its analytical solution $r_{1,1}$ (dotted) on the left and a semi-log plot of the relative error between both on the right for $(k, q, n, \varepsilon) = (4, 4, 180, 0.01)$ from Example 5.7.

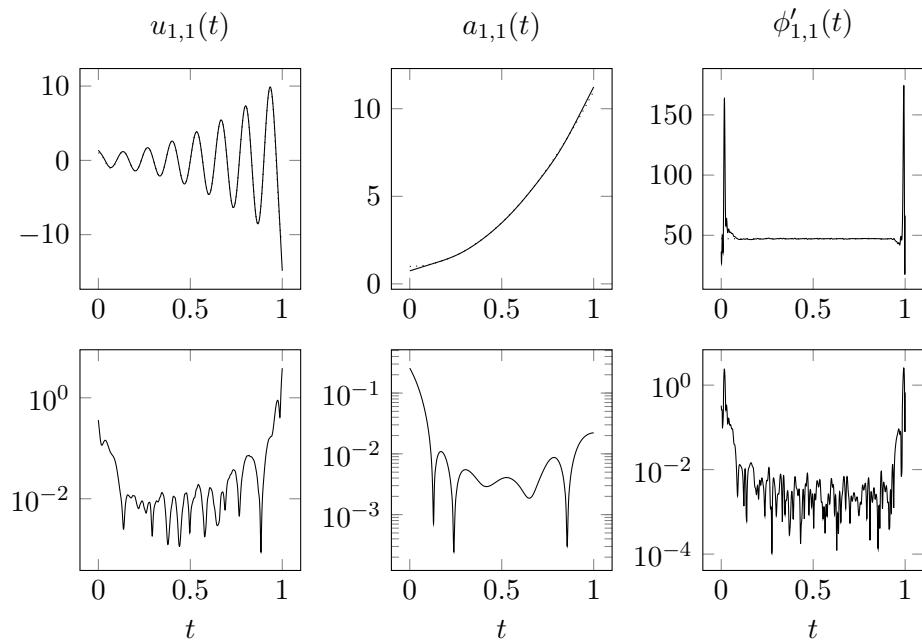


Figure 5.16.: Plots of the second extracted IMF-component $\tilde{u}_{1,1}$ of s_1 (see (5.8)) and its respective instantaneous amplitude $\tilde{a}_{1,1}$ and frequency $\tilde{\phi}'_{1,1}$ in the first row (with analytical solutions $u_{1,1}, a_{1,1}$ and $\phi'_{1,1}$ (dotted)) with semi-log plots of the absolute (for $u_{1,1}(t)$) and relative errors (for $a_{1,1}(t)$ and $\phi'_{1,1}(t)$) compared to the analytical solutions in the second row for $(k, q, n, \varepsilon) = (4, 4, 180, 0.01)$ from Example 5.7.

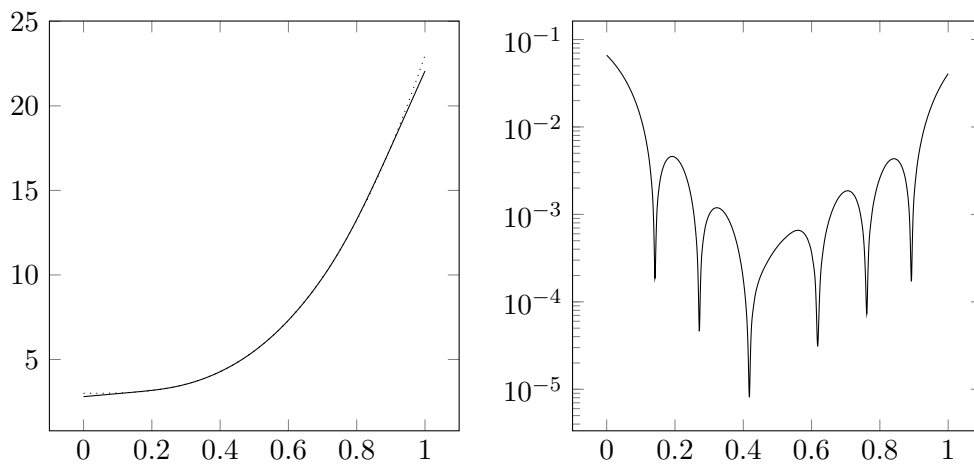


Figure 5.17.: Plots of the calculated second residual $\tilde{r}_{1,2}$ (see (5.10)) and its analytical solution $r_{1,2}$ (dotted) on the left and a semi-log plot of the relative error between both on the right for $(k, q, n, \varepsilon) = (4, 4, 180, 0.01)$ from Example 5.7.

6. Summary and Outlook

In the course of this thesis we started off with the construction of an analytical model of the empirical mode decomposition and showed that it satisfies strong duality, namely due to being SLATER regular, using B-spline properties and the theory of convex-like optimization. This strong duality yielded a theoretical justification for reformulating the constrained optimization problem into an unconstrained optimization problem with a regularization term that enforces the constraints.

In the context of EMD, we examined one possible modern approach to such a regularization term: The operator-based signal-separation (OSS) null-space-pursuit (NSP) method that makes use of adaptive differential operators to determine instantaneous amplitude and phase from a given IMF. We observed that the operator can only yield unique results when the IMF that is to be regularized has constant amplitude 1, which is a strong limitation.

We considered the classic EMD algorithm and noted the following: Sifting, the process in which the signal is separated into an IMF and a residual, is highly dependent on a good method for estimating the upper envelope of a multicomponent signal. We identified the weakness in the classic method that the envelope may intersect with the signal itself, violating the definition of an envelope. We presented a new approach called iterative slope envelope estimation that solves this problem. Additionally, it is a generalization of the classic envelope estimation method. We also made the following observation: During sifting we also obtain the amplitude of the IMF. This in turn meant that we can just divide the IMF by its amplitude and obtain an IMF with constant instantaneous amplitude 1. This meant that we could use the differential operator from the NSP method mentioned earlier and be sure that it behaved properly.

Using both the new envelope estimation method and the differential operator, we have obtained an approach that is a mix of classic and modern methods. Consequently, we defined a hybrid EMD method and examined it using multiple examples. These examples were implemented in a toolbox called ETHOS using the GNU Scientific Library, which was explained and documented subsequently. One newly discovered approach in this process was to evaluate the quality of each extracted IMF by calculating its characteristic.

It is clear that only by building a strict theoretical foundation that went further than previous works it was possible to obtain the results laid out in this thesis. This foundation included convex constraints instead of regularization terms, using B-splines for the theoretical and practical modelling of functions and the theory of convex-like optimization. The author suspects that given the underlying EMD optimization-problem is not convex, previous attempts to show regularity were not followed through. This is because it is widely assumed that convexity is a requirement for showing SLATER regularity. This is wrong, as convex-likeness is sufficient, but generally not well-known. The

6. Summary and Outlook

attractiveness of SLATER regularity is due to the fact that it applies to the entire optimization problem instead of just specific points, and showing it for the EMD optimization problem yields the regularity for any scenario.

A possible outlook for further works would be to expand the iterative slope sifting algorithm to higher dimensions to explore their usefulness in multidimensional EMD. In the context of the ETHOS toolbox, a possible field of research would be to use more specific tools for sparse optimization, possibly based on the modern GHOST (General, Hybrid and Optimized Sparse Toolkit) sparse library (see [KTRZ⁺17]), and refine the B-spline data fitting process, especially concerning preventing overfitting and underfitting.

In the end, what is easy to see is that signal analysis as a whole and EMD in particular are complex topics with many open questions, not only in the theoretical sense but also in practical terms. Examples include problems like mode mixing and noise distortion of an input signal. What remains to be seen is how these problems can be solved most effectively: In a preprocessing step before applying the EMD method or as a part of a newly devised EMD method. Or maybe they are simply unsolvable in terms of information theory. No matter the outcome, given the far-reaching applications it has in many different fields, every little problem solved in signal analysis may have far-reaching consequences.

A. Function Space Order and Operators

This thesis makes use of operations on functions rather than scalars, for instance as candidates in optimization problems. Because of that we want to understand how function spaces work and how we can map them to other vector spaces we can handle more easily. Even though the concepts laid out as follows seem to be very intuitive and might not even need further explanation beyond notation, the formal aspect of this topic shall not be missed for completeness sake but also not unnecessarily complicate the main matter, which is why this chapter is in the appendix.

The functions we are dealing with are relatively smooth functions $\mathbb{R} \rightarrow \mathbb{R}$. Formally speaking, we have a $p \geq 0$ such that our function can be differentiated p times and the p th derivative is continuous. This set is commonly denoted as $\mathcal{C}^p(\mathbb{R}, \mathbb{R})$, the set of p -continuously differentiable functions. It is easy to see that $\mathcal{C}^0(\mathbb{R}, \mathbb{R}) \supseteq \mathcal{C}^1(\mathbb{R}, \mathbb{R}) \supseteq \mathcal{C}^2(\mathbb{R}, \mathbb{R}) \supseteq \dots \supseteq \mathcal{C}^\infty(\mathbb{R}, \mathbb{R})$, so if we define something for $\mathcal{C}^0(\mathbb{R}, \mathbb{R})$ it automatically holds for all functions from $\mathcal{C}^p(\mathbb{R}, \mathbb{R})$ with $p \geq 0$. This is why, as follows, we will only use the set of continuous functions $\mathcal{C}^0(\mathbb{R}, \mathbb{R})$ in our definitions to keep everything relatively general.

One aspect of interest is to be able to compare two functions in some way. In other words, we want to find an order relation on $\mathcal{C}^0(\mathbb{R}, \mathbb{R})$. One way to do that is as follows: We say that a function succeeds another function if and only if the former is pointwise greater than or equal to the latter. We define precedence respectively and note that, obviously, there are functions which can not be compared this way. This concept is illustrated in Figure A.1 and is the function space order used in the course of this thesis.

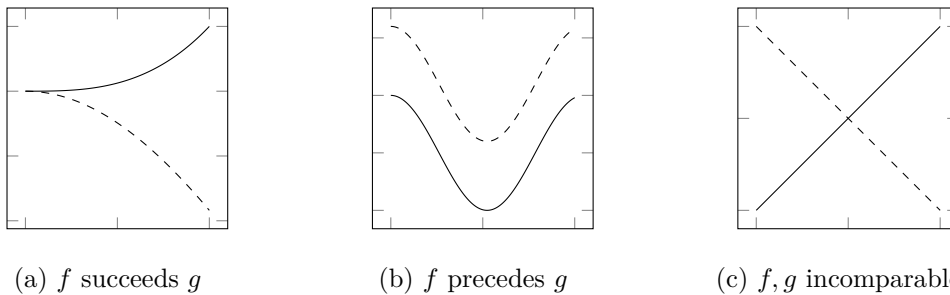


Figure A.1.: Illustration of an intuitive concept for a partial function space order (see Proposition A.4) exemplified with two functions f (solid) and g (dashed).

Before we are able to further formalize this idea, we first need to introduce some preliminary definitions of what an order is and how to define ordered vector spaces.

A. Function Space Order and Operators

Definition A.1 (Preorder [Cie97, Section 2.4]). *Let S be a set and \leq a binary relation on S . \leq is a preorder on S if and only if*

1. Reflexivity:

$$\forall x \in S: x \leq x,$$

2. Transitivity:

$$\forall x, y, z \in S: a \leq b \wedge b \leq c \Rightarrow a \leq c.$$

A preorder is the weakest order we can find for a vector space. If we can also show antisymmetry of a preorder, we obtain a partial order, given in the following

Definition A.2 (Partial order [Cie97, Section 2.4]). *Let S be a set and \leq a preorder on S . \leq is a partial order on S if and only if \leq is antisymmetric, i.e.*

$$\forall a, b \in S: a \leq b \wedge b \leq a \Rightarrow a = b.$$

One step higher would be a total order, which adds the connex property meaning that all elements of the set are comparable. As we've seen in Figure A.1 this is not possible for vector spaces given the presence of indeterminate relations.

If we find a binary relation on a vector space that is either a preorder or partial order we would, as the next step, hope that the orders are compatible with vector space operations. In other words, this means that addition and scalar multiplication preserve relations intuitively. This is reflected in the following

Definition A.3 ((Pre)ordered vector space [Bou03, Chapter II, §2.5]). *Let V be a real vector space and \leq a binary relation on V . V is a (pre)ordered vector space if and only if*

1. \leq is a preorder or partial order respectively,

2. Addition compatibility:

$$\forall x, y, z \in V: x \leq y \Rightarrow x + z \leq y + z,$$

3. Scalar multiplication compatibility:

$$\forall x, y \in V: \forall \lambda \geq 0: x \leq y \Rightarrow \lambda \cdot x \leq \lambda \cdot y.$$

With the definitions in place we can now formalize what has been discussed at the beginning of the section and illustrated in Figure A.1.

Proposition A.4. *Let $a, b \in \mathcal{C}^0(\mathbb{R}, \mathbb{R})$. $(\mathcal{C}^0(\mathbb{R}, \mathbb{R}), \preceq)$ is an ordered vector space with*

$$a \preceq b \Leftrightarrow \forall t \in \mathbb{R}: a(t) \leq b(t).$$

Proof. Let $a, b, c \in \mathcal{C}^0(\mathbb{R}, \mathbb{R})$. We first show that \preceq is a partial order.

1. *Reflexivity:*

$$\forall t \in \mathbb{R}: a(t) \leq a(t) \Leftrightarrow a \preceq a,$$

2. *Transitivity:*

$$\begin{aligned} a \preceq b \wedge b \preceq c &\Leftrightarrow \forall t \in \mathbb{R}: (a(t) \leq b(t) \wedge b(t) \leq c(t)) \\ &\Rightarrow \forall t \in \mathbb{R}: a(t) \leq c(t) \\ &\Leftrightarrow a \preceq c, \end{aligned}$$

3. *Antisymmetry:*

$$\begin{aligned} a \preceq b \wedge b \preceq a &\Leftrightarrow \forall t \in \mathbb{R}: (a(t) \leq b(t) \wedge b(t) \leq a(t)) \\ &\Leftrightarrow \forall t \in \mathbb{R}: a(t) = b(t) \\ &\Leftrightarrow a = b. \end{aligned}$$

Let $\lambda \geq 0$. We now show that $(\mathcal{C}^0(\mathbb{R}, \mathbb{R}), \preceq)$ satisfies the two axioms of an ordered vector space such that the order is compatible with the vector space operations.

1. *Addition compatibility:*

$$\begin{aligned} a \preceq b &\Leftrightarrow \forall t \in \mathbb{R}: a(t) \leq b(t) \\ &\Leftrightarrow \forall t \in \mathbb{R}: a(t) + c(t) \leq b(t) + c(t) \\ &\Leftrightarrow \forall t \in \mathbb{R}: (a + c)(t) \leq (b + c)(t) \\ &\Leftrightarrow a + c \preceq b + c, \end{aligned}$$

2. *Scalar multiplication compatibility:*

$$\begin{aligned} a \preceq b &\Leftrightarrow \forall t \in \mathbb{R}: a(t) \leq b(t) \\ &\Leftrightarrow \forall t \in \mathbb{R}: \lambda \cdot a(t) \leq \lambda \cdot b(t) \\ &\Leftrightarrow \forall t \in \mathbb{R}: (\lambda \cdot a)(t) \leq (\lambda \cdot b)(t) \\ &\Leftrightarrow \lambda \cdot a \preceq \lambda \cdot b. \end{aligned}$$

□

We have now shown that $\mathcal{C}^0(\mathbb{R}, \mathbb{R})$ is an ordered vector space with the order relation \preceq , but this is just one point of interest. It is often useful to transform objects that are hard to work with to a space where that is easy, perform operations on them and then transform them back. One common example are polar coordinate transforms which dramatically simplify many complicated integrals. A requirement for such a transform in the general sense is that it is an isomorphism and preserves the nature and/or relations of the objects. In the context of optimization problems this means that a transform shall preserve the relative order of objects. If a function precedes another its transform shall do the same relative to the transform of the other function.

The motivation for this approach in this thesis is found within the strong link between spline functions and their B-spline base coefficients, as introduced in Chapter 2. The

A. Function Space Order and Operators

base coefficients of a spline function is a vector in \mathbb{R}^n and fully describes it. Due to the nature of the B-splines the intuitive partial order \leq on \mathbb{R}^n with regard to the base coefficients is equivalent to the partial order \preceq on the set of spline functions Σ_k . To put it differently, if a spline function succeeds another, so do their base coefficients. The advantage this brings is apparent: Vectors in \mathbb{R}^n are much easier to handle both theoretically and numerically, and any optimization problem can be trivially transformed between both representations.

Now that we have understood the motivation behind this approach, we can formalize such a transform between ordered vector spaces in the following

Definition A.5 (Order isomorphism of ordered vector-spaces [Cie97, Section 4.1]). *Let $(V, \leq_V), (W, \leq_W)$ be ordered vector spaces and $f: V \rightarrow W$. f is an order isomorphism of ordered vector-spaces if and only if*

1. f is an isomorphism,
2. $\forall x, y \in V: x \leq_V y \Leftrightarrow f(x) \leq_W f(y)$.

As we can see, preserving the order structure opens up new possibilities with regard to optimization problems. In our case, even though we formulate it over a function space, we can transform our candidates into \mathbb{R}^n and examine the equivalent optimization problem over \mathbb{R}^n , which is much more accessible than the function space in many aspects.

As another remark we define the following operators on functions that serve notational purposes but can be considered to be more or less intuitive.

Definition A.6 (Modulus operator). *Let $a \in \mathcal{C}^0(\mathbb{R}, \mathbb{R})$. The modulus operator $|\cdot|: \mathcal{C}^0(\mathbb{R}, \mathbb{R}) \rightarrow \mathcal{C}^0(\mathbb{R}, \mathbb{R})$ is defined as*

$$|a|(t) := |a(t)|.$$

Definition A.7 (Power operator). *Let $p \geq 0$ and $a \in \mathcal{C}^0(\mathbb{R}, \mathbb{R})$. The power operator $^p: \mathcal{C}^0(\mathbb{R}, \mathbb{R}) \rightarrow \mathcal{C}^0(\mathbb{R}, \mathbb{R})$ is defined as*

$$a^p(t) := (a(t))^p.$$

Definition A.8 (Differentiation operator). *Let $p \in \mathbb{N}_0$ and $a \in \mathcal{C}^0(\mathbb{R}, \mathbb{R})$. The differentiation operator $D^p: \mathcal{C}^0(\mathbb{R}, \mathbb{R}) \rightarrow \mathcal{C}^0(\mathbb{R}, \mathbb{R})$ is defined as*

$$(D^p a)(t) := \begin{cases} a(t) & p = 0 \\ \frac{d^p a}{dt^p}(t) & p > 0 \end{cases}$$

What shall be apparent from the results of this chapter is that this approach saves us from a lot of cumbersome notation and complexity down the road. The alternative of always thinking of a function as a set of samples may also solve the discretization problem, but requires much more care in terms of parametrization and is much harder to access theoretically. The latter is especially apparent when it comes to derivatives, which are a crucial part of the theory of this thesis.

B. Convexity Theory

The theory of convex sets and functions plays a central role in this thesis and we will introduce it in this chapter. Even though most of the given definitions may be known to the reader, the resulting Theorem B.7 is used in all proofs in the thesis for showing function convexity. Before we dive in further, we introduce both concepts of convex sets and convex functions.

Definition B.1 (Convex set). *Let V be a real or complex vector space and $C \subseteq V$. C is convex if and only if*

$$\forall a, b \in C: \forall \lambda \in [0, 1]: \lambda \cdot a + (1 - \lambda) \cdot b \in C.$$

Definition B.2 ((Strictly) convex function). *Let $n \in \mathbb{N}$, $C \subseteq \mathbb{R}^n$ convex and $f: C \rightarrow \mathbb{R}$. f is a strictly convex function or convex function if and only if*

$$\forall a, b \in C: \forall \lambda \in [0, 1]: f(\lambda \cdot a + (1 - \lambda) \cdot b) < \lambda \cdot f(a) + (1 - \lambda) \cdot f(b)$$

or

$$\forall a, b \in C: \forall \lambda \in [0, 1]: f(\lambda \cdot a + (1 - \lambda) \cdot b) \leq \lambda \cdot f(a) + (1 - \lambda) \cdot f(b)$$

respectively.

For the purpose of determining convexity later the multidimensional pendant of a second derivative is introduced as the Hessian matrix, the matrix that contains all possible combinations of mixed second partial derivatives.

Definition B.3 (Hessian matrix [NP06, Section 3.9]). *Let $n \in \mathbb{N}$ and $f \in \mathcal{C}^2(\mathbb{R}^n, \mathbb{R})$. The Hessian matrix $H_f(x) \in \mathbb{R}^{n \times n}$ of f in $x \in \mathbb{R}^n$ is defined as*

$$H_f(x) := \left(\frac{\partial^2 f(x)}{\partial x_i \partial x_j} \right)_{i, j \in \{1, \dots, n\}}.$$

Another important concept is the positive definiteness that can more or less be imagined to be a generalization of positivity of scalars into the realm of matrices.

Definition B.4 (Positive (semi)definite). *Let $n \in \mathbb{N}$ and $A \in \mathbb{R}^{n \times n}$. A is positive definite or positive semidefinite if and only if*

$$\forall v \in \mathbb{R}^n: v^T \cdot A \cdot v > 0$$

or

$$\forall v \in \mathbb{R}^n: v^T \cdot A \cdot v \geq 0$$

respectively.

B. Convexity Theory

One thing to note here though is that a matrix can in fact have negative entries and be positive definite, but also have only positive entries and still not be positive definite. Using these definitions, we can give the following condition for a sufficiently smooth function to be convex.

Proposition B.5 (Hessian (strict) convexity condition). *Let $n \in \mathbb{N}$ and $f \in \mathcal{C}^2(\mathbb{R}^n, \mathbb{R})$. f is strictly convex or convex if and only if for all $x \in \mathbb{R}^n$ the Hessian matrix $H_f(x)$ is positive definite or positive semidefinite respectively.*

Proof. See [NP06, Corollary 3.9.5]. □

The result is that object of interest is the Hessian matrix of a given function we want to examine and its definiteness. The direct approach to check definiteness is complicated, especially for large systems like the ones we are dealing with in this thesis. One useful result to simplify this process is the GERSHGORIN-HADAMARD-theorem that gives conditions which are easy to check, yielding a positive definite matrix. To formulate the theorem we must first consider so-called strictly diagonally dominant matrices where the absolute value of a diagonal entry is strictly larger than the sum of the absolute values of all other entries in that row.

Definition B.6 (Strictly diagonally dominant [HJ12, Definition 6.1.9]). *Let $n \in \mathbb{N}$ and $A \in \mathbb{R}^{n \times n}$. A is strictly diagonally dominant if and only if*

$$\forall i \in \{1, \dots, n\}: |a_{ii}| > \sum_{j \in \{1, \dots, n\} \setminus \{i\}} |a_{ij}|.$$

Theorem B.7 (GERŠGORIN-HADAMARD [HJ12, Theorem 6.1.10]). *Let $n \in \mathbb{N}$ and $M \in \mathbb{R}^{n \times n}$ symmetric, diagonally dominant and $\forall i \in \{1, \dots, n\}: a_{ii} > 0$. Then M is positive definite, non-singular and every eigenvalue of M is positive.*

Proof. See [HJ12, Theorem 6.1.10]. □

Using this theorem it shall be possible to approach even large systems in regard to positive definiteness. When we show positive definiteness of the Hessian matrix, convexity follows and we have obtained our desired result.

C. Notation Directory

C.1. Chapter 1: Introduction

$\Phi(t)$	1-periodic function; see Equation (1.1)
c_j	FOURIER coefficients; see Equation (1.2)
$(\mathcal{F}s)(f)$	FOURIER transform; see Equation (1.4)
$\langle \cdot, \cdot \rangle$	standard inner product; see Equation (1.5)
$\psi_{j,k}$	wavelet basis function; see Equation (1.6)
ψ	mother wavelet; see Equation (1.6)
$c_{j,k}$	wavelet coefficients; see Equation (1.8)
$\ \cdot \ _2$	2-norm based on the standard inner product

C.2. Chapter 2: B-Splines

Π_p	set of polynomials of order p ; see Definition 2.1
$\Sigma_{k,T}$	spline function space; see Definition 2.2
Σ_k	shorthand notation for $\Sigma_{k,T}$; see Remark 2.14
k	spline function order; see Definition 2.2
ℓ	size of spline knot vector; see Definition 2.2
T	spline knot vector; see Definition 2.2
$\chi(A)$	indicator function on set A ; see Definition 2.4
$B_{i,k,T}$	B-spline function; see Definition 2.5
$B_{i,k}$	shorthand notation for $B_{i,k,\Delta_k(T)}$; see Remark 2.14
$\Delta_k(T)$	extended knot vector; see Definition 2.8
n	number of B-spline functions ($k + \ell - 2$); see Definition 2.8
$\mathbb{B}_{k,T}$	coefficient spline mapping; see Definition 2.10
\mathbb{B}_k	shorthand notation for $\mathbb{B}_{k,T}$; see Remark 2.14
$c_{k,\infty}$	B-spline condition constant; see Proposition 2.12

C.3. Chapter 3: Empirical Mode Decomposition Model and Analysis

a	instantaneous amplitude; see Definition 3.1
ϕ	instantaneous phase; see Definition 3.1
ϕ'	instantaneous frequency; see Definition 3.1

C. Notation Directory

$\mathcal{S}_{\mu_0, \mu_1, \mu_2}$	set of intrinsic mode function souls (IMFS) with characteristic (μ_0, μ_1, μ_2) ; see Definition 3.1
$\mathcal{S}_{\mu_0, \mu_1, \mu_2}$	set of intrinsic mode spline function souls (IMSpFS); see Definition 3.10
$\mathcal{I}[a, \phi]$	intrinsic mode function operator; see Definition 3.5
$c_1[s](a, \phi)$	canonical EMD cost function; see Definition 3.11
$\mathbf{c}_1[s](\mathbf{a}, \phi)$	canonical spline EMD cost function; see Definition 3.12
$c_\ell[s](a, \phi)$	leakage factor EMD cost function; see Definition 3.14
$\mathbf{c}_\ell[s](\mathbf{a}, \phi)$	leakage factor spline EMD cost function; see Definition 3.15
V^+	positive cone of cone V ; see Definition 3.21
V'	dual cone of cone V ; see Definition 3.35
$\Lambda(x, \lambda)$	LAGRANGE function; see Definition 3.36
$\underline{\Lambda}(\lambda)$	LAGRANGE dual function; see Definition 3.37

C.4. Chapter 4: Operator-Based Analysis of Intrinsic Mode Functions

$A[a]$	instantaneous envelope derivation operator; see Definition 4.1
$\Omega[\phi]$	inverse square continuous frequency operator; see Definition 4.2
$\mathcal{D}_{(a, \phi)}$	IMF differential operator; see Definition 4.3
$\tilde{\mathcal{D}}_{(A, \Omega)}$	modified IMF differential operator; see Definition 4.5

C.5. Chapter A: Function Space Order and Operators

\mathbb{N}	set of natural numbers ≥ 1
\mathbb{N}_0	set of natural numbers ≥ 0
$\mathcal{C}^p(A, B)$	set of p -continuously differentiable functions $A \rightarrow B$
\preceq	partial order on $\mathcal{C}^0(\mathbb{R}, \mathbb{R})$; see Proposition A.4
$ \cdot $	modulus operator; see Definition A.6
$(\cdot)^p$	power operator; see Definition A.7
D^p	differentiation operator; see Definition A.8

C.6. Chapter B: Convexity Theory

$H_f(x)$	Hessian matrix of f in x ; see Definition B.3
----------	---

D. Code Listings

D.1. ETHOS Toolbox

D.1.1. ethos.h

```
1  /* See LICENSE file for copyright and license details. */
2  #ifndef ETHOS_H
3  #define ETHOS_H
4
5  #include <sys/types.h>
6
7  enum ethos_plot_format {
8      ETHOS_PLOT_CSV,
9      ETHOS_PLOT_GRAPH,
10 };
11
12 struct ethos {
13     void *bw;
14     size_t n;
15     double a;
16     double b;
17     int k;
18     int q;
19     double *grid;
20     size_t ngrid;
21     double *extgrid;
22     size_t nextgrid;
23     double ***dB;
24     size_t *istart;
25     size_t *iend;
26 };
27
28 enum ethos_grid {
29     ETHOS_GRID_UNIFORM,
30 };
31
32 int ethos_init(struct ethos *e, const double *T, size_t N, int k, int q,
33               double dens, enum ethos_grid g);
```

D. Code Listings

```
34 void ethos_free(struct ethos *e);
35
36 int ethos_extend_boundary(double ratio, const double *T, const double *S,
37                          size_t N, double **Te, double **Se,
38                          size_t *Ne);
39 int ethos_fit(const struct ethos *e, double *s, const double *T,
40              const double *S, size_t N);
41
42 int ethos_plot_points(double *T, double *S, size_t N, const char *fname,
43                     enum ethos_plot_format p);
44 int ethos_plot_spline(const struct ethos *e, const double *c,
45                      const char *fname, enum ethos_plot_format p);
46
47 int ethos_upper_envelope(const struct ethos *e, double *m,
48                          const double *s, double eps);
49 int ethos_frequency_from_simple_imf(const struct ethos *e, double *u);
50 int ethos_emd(const struct ethos *e, double *u, double *a, double *freq,
51              double *s, double eps);
52
53 int ethos_characteristic(const struct ethos *e, double mu[static 3],
54                          const double *a, const double *freq);
55
56 double ethos_norm_sup_bound_spline(const struct ethos *e,
57                                   const double *c);
58 int ethos_relerror(const struct ethos *e, double *relerror, double *c,
59                  double *c_analytic);
60
61 #endif /* ETHOS_H */
```

D.1.2. ethos.c

```
1  /* See LICENSE file for copyright and license details. */
2  #include <errno.h>
3  #include <gsl/gsl_bspline.h>
4  #include <gsl/gsl_linalg.h>
5  #include <gsl/gsl_matrix.h>
6  #include <gsl/gsl_multifit.h>
7  #include <gsl/gsl_statistics.h>
8  #include <gsl/gsl_vector.h>
9  #include <limits.h>
10 #include <math.h>
11 #include <stdarg.h>
12 #include <stddef.h>
```

```

13 #include <stdint.h>
14 #include <stdio.h>
15 #include <stdlib.h>
16 #include <string.h>
17 #include <sys/types.h>
18
19 #include "ethos.h"
20
21 #undef MIN
22 #define MIN(x,y) ((x) < (y) ? (x) : (y))
23 #undef MAX
24 #define MAX(x,y) ((x) > (y) ? (x) : (y))
25 #undef LEN
26 #define LEN(x) (sizeof (x) / sizeof *(x))
27
28 static void
29 warn(const char *fmt, ...)
30 {
31     va_list ap;
32
33     fprintf(stderr, "libethos:␣");
34
35     va_start(ap, fmt);
36     vfprintf(stderr, fmt, ap);
37     va_end(ap);
38
39     if (fmt[0] && fmt[strlen(fmt) - 1] == ':') {
40         fputc('␣', stderr);
41         perror(NULL);
42     } else {
43         fputc('\n', stderr);
44     }
45 }
46
47 /*
48  * This is sqrt(SIZE_MAX+1), as s1*s2 <= SIZE_MAX
49  * if both s1 < MUL_NO_OVERFLOW and s2 < MUL_NO_OVERFLOW
50  */
51 #define MUL_NO_OVERFLOW ((size_t)1 << (sizeof(size_t) * 4))
52
53 static void *
54 _reallocarray(void *optr, size_t nmemb, size_t size)
55 {
56     if ((nmemb >= MUL_NO_OVERFLOW || size >= MUL_NO_OVERFLOW) &&

```

D. Code Listings

```
57         nmemb > 0 && SIZE_MAX / nmemb < size) {
58             errno = ENOMEM;
59             return NULL;
60         }
61         return realloc(optr, size * nmemb);
62     }
63
64     static void *
65     rereallocarray(void *optr, size_t nmemb, size_t size)
66     {
67         void *p;
68
69         if (!(p = _reallocarray(optr, nmemb, size))) {
70             warn("reallocarray: Out of memory");
71             exit(1);
72         }
73
74         return p;
75     }
76
77     static void
78     util_array_vector_wrap(gsl_vector *v, const double *arr, size_t len)
79     {
80         v->size = len;
81         v->stride = 1;
82         v->data = (double *)arr;
83         v->block = NULL;
84         v->owner = 0;
85     }
86
87     int
88     ethos_init(struct ethos *e, const double *T, size_t N, int k, int q,
89               double dens, enum ethos_grid g)
90     {
91         gsl_matrix *dB;
92         gsl_vector *gridv;
93         size_t i, j, m, nderiv;
94         double t;
95
96         /* input validation */
97         if (dens <= 0 || dens > 1) {
98             warn("ethos_init: Grid-density dens must be in [0,1]");
99             return 1;
100        }
```

```

101     if (k < 1) {
102         warn("ethos_init: Parameter k must be larger than 0");
103         return 1;
104     }
105     if (q < 0) {
106         warn("ethos_init: The parameter q must be positive");
107         return 1;
108     }
109     if (N == 0) {
110         warn("ethos_init: Empty time vector");
111         return 1;
112     }
113
114     /* initialization */
115     e->ngrid = (size_t)(dens * N);
116     if (e->ngrid + k <= 2) {
117         warn("ethos_init: Density too low for given parameters");
118         return 1;
119     }
120     e->bw = gsl_bspline_alloc(k, e->ngrid);
121     e->n = e->ngrid + k - 2;
122     e->k = k;
123     e->q = q;
124     e->a = T[0];
125     e->b = T[N - 1];
126
127     /* breakpoint vector */
128     e->grid = ereallocarray(NULL, e->ngrid, sizeof(*e->grid));
129     switch (g) {
130     case ETHOS_GRID_UNIFORM:
131         for (i = 0; i < e->ngrid; i++) {
132             e->grid[i] = e->a + (double)(e->b - e->a) /
133                 (e->ngrid - 1) * i;
134         }
135         break;
136     default:
137         warn("ethos_init: Invalid grid style");
138         free(e->grid);
139         gsl_bspline_free(e->bw);
140         return 1;
141     }
142
143     gridv = gsl_vector_alloc(e->ngrid);
144     for (i = 0; i < e->ngrid; i++) {

```

D. Code Listings

```

145         gsl_vector_set(gridv, i, e->grid[i]);
146     }
147     gsl_bspline_knots(gridv, e->bw);
148     gsl_vector_free(gridv);
149
150     /* build extended grid */
151     e->nextgrid = e->ngrid + q * (e->ngrid - 1);
152     e->extgrid = ereallocarray(NULL, e->nextgrid,
153                               sizeof(*e->extgrid));
154     for (i = 0; i < (e->ngrid - 1); i++) {
155         for (j = 0; j <= (size_t)q; j++) {
156             e->extgrid[i * (q + 1) + j] = e->grid[i] + j *
157                 (e->grid[i + 1] - e->grid[i]) / (q + 1);
158         }
159     }
160     e->extgrid[e->ngrid + q * (e->ngrid - 1) - 1] =
161         e->grid[e->ngrid - 1];
162
163     /* evaluate derivatives 0, 1, 2 on extended grid */
164     nderiv = 2;
165     dB = gsl_matrix_alloc(e->k, nderiv + 1);
166
167     e->dB = ereallocarray(NULL, e->nextgrid, sizeof(*(e->dB)));
168     for (m = 0; m < e->nextgrid; m++) {
169         e->dB[m] = ereallocarray(NULL, e->k, sizeof(**(e->dB)));
170         for (i = 0; i <= (size_t)e->k; i++) {
171             e->dB[m][i] = ereallocarray(NULL, nderiv + 1,
172                                       sizeof(***(e->dB)));
173         }
174     }
175     e->istart = ereallocarray(NULL, e->nextgrid,
176                               sizeof(*(e->istart)));
177     e->iend = ereallocarray(NULL, e->nextgrid, sizeof(*(e->iend)));
178
179     for (m = 0; m < e->nextgrid; m++) {
180         t = e->extgrid[m];
181
182         /* B_i(e->extgrid[m]) for all i where B_i is non-zero */
183         gsl_bspline_deriv_eval_nonzero(t, nderiv, dB,
184                                       &(e->istart[m]),
185                                       &(e->iend[m]), e->bw);
186
187         /* store in ethos-struct */
188         for (i = e->istart[m]; i <= e->iend[m]; i++) {

```



```

189         for (j = 0; j <= nderiv; j++) {
190             e->dB[m][i - e->istart[m]][j] =
191                 gsl_matrix_get(dB,
192                             i - e->istart[m],
193                             j);
194         }
195     }
196 }
197 gsl_matrix_free(dB);
198
199 return 0;
200 }
201
202 void
203 ethos_free(struct ethos *e)
204 {
205     size_t m, i;
206
207     gsl_bspline_free(e->bw);
208     e->bw = NULL;
209
210     free(e->grid);
211     e->grid = NULL;
212
213     free(e->extgrid);
214     e->extgrid = NULL;
215
216     for (m = 0; m < e->nextgrid; m++) {
217         for (i = 0; i <= (size_t)e->k; i++) {
218             free(e->dB[m][i]);
219             e->dB[m][i] = NULL;
220         }
221         free(e->dB[m]);
222         e->dB[m] = NULL;
223     }
224     free(e->dB);
225     e->dB = NULL;
226
227     free(e->istart);
228     e->istart = NULL;
229     free(e->iend);
230     e->iend = NULL;
231 }
232

```

D. Code Listings

```
233 int
234 ethos_extend_boundary(double ratio, const double *T, const double *S,
235                      size_t N, double **Te, double **Se, size_t *Ne)
236 {
237     double a, b, delta;
238     size_t nmirr_l, nmirr_r, i, ind;
239
240     if (ratio < 0 || ratio > 1) {
241         warn("ethos_mirror_boundary: Ratio must be in [0,1]");
242         return 1;
243     }
244
245     /* get extent of the array and range of mirror */
246     a = T[0];
247     b = T[N - 1];
248     delta = (b - a) * ratio;
249     for (nmirr_l = 0; nmirr_l < N; nmirr_l++) {
250         if (T[nmirr_l] >= a + delta) {
251             break;
252         }
253     }
254     for (nmirr_r = 0; nmirr_r < N; nmirr_r++) {
255         if (T[N - nmirr_r - 1] <= b - delta) {
256             break;
257         }
258     }
259
260     /* allocate new vectors */
261     *Ne = N + (nmirr_l - 1) + (nmirr_r - 1);
262     *Te = ereallocarray(NULL, *Ne, sizeof(**Te));
263     *Se = ereallocarray(NULL, *Ne, sizeof(**Se));
264
265     /* fill mirror vectors */
266     for (i = 0; i < nmirr_l - 1; i++) {
267         ind = nmirr_l - 1 - i;
268         (*Te)[i] = a - (T[ind] - a);
269         (*Se)[i] = S[ind];
270     }
271     for (i = 0; i < N; i++) {
272         ind = i + (nmirr_l - 1);
273         (*Te)[ind] = T[i];
274         (*Se)[ind] = S[i];
275     }
276     for (i = 0; i < nmirr_r - 1; i++) {
```

```

277         ind = i + (nmirr_l - 1) + N;
278         (*Te)[ind] = b + (b - T[N - 2 - i]);
279         (*Se)[ind] = S[N - 2 - i];
280     }
281
282     return 0;
283 }
284
285 int
286 ethos_fit(const struct ethos *e, double *s, const double *T,
287           const double *S, size_t N)
288 {
289     gsl_matrix *F, *cov;
290     gsl_multifit_linear_workspace *mw;
291     gsl_vector s_v, *y, *w, *B;
292     size_t neq, i, start, end, j, m;
293     double chisq, tss, Rsq;
294     int ud;
295
296     /* check S if it is contained in spline knot vector */
297     if (T[0] < e->a || (N > 0 && T[N - 1] > e->b)) {
298         warn("ethos_fit: input data exceeds spline bounds");
299         return 1;
300     }
301
302     /* coefficient vector */
303     util_array_vector_wrap(&s_v, s, e->n);
304
305     /* is the system underdetermined? */
306     ud = (e->n > N);
307     neq = N + (ud ? e->nextgrid : 0);
308
309     /* fit matrix */
310     F = gsl_matrix_alloc(neq, e->n);
311
312     B = gsl_vector_alloc(e->k);
313     for (i = 0; i < N; i++) {
314         /* compute B_j(T[i]) for all j where B_j is non-zero */
315         gsl_bspline_eval_nonzero(T[i], B, &start, &end, e->bw);
316
317         /* fill row i */
318         for (j = start; j <= end; j++) {
319             gsl_matrix_set(F, i, j,
320                           gsl_vector_get(B, j - start));

```

D. Code Listings

```
321         }
322     }
323     gsl_vector_free(B);
324
325     if (ud) {
326         /* fill smoothness terms */
327         for (m = 0; m < e->nextgrid; m++) {
328             for (i = e->istart[m]; i <= e->iend[m]; i++) {
329                 gsl_matrix_set(F, N + m, i,
330                             e->dB[m][i -
331                             e->istart[m]][2]);
332             }
333         }
334     }
335
336     /* run the fit */
337     cov = gsl_matrix_alloc(e->n, e->n);
338
339     /* weight vector and right hand side */
340     y = gsl_vector_alloc(neq);
341     w = gsl_vector_alloc(neq);
342     for (i = 0; i < neq; i++) {
343         gsl_vector_set(y, i, (i < N) ? S[i] : 0.0);
344         gsl_vector_set(w, i, (i < N) ? 1.0 : 1E-12);
345     }
346
347     mw = gsl_multifit_linear_alloc(neq, e->n);
348     gsl_multifit_wlinear(F, w, y, &s_v, cov, &chisq, mw);
349     /*gsl_multifit_linear_free(mw); GSL-BUG */
350
351     /* statistics (total sum of squares) (dof = neq - e->n) */
352     tss = gsl_stats_wtss(y->data, 1, s, 1, e->n);
353     Rsq = 1.0 - chisq / tss;
354     (void)Rsq;
355
356     /* cleanup */
357     gsl_vector_free(y);
358     gsl_vector_free(w);
359     gsl_matrix_free(cov);
360     /* gsl_matrix_free(F); GSL-BUG */
361
362     return 0;
363 }
364
```

```

365 int
366 ethos_plot_points(double *T, double *S, size_t N, const char *fname,
367                 enum ethos_plot_format p)
368 {
369     FILE *fp;
370     size_t i;
371
372     if (fname) {
373         if (!(fp = fopen(fname, "w"))) {
374             warn("fopen: '%s': %s\n", fname, strerror(errno));
375             return 1;
376         }
377     } else {
378         fp = stdout;
379     }
380
381     switch (p) {
382     case ETHOS_PLOT_GRAPH:
383         fprintf(fp, "#m=0,S=3\n");
384         for (i = 0; i < N; i++) {
385             fprintf(fp, "%g %g\n", T[i], S[i]);
386         }
387         fprintf(fp, "\n\n");
388         break;
389     case ETHOS_PLOT_CSV:
390         fprintf(fp, "x,y\n");
391         for (i = 0; i < N; i++) {
392             fprintf(fp, "%g,%g\n", T[i], S[i]);
393         }
394         break;
395     default:
396         warn("ethos_plot_points: Invalid plot format");
397         return 1;
398     }
399
400     if (fname && fclose(fp)) {
401         warn("fclose: %s\n", strerror(errno));
402         return 1;
403     }
404
405     return 0;
406 }
407
408 int

```

D. Code Listings

```
409 ethos_plot_spline(const struct ethos *e, const double *c,
410                  const char *fname, enum ethos_plot_format p)
411 {
412     FILE *fp;
413     size_t m, i;
414     double s;
415
416     if (fname) {
417         if (!(fp = fopen(fname, "w"))) {
418             warn("fopen, '%s': %s\n", fname, strerror(errno));
419             return 1;
420         }
421     } else {
422         fp = stdout;
423     }
424
425     switch (p) {
426     case ETHOS_PLOT_GRAPH:
427         fprintf(fp, "#m=1,S=0\n");
428         for (m = 0; m < e->nextgrid; m++) {
429             s = 0;
430             for (i = e->istart[m]; i <= e->iend[m]; i++) {
431                 s += c[i] * e->dB[m][i -
432                     e->istart[m]][0];
433             }
434             fprintf(fp, "%g %g\n", e->extgrid[m], s);
435         }
436         fprintf(fp, "\n\n");
437         break;
438     case ETHOS_PLOT_CSV:
439         fprintf(fp, "x,y\n");
440         for (m = 0; m < e->nextgrid; m++) {
441             s = 0;
442             for (i = e->istart[m]; i <= e->iend[m]; i++) {
443                 s += c[i] * e->dB[m][i -
444                     e->istart[m]][0];
445             }
446             fprintf(fp, "%g,%g\n", e->extgrid[m], s);
447         }
448         break;
449     default:
450         warn("ethos_plot_spline: Invalid plot format");
451         return 1;
452     }
```

```

453
454     if (fname && fclose(fp)) {
455         warn("fclose_ '%s':_ '%s\n", fname, strerror(errno));
456         return 1;
457     }
458
459     return 0;
460 }
461
462 static int
463 ethos_upper_envelope_step(const struct ethos *e, double *r,
464                          const double *s)
465 {
466     struct {
467         double *t;
468         double *v;
469         size_t len;
470     } amp;
471     size_t i, m;
472     double s0, s0prev, s1, s1prev, s2, r1, r1prev;
473     int r1_gt_s1_prev;
474
475     amp.len = 0;
476     amp.t = ereallocarray(NULL, amp.len, sizeof(*amp.t));
477     amp.v = ereallocarray(NULL, amp.len, sizeof(*amp.v));
478
479     /*
480      * identify spots where derivatives match up and curvature is
481      * negative
482      */
483     for (m = 0; m < e->nextgrid; s0prev = s0, s1prev = s1,
484          r1prev = r1, r1_gt_s1_prev = (r1 > s1), m++) {
485         s0 = 0.0;
486         s1 = 0.0;
487         s2 = 0.0;
488         r1 = 0.0;
489
490         for (i = e->istart[m]; i <= e->iend[m]; i++) {
491             s0 += s[i] * e->dB[m][i - e->istart[m]][0];
492             s1 += s[i] * e->dB[m][i - e->istart[m]][1];
493             s2 += s[i] * e->dB[m][i - e->istart[m]][2];
494             r1 += r[i] * e->dB[m][i - e->istart[m]][1];
495         }
496

```

D. Code Listings

```
497         if (m > 0) {
498             /*
499              * check if r1_gt_s1_prev != (r1 > s1)
500              * -> there was a match r1 = s1
501              */
502             if (r1_gt_s1_prev != (r1 > s1) && s2 <= 0) {
503                 goto addpoint;
504             }
505         }
506         continue;
507 addpoint:
508         amp.len++;
509         amp.t = ereallocarray(amp.t, amp.len, sizeof(*amp.t));
510         amp.v = ereallocarray(amp.v, amp.len, sizeof(*amp.v));
511
512         if (fabs(s1 - r1) > fabs(s1prev - r1prev)) {
513             /* the previous gridpoint is closer to the max */
514             amp.t[amp.len - 1] = e->extgrid[m - 1];
515             amp.v[amp.len - 1] = s0prev;
516         } else {
517             amp.t[amp.len - 1] = e->extgrid[m];
518             amp.v[amp.len - 1] = s0;
519         }
520     }
521
522     if (ethos_fit(e, r, amp.t, amp.v, amp.len)) {
523         warn("ethos_fit: Failed");
524         free(amp.t);
525         free(amp.v);
526         return 1;
527     }
528
529     free(amp.t);
530     free(amp.v);
531
532     return 0;
533 }
534
535 int
536 ethos_upper_envelope(const struct ethos *e, double *m, const double *s,
537                     double eps)
538 {
539     size_t i, steps;
540     double *mt, *diff;
```



```

541
542     if (eps <= 0) {
543         warn("ethos_upper_envelope: Tolerance must be strictly"
544             "positive");
545         return 1;
546     }
547
548     mt = ereallocarray(NULL, e->n, sizeof(*mt));
549     diff = ereallocarray(NULL, e->n, sizeof(*diff));
550
551     /* set m to zero-function */
552     for (i = 0; i < e->n; i++) {
553         m[i] = 0.0;
554     }
555
556     steps = 0;
557     do {
558         /* set mt to m */
559         for (i = 0; i < e->n; i++) {
560             mt[i] = m[i];
561         }
562
563         if (ethos_upper_envelope_step(e, m, s)) {
564             return 1;
565         }
566
567         /* calculate difference */
568         for (i = 0; i < e->n; i++) {
569             diff[i] = m[i] - mt[i];
570         }
571
572         /* premature termination after 10 steps */
573         if (++steps >= 10) {
574             warn("ethos_upper_envelope: could not satisfy"
575                 "bound");
576             break;
577         }
578     } while (ethos_norm_sup_bound_spline(e, diff) > eps);
579
580     free(mt);
581     free(diff);
582
583     return 0;
584 }

```

D. Code Listings

```
585
586 static int
587 ethos_divide_spline(const struct ethos *e, double *a, const double *b)
588 {
589     size_t m, i;
590     double *eval, a_ev, b_ev;
591
592     eval = ereallocarray(NULL, e->nextgrid, sizeof(*eval));
593
594     for (m = 0; m < e->nextgrid; m++) {
595         a_ev = 0.0;
596         b_ev = 0.0;
597
598         for (i = e->istart[m]; i <= e->iend[m]; i++) {
599             a_ev += a[i] * e->dB[m][i - e->istart[m]][0];
600             b_ev += b[i] * e->dB[m][i - e->istart[m]][0];
601         }
602
603         eval[m] = a_ev / b_ev;
604     }
605
606     return (ethos_fit(e, a, e->extgrid, eval, e->nextgrid) ? 1 : 0);
607 }
608
609 int
610 ethos_frequency_from_simple_imf(const struct ethos *e, double *u)
611 {
612     gsl_matrix *F, *cov;
613     gsl_multifit_linear_workspace *mw;
614     gsl_vector *freq, *y;
615     size_t i, m;
616     double tmp1, chisq, tss, Rsq, *freqeval, om;
617
618     /* coefficient vector */
619     freq = gsl_vector_alloc(e->n);
620
621     /* fit matrix */
622     F = gsl_matrix_alloc(e->nextgrid, e->n);
623
624     for (m = 0; m < e->nextgrid; m++) {
625         for (i = e->istart[m]; i <= e->iend[m]; i++) {
626             /*
627              * Omega s''
628              */
```

```

629
630      /* preprocess sum_{i=0}^{n-1} s_j B_j' */
631      tmp1 = 0.0;
632      for (i = e->istart[m]; i <= e->iend[m]; i++) {
633          tmp1 += u[i] * e->dB[m][i -
634              e->istart[m]][2];
635      }
636
637      /* initialize entry */
638      for (i = e->istart[m]; i <= e->iend[m]; i++) {
639          gsl_matrix_set(F, m, i, tmp1 *
640              e->dB[m][i -
641              e->istart[m]][0]);
642      }
643
644      /*
645       * 1/2 Omega' s'
646       */
647
648      /* preprocess sum_{i=0}^{n-1} s_j B_j' */
649      tmp1 = 0.0;
650      for (i = e->istart[m]; i <= e->iend[m]; i++) {
651          tmp1 += u[i] * e->dB[m][i -
652              e->istart[m]][1];
653      }
654
655      for (i = e->istart[m]; i <= e->iend[m]; i++) {
656          gsl_matrix_set(F, m, i,
657              gsl_matrix_get(F, m, i) +
658              0.5 * tmp1 *
659              e->dB[m][i -
660              e->istart[m]][1]);
661      }
662  }
663 }
664
665 /* run the fit */
666 cov = gsl_matrix_alloc(e->n, e->n);
667
668 /* right hand side */
669 y = gsl_vector_alloc(e->nextgrid);
670 for (m = 0; m < e->nextgrid; m++) {
671     tmp1 = 0.0;
672     for (i = e->istart[m]; i <= e->iend[m]; i++) {

```

D. Code Listings

```
673         tmp1 += -u[i] * e->dB[m][i - e->istart[m]][0];
674     }
675     gsl_vector_set(y, m, tmp1);
676 }
677
678 mw = gsl_multifit_linear_alloc(e->nextgrid, e->n);
679
680 gsl_multifit_linear(F, y, freq, cov, &chisq, mw);
681 /*gsl_multifit_linear_free(mw); GSL-BUG */
682
683 /* statistics (total sum of squares) (dof = e->nrg + 2 - e->n) */
684 tss = gsl_stats_wtss(y->data, 1, freq->data, 1, e->n);
685 Rsq = 1.0 - chisq / tss;
686 (void)Rsq;
687
688 /* fill output */
689 for (i = 0; i < e->n; i++) {
690     u[i] = gsl_vector_get(freq, i);
691 }
692
693 /* convert omega to frequency */
694 freqeval = ereallocarray(NULL, e->nextgrid, sizeof(*freqeval));
695
696 for (m = 0; m < e->nextgrid; m++) {
697     om = 0.0;
698
699     for (i = e->istart[m]; i <= e->iend[m]; i++) {
700         om += u[i] * e->dB[m][i - e->istart[m]][0];
701     }
702
703     freqeval[m] = 1 / sqrt(fabs(om));
704 }
705
706 if (ethos_fit(e, u, e->extgrid, freqeval, e->nextgrid)) {
707     return 1;
708 }
709 free(freqeval);
710
711 /* cleanup */
712 gsl_vector_free(freq);
713 gsl_vector_free(y);
714 gsl_matrix_free(cov);
715 /* gsl_matrix_free(F); GSL-BUG */
716
```

```

717     return 0;
718 }
719
720 int
721 ethos_emd(const struct ethos *e, double *u, double *a, double *freq,
722          double *s, double eps)
723 {
724     double *upp, *low, r;
725     size_t i;
726
727     /*
728      * upper and lower envelopes
729      */
730     upp = ereallocarray(NULL, e->n, sizeof(*upp));
731     low = ereallocarray(NULL, e->n, sizeof(*low));
732
733     if (ethos_upper_envelope(e, upp, s, eps)) {
734         warn("ethos_shift:␣Failed");
735         free(upp);
736         free(low);
737         return 1;
738     }
739
740     /* flip signal */
741     for (i = 0; i < e->n; i++) {
742         s[i] = -s[i];
743     }
744
745     if (ethos_upper_envelope(e, low, s, eps)) {
746         warn("ethos_shift:␣Failed");
747         free(upp);
748         free(low);
749         return 1;
750     }
751
752     /* un-flip signal and lower envelope */
753     for (i = 0; i < e->n; i++) {
754         s[i] = -s[i];
755         low[i] = -low[i];
756     }
757
758     /*
759      * IMF and residual (stored in s)
760      */

```

D. Code Listings

```
761     for (i = 0; i < e->n; i++) {
762         r = (upp[i] + low[i]) / 2.0;
763         u[i] = s[i] - r;
764         s[i] = r;
765     }
766
767     /*
768      * instantaneous amplitude
769      */
770     for (i = 0; i < e->n; i++) {
771         a[i] = upp[i] - s[i];
772     }
773
774     /* cleanup */
775     free(low);
776     free(upp);
777
778     /*
779      * instantaneous frequency
780      */
781
782     /* calculate simple imf from u and a */
783     for (i = 0; i < e->n; i++) {
784         freq[i] = u[i];
785     }
786     if (ethos_divide_spline(e, freq, a)) {
787         return 1;
788     }
789
790     /* extract frequency */
791     if (ethos_frequency_from_simple_imf(e, freq)) {
792         return 1;
793     }
794
795     return 0;
796 }
797
798 int
799 ethos_characteristic(const struct ethos *e, double mu[static 3],
800                    const double *a, const double *freq)
801 {
802     size_t m, i;
803     double a1, freq0, freq1;
804
```

```

805     mu[0] = INFINITY;
806     mu[1] = mu[2] = DBL_EPSILON;
807
808     for (m = 0; m < e->nextgrid; m++) {
809         /* evaluate a', freq, freq' */
810         a1 = freq0 = freq1 = 0.0;
811         for (i = e->istart[m]; i <= e->iend[m]; i++) {
812             a1 += a[i] * e->dB[m][i - e->istart[m]][1];
813             freq0 += freq[i] * e->dB[m][i - e->istart[m]][0];
814             freq1 += freq[i] * e->dB[m][i - e->istart[m]][1];
815         }
816
817         /* take the absolute value */
818         a1 = fabs(a1);
819         freq0 = fabs(freq0);
820         freq1 = fabs(freq1);
821
822         /* mu_0 */
823         if (freq0 < mu[0]) {
824             mu[0] = freq0;
825         }
826
827         /* mu_1 */
828         if (a1 / freq0 > mu[1]) {
829             mu[1] = a1 / freq0;
830         }
831
832         /* mu_2 */
833         if (freq1 / freq0 > mu[2]) {
834             mu[2] = freq1 / freq0;
835         }
836     }
837
838     return 0;
839 }
840
841 double
842 ethos_norm_sup_bound_spline(const struct ethos *e, const double *c)
843 {
844     size_t i;
845     double res;
846
847     res = -INFINITY;
848

```

D. Code Listings

```
849     for (i = 0; i < e->n; i++) {
850         if (fabs(c[i]) > res) {
851             res = fabs(c[i]);
852         }
853     }
854
855     return res;
856 }
857
858 int
859 ethos_relerror(const struct ethos *e, double *relerror, double *c,
860               double *c_analytic)
861 {
862     size_t m, i;
863     int ret;
864     double *relerror_eval, c0, c_an0;
865
866     relerror_eval = ereallocarray(NULL, e->nextgrid,
867                                   sizeof(*relerror_eval));
868
869     for (m = 0; m < e->nextgrid; m++) {
870         c0 = c_an0 = 0.0;
871
872         for (i = e->istart[m]; i <= e->iend[m]; i++) {
873             c0 += c[i] * e->dB[m][i - e->istart[m]][0];
874             c_an0 += c_analytic[i] * e->dB[m][i -
875                                     e->istart[m]][0];
876         }
877
878         relerror_eval[m] = fabs((c0 - c_an0) / c_an0);
879     }
880
881     ret = ethos_fit(e, relerror, e->extgrid, relerror_eval,
882                   e->nextgrid);
883
884     free(relerror_eval);
885
886     return ret;
887 }
```

D.1.3. config.mk

```
1 # Customize below to fit your system
```



```

2
3 # paths
4 PREFIX = /usr/local
5 MANPREFIX = $(PREFIX)/share/man
6
7 # flags
8 CPPFLAGS = -D_DEFAULT_SOURCE
9 CFLAGS   = -std=c99 -pedantic -Wall -Wextra -Os
10 ARFLAGS  = rcs
11
12 # compiler, linker and archiver
13 CC = cc
14 AR = ar

```

D.1.4. Makefile

```

1 # See LICENSE file for copyright and license details
2 # ETHOS - EMD Toolbox using Hybrid Operator-Based Methods and B-Splines
3 .POSIX:
4
5 include config.mk
6
7 all: libethos.a
8
9 ethos.o: ethos.c config.mk ethos.h
10
11 libethos.a: ethos.o
12     $(AR) $(ARFLAGS) $@ $^
13
14 .c.o:
15     $(CC) -c $(CPPFLAGS) $(CFLAGS) $<
16
17 clean:
18     rm -f libethos.a ethos.o

```

D.2. Examples

These programs expect `libethos.a` and `ethos.h` somewhere in the environment. Set the variable `ETHOS` in `config.mk` (see Listing D.2.6) to point to the directory containing both files. This in turn will properly set the I- and L-flags in the preprocessor flags `CPPFLAGS` and the linker flags `LDFLAGS` respectively.

D.2.1. emd.c

```
1  /* See LICENSE file for copyright and license details. */
2  #include <ethos.h>
3  #include <gsl/gsl_matrix.h>
4  #include <limits.h>
5  #include <math.h>
6  #include <string.h>
7
8  #include "util.h"
9
10 double
11 a_0_0(double t)
12 {
13     return t + 1;
14 }
15
16 double
17 phi_0_0(double t)
18 {
19     return (15 * t + 21) * M_PI * t;
20 }
21
22 double
23 freq_0_0(double t)
24 {
25     return 15 * M_PI * t + (15 * t + 21) * M_PI;
26 }
27
28 double
29 a_0_1(double t)
30 {
31     return 3 * t + 1;
32 }
33
34 double
35 phi_0_1(double t)
36 {
37     return 5 * M_PI * t;
38 }
39
40 double
41 freq_0_1(double t)
42 {
```

```
43     (void)t;
44
45     return 5 * M_PI;
46 }
47
48 double
49 s_0(double t)
50 {
51     return a_0_0(t) * cos(phi_0_0(t)) +
52           a_0_1(t) * cos(phi_0_1(t)) +
53           20 * (t + 1);
54 }
55
56 double
57 a_1_0(double t)
58 {
59     return 1 + pow(t, 3.0);
60 }
61
62 double
63 phi_1_0(double t)
64 {
65     return 80 * M_PI * t;
66 }
67
68 double
69 freq_1_0(double t)
70 {
71     (void)t;
72
73     return 80 * M_PI;
74 }
75
76 double
77 a_1_1(double t)
78 {
79     return 1 + 10 * pow(t, 2.0);
80 }
81
82 double
83 phi_1_1(double t)
84 {
85     return 15 * M_PI * t;
86 }
```

D. Code Listings

```
87
88 double
89 freq_1_1(double t)
90 {
91     (void)t;
92
93     return 15 * M_PI;
94 }
95
96 double
97 s_1(double t)
98 {
99     return a_1_0(t) * cos(phi_1_0(t)) +
100           a_1_1(t) * cos(phi_1_1(t)) +
101           (20 * pow(t, 3.0) + 3);
102 }
103
104 struct imf {
105     double (*a)(double);
106     double (*phi)(double);
107     double (*freq)(double);
108 };
109
110 struct imf imfs_0[] = {
111     { a_0_0, phi_0_0, freq_0_0 },
112     { a_0_1, phi_0_1, freq_0_1 },
113 };
114
115 struct imf imfs_1[] = {
116     { a_1_0, phi_1_0, freq_1_0 },
117     { a_1_1, phi_1_1, freq_1_1 },
118 };
119
120 struct example {
121     char *name;
122     double a;
123     double b;
124     size_t N;
125     int q;
126     double dens;
127     double (*s)(double);
128     size_t ncomp;
129     struct imf *comp;
130     double eps;
```

```

131 } examples[] = {
132     {
133         .name = "emd.data/0",
134         .a    = 0.0,
135         .b    = 1.0,
136         .N    = 596,
137         .q    = 4,
138         .dens = 0.3,
139         .s    = s_0,
140         .ncomp = 2,
141         .comp = imfs_0,
142         .eps  = 0.01,
143     },
144     {
145         .name = "emd.data/1",
146         .a    = 0.0,
147         .b    = 1.0,
148         .N    = 596,
149         .q    = 4,
150         .dens = 0.3,
151         .s    = s_1,
152         .ncomp = 2,
153         .comp = imfs_1,
154         .eps  = 0.01,
155     },
156 };
157
158 int
159 process(struct example *ex)
160 {
161     struct comp_data {
162         double *U_an;
163         double *A_an;
164         double *Freq_an;
165         double *u_an;
166         double *a_an;
167         double *freq_an;
168         double *u;
169         double *a;
170         double *freq;
171         double *u_abserr;
172         double *a_relerr;
173         double *freq_relerr;

```

D. Code Listings

```

175     } *cd;
176     struct ethos *e;
177     double *T, *S, *s, *s_an, *tmp, mu[3];
178     size_t i, k;
179
180     e = ereallocarray(NULL, 1, sizeof(struct ethos));
181
182     /* generate analytical input points */
183     T = ereallocarray(NULL, ex->N, sizeof(*T));
184     S = ereallocarray(NULL, ex->N, sizeof(*S));
185     cd = ereallocarray(NULL, ex->ncomp, sizeof(*cd));
186     for (i = 0; i < ex->ncomp; i++) {
187         cd[i].U_an = ereallocarray(NULL, ex->N,
188                                   sizeof(*(cd[i].U_an)));
189         cd[i].A_an = ereallocarray(NULL, ex->N,
190                                   sizeof(*(cd[i].A_an)));
191         cd[i].Freq_an = ereallocarray(NULL, ex->N,
192                                       sizeof(*(cd[i].Freq_an)));
193     }
194     for (i = 0; i < ex->N; i++) {
195         T[i] = ex->a + (double)(ex->b - ex->a) / (ex->N - 1) * i;
196         S[i] = ex->s(T[i]);
197         for (k = 0; k < ex->ncomp; k++) {
198             cd[k].U_an[i] = ex->comp[k].a(T[i]) *
199                             cos(ex->comp[k].phi(T[i]));
200             cd[k].A_an[i] = ex->comp[k].a(T[i]);
201             cd[k].Freq_an[i] = ex->comp[k].freq(T[i]);
202         }
203     }
204
205     /* initialize ethos */
206     if (ethos_init(e, T, ex->N, 4, ex->q, ex->dens,
207                 ETHOS_GRID_UNIFORM)) {
208         warn("ethos_init: Failed");
209         return 1;
210     }
211
212     fprintf(stderr, "%s: n=%zu\n", ex->name, e->n);
213
214     /* fit */
215     s = ereallocarray(NULL, e->n, sizeof*(s));
216     if (ethos_fit(e, s, T, S, ex->N)) {
217         warn("ethos_fit: Failed");
218         return 1;

```

```

219     }
220     plot_spline_fmt(e, s, ETHOS_PLOT_CSV, "%s-s.csv", ex->name);
221
222     s_an = ereallocarray(NULL, e->n, sizeof(*s_an));
223     for (i = 0; i < e->n; i++) {
224         s_an[i] = s[i];
225     }
226
227     for (k = 0; k < ex->ncomp; k++) {
228         /* fit analytical solutions */
229         cd[k].u_an = ereallocarray(NULL, e->n,
230                                   sizeof(*(cd[k].u_an)));
231         cd[k].a_an = ereallocarray(NULL, e->n,
232                                   sizeof(*(cd[k].a_an)));
233         cd[k].freq_an = ereallocarray(NULL, e->n,
234                                       sizeof(*(cd[k].freq_an)));
235
236         if (ethos_fit(e, cd[k].u_an, T, cd[k].U_an, ex->N) ||
237             ethos_fit(e, cd[k].a_an, T, cd[k].A_an, ex->N) ||
238             ethos_fit(e, cd[k].freq_an, T, cd[k].Freq_an, ex->N)
239         ) {
240             warn("ethos_fit:␣Failed");
241             return 1;
242         }
243
244         /* plot analytical solutions */
245         plot_spline_fmt(e, cd[k].u_an, ETHOS_PLOT_CSV,
246                       "%s-u-%zu-analytic.csv", ex->name, k);
247         plot_spline_fmt(e, cd[k].a_an, ETHOS_PLOT_CSV,
248                       "%s-a-%zu-analytic.csv", ex->name, k);
249         plot_spline_fmt(e, cd[k].freq_an, ETHOS_PLOT_CSV,
250                       "%s-freq-%zu-analytic.csv", ex->name, k);
251
252         /* analytical IMF characteristic */
253         ethos_characteristic(e, mu, cd[k].a_an, cd[k].freq_an);
254         fprintf(stderr, "%s:␣IMF-%zu:␣characteristic␣"
255                   " (%e,␣%e,␣%e)\n", ex->name, k, mu[0], mu[1],
256                   mu[2]);
257
258         cd[k].u = ereallocarray(NULL, e->n, sizeof(*(cd[k].u)));
259         cd[k].a = ereallocarray(NULL, e->n, sizeof(*(cd[k].a)));
260         cd[k].freq = ereallocarray(NULL, e->n,
261                                   sizeof(*(cd[k].freq)));
262         if (ethos_emd(e, cd[k].u, cd[k].a, cd[k].freq, s,

```

D. Code Listings

```

263         ex->eps)) {
264             return 1;
265     }
266
267     /* plot solutions */
268     plot_spline_fmt(e, cd[k].u, ETHOS_PLOT_CSV,
269                   "%s-u-%zu.csv", ex->name, k);
270     plot_spline_fmt(e, cd[k].a, ETHOS_PLOT_CSV,
271                   "%s-a-%zu.csv", ex->name, k);
272     plot_spline_fmt(e, cd[k].freq, ETHOS_PLOT_CSV,
273                   "%s-freq-%zu.csv", ex->name, k);
274
275     /* plot error */
276     cd[k].u_abserr = ereallocarray(NULL, e->n,
277                                   sizeof(*(cd[k].
278                                           u_abserr)));
279     cd[k].a_relerr = ereallocarray(NULL, e->n,
280                                   sizeof(*(cd[k].
281                                           a_relerr)));
282     cd[k].freq_relerr = ereallocarray(NULL, e->n,
283                                       sizeof(*(cd[k].
284                                               freq_relerr)));
285
286     for (i = 0; i < e->n; i++) {
287         cd[k].u_abserr[i] = fabs(cd[k].u[i] -
288                                 cd[k].u_an[i]);
289     }
290     ethos_relerror(e, cd[k].a_relerr, cd[k].a, cd[k].a_an);
291     ethos_relerror(e, cd[k].freq_relerr, cd[k].freq,
292                   cd[k].freq_an);
293
294     plot_spline_fmt(e, cd[k].u_abserr, ETHOS_PLOT_CSV,
295                   "%s-u-%zu-abserr.csv", ex->name, k);
296     plot_spline_fmt(e, cd[k].a_relerr, ETHOS_PLOT_CSV,
297                   "%s-a-%zu-relerr.csv", ex->name, k);
298     plot_spline_fmt(e, cd[k].freq_relerr, ETHOS_PLOT_CSV,
299                   "%s-freq-%zu-relerr.csv", ex->name, k);
300
301     /* subtract u from s in the analytical solution */
302     for (i = 0; i < e->n; i++) {
303         s_an[i] -= cd[k].u_an[i];
304     }
305     plot_spline_fmt(e, s_an, ETHOS_PLOT_CSV,
306                   "%s-r-%zu-analytic.csv", ex->name,

```



```

307         k + 1);
308     plot_spline_fmt(e, s, ETHOS_PLOT_CSV,
309         "%s-r-%zu.csv", ex->name, k + 1);
310
311     tmp = ereallocarray(NULL, e->n, sizeof(*tmp));
312     ethos_relerror(e, tmp, s, s_an);
313     plot_spline_fmt(e, tmp, ETHOS_PLOT_CSV,
314         "%s-r-%zu-relerr.csv", ex->name, k + 1);
315     free(tmp);
316 }
317
318 /* cleanup */
319 free(T);
320 free(S);
321 free(s);
322
323     return 0;
324 }
325
326 int
327 main(int argc, char *argv[])
328 {
329     int ret;
330     size_t i;
331
332     ret = 0;
333
334     for (i = 0; i < LEN(examples); i++) {
335         if (argc <= 1 || !strcmp(examples[i].name, argv[1])) {
336             ret |= process(&examples[i]);
337
338             if (argv[1]) {
339                 break;
340             }
341         }
342     }
343
344     return ret;
345 }

```

D.2.2. envelope.c

```

1 /* See LICENSE file for copyright and license details. */

```

D. Code Listings

```
2 #include <ethos.h>
3 #include <gsl/gsl_matrix.h>
4 #include <limits.h>
5 #include <math.h>
6 #include <string.h>
7
8 #include "util.h"
9
10 double
11 s_x(double t)
12 {
13     return 20 * t + (2 + cos(4 * M_PI * t)) * cos(13 * M_PI * t);
14 }
15
16 double
17 m_x(double t)
18 {
19     return 20 * t + (2 + cos(4 * M_PI * t));
20 }
21
22 double
23 s_0(double t)
24 {
25     return 40 * t + (20 + 10 * cos(5 * M_PI * t)) *
26         cos(25 * M_PI * t);
27 }
28
29 double
30 m_0(double t)
31 {
32     return 40 * t + (20 + 10 * cos(5 * M_PI * t));
33 }
34
35 double
36 s_1(double t)
37 {
38     return 1.0 / 16.0 * (pow(t, 2.0) + 2) *
39         cos(M_PI * sin(8 * t) + M_PI);
40 }
41
42 double
43 m_1(double t)
44 {
45     return 1.0 / 16.0 * (pow(t, 2.0) + 2);
```

```
46 }
47
48 struct example {
49     char *name;
50     double a;
51     double b;
52     size_t N;
53     int q;
54     double dens;
55     double (*s)(double);
56     double (*m)(double);
57     double eps;
58 } examples[] = {
59     {
60         .name = "envelope.data/x",
61         .a    = 0.0,
62         .b    = 1.0,
63         .N    = 596,
64         .q    = 4,
65         .dens = 0.3,
66         .s    = s_x,
67         .m    = m_x,
68         .eps  = 0.01,
69     },
70     {
71         .name = "envelope.data/0",
72         .a    = 0.0,
73         .b    = 1.0,
74         .N    = 596,
75         .q    = 4,
76         .dens = 0.3,
77         .s    = s_0,
78         .m    = m_0,
79         .eps  = 0.01,
80     },
81     {
82         .name = "envelope.data/1",
83         .a    = -4.0,
84         .b    = 4.0,
85         .N    = 596,
86         .q    = 4,
87         .dens = 0.3,
88         .s    = s_1,
89         .m    = m_1,
```

D. Code Listings

```
90         .eps = 0.10,
91     },
92 };
93
94 int
95 process(struct example *ex)
96 {
97     struct ethos *e;
98     double *T, *S, *A, *s, *a_an, *a, *a_class, *err,
99         *releror;
100    size_t i;
101
102    e = reallocarray(NULL, 1, sizeof(struct ethos));
103
104    T = ereallocarray(NULL, ex->N, sizeof(*T));
105    S = ereallocarray(NULL, ex->N, sizeof(*S));
106    A = ereallocarray(NULL, ex->N, sizeof(*A));
107
108    /* generate input points */
109    for (i = 0; i < ex->N; i++) {
110        T[i] = ex->a + (double)(ex->b - ex->a) / (ex->N - 1) * i;
111        S[i] = ex->s(T[i]);
112        A[i] = ex->m(T[i]);
113    }
114
115    plot_points_fmt(T, S, ex->N, ETHOS_PLOT_CSV,
116                  "%s-s-points.csv", ex->name);
117
118    /* initialize ethos */
119    if (ethos_init(e, T, ex->N, 4, ex->q, ex->dens,
120                ETHOS_GRID_UNIFORM)) {
121        warn("ethos_init: Failed");
122        return 1;
123    }
124
125    fprintf(stderr, "%s: n=%zu\n", ex->name, e->n);
126
127    /* fit */
128    s = ereallocarray(NULL, e->n, sizeof(*s));
129    if (ethos_fit(e, s, T, S, ex->N)) {
130        warn("ethos_fit: Failed");
131        return 1;
132    }
133    plot_spline_fmt(e, s, ETHOS_PLOT_CSV,
```

```

134         "%s-s.csv", ex->name);
135
136     a_an = ereallocarray(NULL, e->n, sizeof(*a_an));
137     if (ethos_fit(e, a_an, T, A, ex->N)) {
138         warn("ethos_fit:␣Failed");
139         return 1;
140     }
141     plot_spline_fmt(e, a_an, ETHOS_PLOT_CSV,
142         "%s-a-analytic.csv", ex->name);
143
144     double *r = ereallocarray(NULL, e->n, sizeof(*r));
145     for (i = 0; i < e->n; i++) {
146         r[i] = 0.0;
147     }
148     a_class = ereallocarray(NULL, e->n, sizeof(*a_class));
149     if (ethos_upper_envelope(e, a_class, s, INFINITY)) {
150         warn("ethos_sift:␣Failed");
151         return 1;
152     }
153     plot_spline_fmt(e, a_class, ETHOS_PLOT_CSV,
154         "%s-a-classic.csv", ex->name);
155
156     a = ereallocarray(NULL, e->n, sizeof(*a));
157     if (ethos_upper_envelope(e, a, s, ex->eps)) {
158         warn("ethos_sift:␣Failed");
159         return 1;
160     }
161     plot_spline_fmt(e, a, ETHOS_PLOT_CSV,
162         "%s-a.csv", ex->name);
163
164     /* error */
165     err = ereallocarray(NULL, e->n, sizeof(*err));
166     for (i = 0; i < e->n; i++) {
167         err[i] = a[i] - a_an[i];
168     }
169     plot_spline_fmt(e, err, ETHOS_PLOT_CSV,
170         "%s-err.csv", ex->name);
171
172     relerror = ereallocarray(NULL, e->n, sizeof(*relerror));
173
174     ethos_relerror(e, relerror, a, a_an);
175     plot_spline_fmt(e, relerror, ETHOS_PLOT_CSV,
176         "%s-relerr.csv", ex->name);
177

```

D. Code Listings

```
178     /* classic error */
179     for (i = 0; i < e->n; i++) {
180         err[i] = a_class[i] - a_an[i];
181     }
182     plot_spline_fmt(e, err, ETHOS_PLOT_CSV,
183         "%s-err-classic.csv", ex->name);
184
185     ethos_relerror(e, relerror, a_class, a_an);
186     plot_spline_fmt(e, relerror, ETHOS_PLOT_CSV,
187         "%s-relerr-classic.csv", ex->name);
188     free(relerror);
189
190
191     /* cleanup */
192     free(T);
193     free(S);
194     free(A);
195     free(s);
196     free(a_an);
197     free(a);
198     free(err);
199
200     return 0;
201 }
202
203 int
204 main(int argc, char *argv[])
205 {
206     int ret;
207     size_t i;
208
209     ret = 0;
210
211     for (i = 0; i < LEN(examples); i++) {
212         if (argc <= 1 || !strcmp(examples[i].name, argv[1])) {
213             ret |= process(&examples[i]);
214
215             if (argv[1]) {
216                 break;
217             }
218         }
219     }
220
221     return ret;
```

222 }

D.2.3. regop.c

```

1  /* See LICENSE file for copyright and license details. */
2  #include <ethos.h>
3  #include <gsl/gsl_matrix.h>
4  #include <limits.h>
5  #include <math.h>
6  #include <string.h>
7
8  #include "util.h"
9
10 double
11 u_0(double t)
12 {
13     return cos(40 * t);
14 }
15
16 double
17 freq_0(double t)
18 {
19     (void)t;
20
21     return 40;
22 }
23
24 double
25 u_1(double t)
26 {
27     return cos(3 * sin(3 * M_PI * t) + 16 * M_PI * t);
28 }
29
30 double
31 freq_1(double t)
32 {
33     return 3 * 3 * M_PI * cos(3 * M_PI * t) + 16 * M_PI;
34 }
35
36 double
37 u_2(double t)
38 {
39     return cos(40 * t + 100.0 / 90.0 * log(1 + exp(90 * (t - 0.5))));

```

D. Code Listings

```
40 }
41
42 double
43 freq_2(double t)
44 {
45     return 40 + 100.0 / (1 + exp(-90 * (t - 0.5)));
46 }
47
48 struct example {
49     char *name;
50     double a;
51     double b;
52     size_t N;
53     int q;
54     double dens;
55     double (*u)(double);
56     double (*freq)(double);
57 } examples[] = {
58     {
59         .name = "regop.data/0",
60         .a    = 0.0,
61         .b    = 1.0,
62         .N    = 596,
63         .q    = 4,
64         .dens = 0.3,
65         .u    = u_0,
66         .freq = freq_0,
67     },
68     {
69         .name = "regop.data/1",
70         .a    = 0.0,
71         .b    = 1.0,
72         .N    = 596,
73         .q    = 4,
74         .dens = 0.3,
75         .u    = u_1,
76         .freq = freq_1,
77     },
78     {
79         .name = "regop.data/2",
80         .a    = 0.0,
81         .b    = 1.0,
82         .N    = 596,
83         .q    = 4,
```



```

84         .dens = 0.3,
85         .u    = u_2,
86         .freq = freq_2,
87     },
88 };
89
90 int
91 process(struct example *ex)
92 {
93     struct ethos *e;
94     double *T, *U, *F, *u, *f_an, *f, *err, *tmp;
95     size_t i;
96
97     e = reallocarray(NULL, 1, sizeof(struct ethos));
98
99     T = ereallocarray(NULL, ex->N, sizeof(*T));
100    U = ereallocarray(NULL, ex->N, sizeof(*U));
101    F = ereallocarray(NULL, ex->N, sizeof(*F));
102
103    /* generate input points */
104    for (i = 0; i < ex->N; i++) {
105        T[i] = (double)(ex->b - ex->a) / (ex->N - 1) * i;
106        U[i] = ex->u(T[i]);
107        F[i] = ex->freq(T[i]);
108    }
109    plot_points_fmt(T, U, ex->N, ETHOS_PLOT_CSV, "%s-u-points.csv",
110                  ex->name);
111
112    /* initialize ethos */
113    if (ethos_init(e, T, ex->N, 4, ex->q, ex->dens,
114                  ETHOS_GRID_UNIFORM)) {
115        warn("ethos_init:␣Failed");
116        return 1;
117    }
118
119    fprintf(stderr, "%s:␣n␣=␣%zu␣\n", ex->name, e->n);
120
121    /* fit */
122    u = ereallocarray(NULL, e->n, sizeof(*u));
123    if (ethos_fit(e, u, T, U, ex->N)) {
124        warn("ethos_fit:␣Failed");
125        return 1;
126    }
127    f_an = ereallocarray(NULL, e->n, sizeof(*f_an));

```

D. Code Listings

```
128     if (ethos_fit(e, f_an, T, F, ex->N)) {
129         warn("ethos_fit: Failed");
130         return 1;
131     }
132     plot_spline_fmt(e, u, ETHOS_PLOT_CSV, "%s-u.csv", ex->name);
133
134     /* calculate instantaneous frequency */
135     f = ereallocarray(NULL, e->n, sizeof(*f));
136     for (i = 0; i < e->n; i++) {
137         f[i] = u[i];
138     }
139     if (ethos_frequency_from_simple_imf(e, f)) {
140         return 1;
141     }
142
143     err = ereallocarray(NULL, e->n, sizeof(*err));
144     for (i = 0; i < e->n; i++) {
145         err[i] = f[i] - f_an[i];
146     }
147
148     plot_spline_fmt(e, err, ETHOS_PLOT_CSV, "%s-abserr.csv",
149                    ex->name);
150     plot_spline_fmt(e, f, ETHOS_PLOT_CSV, "%s-freq.csv", ex->name);
151     plot_spline_fmt(e, f_an, ETHOS_PLOT_CSV, "%s-freq-analytic.csv",
152                    ex->name);
153
154     tmp = ereallocarray(NULL, e->n, sizeof(*tmp));
155     ethos_relerror(e, tmp, f, f_an);
156     plot_spline_fmt(e, tmp, ETHOS_PLOT_CSV, "%s-relerr.csv",
157                    ex->name);
158     free(tmp);
159
160     /* cleanup */
161     free(T);
162     free(U);
163     free(F);
164     free(u);
165     free(f_an);
166     free(f);
167     free(err);
168
169     return 0;
170 }
171
```

```

172 int
173 main(int argc, char *argv[])
174 {
175     int ret;
176     size_t i;
177
178     ret = 0;
179
180     for (i = 0; i < LEN(examples); i++) {
181         if (argc <= 1 || !strcmp(examples[i].name, argv[1])) {
182             ret |= process(&examples[i]);
183
184             if (argv[1]) {
185                 break;
186             }
187         }
188     }
189
190     return ret;
191 }

```

D.2.4. util.h

```

1  /* See LICENSE file for copyright and license details. */
2  #ifndef UTIL_H
3  #define UTIL_H
4
5  #include <gsl/gsl_vector.h>
6  #include <stddef.h>
7  #include <time.h>
8
9  #undef MIN
10 #define MIN(x,y) ((x) < (y) ? (x) : (y))
11 #undef MAX
12 #define MAX(x,y) ((x) > (y) ? (x) : (y))
13 #undef LEN
14 #define LEN(x) (sizeof (x) / sizeof *(x))
15
16 void warn(const char *, ...);
17 void die(const char *, ...);
18
19 long long strtonum(const char *, long long, long long, const char **);
20

```

D. Code Listings

```
21 int esnprintf(char *, size_t, const char *, ...);
22 void *ereallocarray(void *, size_t, size_t);
23
24 void util_array_vector_wrap(const double *, size_t, gsl_vector *);
25
26 int plot_spline_fmt(const struct ethos *, const double *,
27                    enum ethos_plot_format, const char *, ...);
28 int plot_points_fmt(const double *, const double *, size_t,
29                    enum ethos_plot_format, const char *, ...);
30
31 #endif /* UTIL_H */
```

D.2.5. util.c

```
1  /* See LICENSE file for copyright and license details. */
2  #include <errno.h>
3  #include <gsl/gsl_vector.h>
4  #include <limits.h>
5  #include <stdarg.h>
6  #include <stddef.h>
7  #include <stdint.h>
8  #include <stdio.h>
9  #include <stdlib.h>
10 #include <string.h>
11 #include <sys/types.h>
12 #include <time.h>
13
14 #include <ethos.h>
15 #include "util.h"
16
17 static char *argv0;
18
19 static void
20 verr(const char *fmt, va_list ap)
21 {
22     if (argv0 && strcmp(fmt, "usage", sizeof("usage") - 1)) {
23         fprintf(stderr, "%s:\n", argv0);
24     }
25
26     vfprintf(stderr, fmt, ap);
27
28     if (fmt[0] && fmt[strlen(fmt) - 1] == ':') {
29         fputc('\n', stderr);
30     }
31 }
```

```

30         perror(NULL);
31     } else {
32         fputc('\n', stderr);
33     }
34 }
35
36 void
37 warn(const char *fmt, ...)
38 {
39     va_list ap;
40
41     va_start(ap, fmt);
42     verr(fmt, ap);
43     va_end(ap);
44 }
45
46 void
47 die(const char *fmt, ...)
48 {
49     va_list ap;
50
51     va_start(ap, fmt);
52     verr(fmt, ap);
53     va_end(ap);
54
55     exit(1);
56 }
57
58 #define INVALID 1
59 #define TOOSMALL 2
60 #define TOOLARGE 3
61
62 long long
63 strtonum(const char *numstr, long long minval, long long maxval,
64          const char **errstrp)
65 {
66     long long ll = 0;
67     int error = 0;
68     char *ep;
69     struct errval {
70         const char *errstr;
71         int err;
72     } ev[4] = {
73         { NULL, 0 },

```

D. Code Listings

```
74         { "invalid",    EINVAL },
75         { "too_small",  ERANGE },
76         { "too_large",  ERANGE },
77     };
78
79     ev[0].err = errno;
80     errno = 0;
81     if (minval > maxval) {
82         error = INVALID;
83     } else {
84         ll = strtoll(numstr, &ep, 10);
85         if (numstr == ep || *ep != '\0')
86             error = INVALID;
87         else if ((ll == LLONG_MIN && errno == ERANGE) ||
88                 ll < minval)
89             error = TOOSMALL;
90         else if ((ll == LLONG_MAX && errno == ERANGE) ||
91                 ll > maxval)
92             error = TOOLARGE;
93     }
94     if (errstrp != NULL)
95         *errstrp = ev[error].errstr;
96     errno = ev[error].err;
97     if (error)
98         ll = 0;
99
100    return ll;
101 }
102
103 /*
104  * This is sqrt(SIZE_MAX+1), as s1*s2 <= SIZE_MAX
105  * if both s1 < MUL_NO_OVERFLOW and s2 < MUL_NO_OVERFLOW
106  */
107 #define MUL_NO_OVERFLOW ((size_t)1 << (sizeof(size_t) * 4))
108
109 static void *
110 _reallocarray(void *optr, size_t nmemb, size_t size)
111 {
112     if ((nmemb >= MUL_NO_OVERFLOW || size >= MUL_NO_OVERFLOW) &&
113         nmemb > 0 && SIZE_MAX / nmemb < size) {
114         errno = ENOMEM;
115         return NULL;
116     }
117     return realloc(optr, size * nmemb);

```

```

118 }
119
120 int
121 esnprintf(char *str, size_t size, const char *fmt, ...)
122 {
123     va_list ap;
124     int ret;
125
126     va_start(ap, fmt);
127     ret = vsnprintf(str, size, fmt, ap);
128     va_end(ap);
129
130     return (ret < 0 || (size_t)ret >= size);
131 }
132
133 void *
134 ereallocarray(void *optr, size_t nmemb, size_t size)
135 {
136     void *p;
137
138     if (!(p = _reallocarray(optr, nmemb, size))) {
139         die("reallocarray: Out of memory");
140     }
141
142     return p;
143 }
144
145 void
146 util_array_vector_wrap(const double *arr, size_t len, gsl_vector *v)
147 {
148     v->size = len;
149     v->stride = 1;
150     v->data = (double *)arr;
151     v->block = NULL;
152     v->owner = 0;
153 }
154
155 int
156 plot_spline_fmt(const struct ethos *e, const double *c,
157                enum ethos_plot_format p, const char *fmt, ...)
158 {
159     char fname[PATH_MAX];
160     va_list ap;
161

```

D. Code Listings

```
162     va_start(ap, fmt);
163     if ((unsigned)vsnprintf(fname, LEN(fname), fmt, ap) >=
164         LEN(fname)) {
165         warn("vsnprintf: Truncated filename");
166         return 1;
167     }
168     va_end(ap);
169
170     return ethos_plot_spline(e, c, fname, p);
171 }
172
173 int
174 plot_points_fmt(const double *T, const double *S, size_t N,
175                enum ethos_plot_format p, const char *fmt, ...)
176 {
177     char fname[PATH_MAX];
178     va_list ap;
179
180     va_start(ap, fmt);
181     if ((unsigned)vsnprintf(fname, LEN(fname), fmt, ap) >=
182         LEN(fname)) {
183         warn("vsnprintf: Truncated filename");
184         return 1;
185     }
186     va_end(ap);
187
188     return ethos_plot_points((double *)T, (double *)S, N, fname, p);
189 }
```

D.2.6. config.mk

```
1  # Customize below to fit your system
2
3  # paths
4  PREFIX    = /usr/local
5  ETHOS     = ../ethos/
6
7  # flags
8  CPPFLAGS  = -D_DEFAULT_SOURCE -I $(ETHOS)
9  CFLAGS    = -std=c99 -pedantic -Wall -Wextra -Os
10 LDFLAGS    = -s -L $(ETHOS)
11 LDLIBS    = -lethos -lgsl -lgslcblas -lm
12
```



```

13 # compiler and linker
14 CC = cc

```

D.2.7. Makefile

```

1 # See LICENSE file for copyright and license details
2 # ETHOS - EMD Toolbox using Hybrid Operator-Based Methods and B-Splines
3 .POSIX:
4
5 include config.mk
6
7 EXAMPLES = emd envelope regop spline
8
9 all: $(EXAMPLES:=.data/SENTINEL)
10
11 emd.data/SENTINEL: emd
12 envelope.data/SENTINEL: envelope
13 regop.data/SENTINEL: regop
14 spline.data/SENTINEL: spline
15
16 emd: emd.o util.o
17 envelope: envelope.o util.o
18 regop: regop.o util.o
19 spline: spline.o util.o
20
21 emd.o: emd.c config.mk
22 envelope.o: envelope.c config.mk
23 regop.o: regop.c config.mk
24 spline.o: spline.c config.mk
25 util.o: util.c config.mk
26
27 .o:
28     $(CC) -o $@ $(LDFLAGS) $< util.o $(LDLIBS)
29
30 .c.o:
31     $(CC) -c $(CPPFLAGS) $(CFLAGS) $<
32
33 $(EXAMPLES:=.data/SENTINEL):
34     touch $@
35     ./$^
36
37 clean:
38     rm -f $(EXAMPLES) $(EXAMPLES:=.o) util.o

```

D.3. License

This ISC license applies to all code listings in Chapter D.

```
1 Copyright 2019-2020 Laslo Hunhold
2
3 Permission to use, copy, modify, and/or distribute this software for any
4 purpose with or without fee is hereby granted, provided that the above
5 copyright notice and this permission notice appear in all copies.
6
7 THE SOFTWARE IS PROVIDED "AS IS" AND THE AUTHOR DISCLAIMS ALL WARRANTIES
8 WITH REGARD TO THIS SOFTWARE INCLUDING ALL IMPLIED WARRANTIES OF
9 MERCHANTABILITY AND FITNESS. IN NO EVENT SHALL THE AUTHOR BE LIABLE FOR
10 ANY SPECIAL, DIRECT, INDIRECT, OR CONSEQUENTIAL DAMAGES OR ANY DAMAGES
11 WHATSOEVER RESULTING FROM LOSS OF USE, DATA OR PROFITS, WHETHER IN AN
12 ACTION OF CONTRACT, NEGLIGENCE OR OTHER TORTIOUS ACTION, ARISING OUT OF
13 OR IN CONNECTION WITH THE USE OR PERFORMANCE OF THIS SOFTWARE.
```

Bibliography

- [Bou03] Bourbaki, Nicolas: *Topological Vector Spaces: Chapters 1–5*, volume 1 of *Elements of Mathematics*. Springer-Verlag Berlin Heidelberg, Berlin, Germany, 1st edition, 2003, ISBN 978-3-642-61715-7. <https://doi.org/10.1007/978-3-642-61715-7>.
- [Cie97] Ciesielski, Krzysztof: *Set Theory for the Working Mathematician*, volume 39 of *London Mathematical Society Student Texts*. Cambridge University Press, Cambridge, England, UK, 1st edition, 1997, ISBN 978-1-139-17313-1. <https://doi.org/10.1017/CB09781139173131>.
- [Dau92] Daubechies, Ingrid: *Ten Lectures on Wavelets*, volume 61 of *CBMS-NSF Regional Conference Series in Applied Mathematics*. Society for Industrial and Applied Mathematics (SIAM), University City, Philadelphia, PA, USA, 1st edition, June 1992, ISBN 978-1-61197-010-4. <https://doi.org/10.1137/1.9781611970104>.
- [dB01] Boor, Carl-Wilhelm Reinhold de: *A Practical Guide to Splines*, volume 27 of *Applied Mathematical Sciences*. Springer-Verlag New York, New York City, NY, USA, revised edition, April 2001, ISBN 978-0-387-95366-3. <https://www.springer.com/book/978-0-387-95366-3>.
- [Die95] Dierckx, Paul: *Curve and Surface Fitting with Splines*, volume 1 of *Numerical Mathematics and Scientific Computation*. Clarendon Press, Oxford, England, UK, new edition, April 1995, ISBN 978-0-19-853440-2. <https://global.oup.com/academic/product/curve-and-surface-fitting-with-splines-9780198534402>.
- [DLW11] Daubechies, Ingrid, Jianfeng Lu, and Hau Tieng Wu: *Synchrosqueezed wavelet transforms: An empirical mode decomposition-like tool*. *Applied and Computational Harmonic Analysis*, 30(2):243–261, March 2011, ISSN 1063-5203. <https://dx.doi.org/10.1016/j.acha.2010.08.002>.
- [Fou22] Fourier, Jean Baptiste Joseph: *Théorie analytique de la chaleur*. Ambroise Firmin Didot, père et fils, Paris, France, 1st edition, 1822. <https://openlibrary.org/books/OL24141486M/>.
- [GDT⁺18] Galassi, Mark, Jim Davies, James Theiler, Brian Gough, Gerard Jungman, Patrick Alken, Michael Booth, Fabrice Rossi, and Rhys Ulerich: *GNU Scientific Library*. Free Software Foundation, Boston, MA, USA, 2.5 edition,

Bibliography

- June 2018. <https://www.gnu.org/software/gsl/doc/latex/gsl-ref.pdf>.
- [GPHX17] Guo, Baokui, Silong Peng, Xiyuan Hu, and Pengcheng Xu: *Complex-valued differential operator-based method for multi-component signal separation*. Signal Processing, 132:66–76, March 2017, ISSN 0165-1684. <https://dx.doi.org/10.1016/j.sigpro.2016.09.015>.
- [Haa10] Haar, Alfréd: *Zur Theorie der orthogonalen Funktionensysteme*. Mathematische Annalen, 69:331–371, September 1910, ISSN 1432-1807. <https://dx.doi.org/10.1007/BF01456326>.
- [HJ12] Horn, Roger Alan and Charles Royal Johnson: *Matrix Analysis*. Cambridge University Press, Cambridge, England, UK, 2nd edition, October 2012, ISBN 978-0-521-83940-2. <https://dx.doi.org/10.1017/9781139020411>.
- [HK13] Huang, Boqiang and Angela Kunoth: *An optimization based empirical mode decomposition scheme*. Journal of Computational and Applied Mathematics, 240:174–183, March 2013, ISSN 0377-0427. <https://dx.doi.org/10.1016/j.cam.2012.07.012>, MATA 2012.
- [HPH12] Hu, Xiyuan, Silong Peng, and Wen-Liang Hwang: *EMD revisited: A new understanding of the envelope and resolving the mode-mixing problem in AM-FM signals*. IEEE Transactions on Signal Processing, 60(3):1075–1086, March 2012, ISSN 1941-0476. <https://dx.doi.org/10.1109/TSP.2011.2179650>.
- [HS11] Hou, Thomas Yizhao and Zuoqiang Shi: *Adaptive data analysis via sparse time-frequency representation*. Advances in Adaptive Data Analysis, 3(1&2):1–28, April 2011. <https://dx.doi.org/10.1142/S1793536911000647>.
- [HSL⁺98] Huang, Norden Eh, Zheng Shen, Steven R. Long, Manli C. Wu, Hsing H. Shih, Quanan Zheng, Nai-Chyuan Yen, Chi Chao Tung, and Henry H. Liu: *The empirical mode decomposition and the hilbert spectrum for non-linear and non-stationary time series analysis*. Proceedings of the Royal Society of London. Series A: Mathematical, Physical and Engineering Sciences, 454:903–995, March 1998, ISSN 1471-2946. <https://dx.doi.org/10.1098/rspa.1998.0193>.
- [HYY15] Huang, Chao, Lijun Yang, and Lihua Yang: *ϵ -Mono-Component: Its characterization and construction*. IEEE Transactions on Signal Processing, 63:234–243, January 2015, ISSN 1053-587X. <https://dx.doi.org/10.1109/TSP.2014.2370950>.
- [ISO99] ISO/IEC JTC 1/SC 22: *ISO/IEC 9899:1999: Programming Languages — C*. International Organization for Standardization, Geneva, Switzerland,

- 2nd edition, December 1999. <https://www.iso.org/standard/29237.html>.
- [Jah07] Jahn, Johannes: *Introduction to the Theory of Nonlinear Optimization*. Springer-Verlag Berlin Heidelberg, Berlin, Germany, 3rd edition, 2007, ISBN 978-3-540-49379-2. <https://dx.doi.org/10.1007/978-3-540-49379-2>.
- [KK00] Küpfmüller, Karl and Gerhard Kohn: *Theoretische Elektrotechnik und Elektronik: Eine Einführung*. Springer-Lehrbuch. Springer-Verlag Berlin Heidelberg, Berlin, Germany, 15th edition, 2000, ISBN 978-3-662-10425-5. <https://dx.doi.org/10.1007/978-3-662-10425-5>.
- [KTRZ⁺17] Kreutzer, Moritz, Jonas Thies, Melven Röhrig-Zöllner, Andreas Pieper, Faisal Shahzad, Martin Galgon, Achim Basermann, Holger Fehske, Georg Hager, and Gerhard Wellein: *GHOST: Building blocks for high performance sparse linear algebra on heterogeneous systems*. International Journal of Parallel Programming, 45(5):1046–1072, October 2017, ISSN 1573-7640. <https://dx.doi.org/10.1007/s10766-016-0464-z>.
- [Kö88] Körner, Thomas William: *Fourier Analysis*. Cambridge University Press, Cambridge, England, UK, 1st edition, 1988, ISBN 978-1-107-04994-9. <https://dx.doi.org/10.1017/CB09781107049949>.
- [LWW13] Liu, Yanping, Yong Wang, and Zhen Wang: *RBF prediction model based on EMD for forecasting GPS precipitable water vapor and annual precipitation*. In Luo, Xun (editor): *2nd International Conference On Systems Engineering and Modeling (ICSEM-13)*, volume 35 of *Advances in Intelligent Systems Research*, pages 51–55, Paris, France, April 2013. Atlantis Press. <https://dx.doi.org/10.2991/icsem.2013.11>.
- [Mal09] Mallat, Stéphane Georges: *A Wavelet Tour of Signal Processing*. Academic Press, Boston, MA, USA, 3rd edition, 2009, ISBN 978-0-12-374370-1. <https://dx.doi.org/10.1016/B978-0-12-374370-1.50001-9>.
- [NP06] Niculescu, Constantin P. and Lars Erik Persson: *Convex Functions and Their Applications: A Contemporary Approach*, volume 24 of *CMS Books in Mathematics*. Springer-Verlag New York, New York City, NY, USA, 1st edition, 2006, ISBN 978-0-387-31077-0. <https://dx.doi.org/10.1007/0-387-31077-0>.
- [PH08] Peng, Silong and Wen-Liang Hwang: *Adaptive signal decomposition based on local narrow band signals*. IEEE Transactions on Signal Processing, 56(7):2669–2676, June 2008, ISSN 1941-0476. <https://dx.doi.org/10.1109/TSP.2008.917360>.

Bibliography

- [PH10] Peng, Silong and Wen-Liang Hwang: *Null space pursuit: An operator-based approach to adaptive signal separation*. IEEE Transactions on Signal Processing, 58(5):2475–2483, May 2010, ISSN 1941-0476. <https://dx.doi.org/10.1109/TSP.2010.2041606>.
- [Sch46a] Schoenberg, Isaac Jacob: *Contributions to the problem of approximation of equidistant data by analytic functions. Part A. On the problem of smoothing or graduation. A first class of analytic approximation formulae*. Quarterly of Applied Mathematics, 4(1):45–99, April 1946, ISSN 1552-4485. <https://doi.org/10.1090/qam/15914>.
- [Sch46b] Schoenberg, Isaac Jacob: *Contributions to the problem of approximation of equidistant data by analytic functions. Part B. On the problem of osculatory interpolation. A second class of analytic approximation formulae*. Quarterly of Applied Mathematics, 4(2):112–141, July 1946, ISSN 1552-4485. <https://doi.org/10.1090/qam/16705>.
- [SW99] Schaefer, Helmut Heinrich and Michael P. Wolff: *Topological Vector Spaces*, volume 3 of *Graduate Texts in Mathematics*. Springer-Verlag New York, New York City, NY, USA, 2nd edition, June 1999, ISBN 978-1-4612-1468-7. <https://doi.org/10.1007/978-1-4612-1468-7>.
- [WR10] Wu, Qin and Sherman Delbert Riemenschneider: *Boundary extension and stop criteria for empirical mode decomposition*. Advances in Adaptive Data Analysis, 2(2):157–169, April 2010. <https://doi.org/10.1142/S1793536910000434>.
- [YYJ12] Yong, Wang, Liu Yanping, and Yang Jing: *Signal prediction based on empirical mode decomposition and artificial neural networks*. Geodesy and Geodynamics, 3(1):52–56, February 2012, ISSN 1674-9847. <https://dx.doi.org/10.3724/SP.J.1246.2012.00052>.

Eigenständigkeitserklärung

Hiermit versichere ich an Eides statt, daß ich die vorliegende Arbeit selbstständig und ohne die Benutzung anderer als der angegebenen Hilfsmittel angefertigt habe. Alle Stellen, die wörtlich oder sinngemäß aus veröffentlichten und nicht veröffentlichten Schriften entnommen wurden, sind als solche kenntlich gemacht.

Die Arbeit ist in gleicher oder ähnlicher Form oder auszugsweise im Rahmen einer anderen Prüfung noch nicht vorgelegt worden. Ich versichere, daß die eingereichte elektronische Fassung der eingereichten Druckfassung vollständig entspricht.

Laslo Hunhold